Photoinduced Structural Dynamics of Molecular Systems Mapped by Time-Resolved X-ray Methods

Majed Chergui, Eric Collet

▶ **To cite this version:**

Majed Chergui, Eric Collet. Photoinduced Structural Dynamics of Molecular Systems Mapped by Time-Resolved X-ray Methods. Chemical Reviews, 2017, 117 (16), pp.11025-11065. 10.1021/acs.chemrev.6b00831 . hal-01559760

HAL Id: hal-01559760
https://hal.science/hal-01559760

Submitted on 10 Jul 2017

HAL is a multi-disciplinary open access archive for the deposit and dissemination of scientific research documents, whether they are published or not. The documents may come from teaching and research institutions in France or abroad, or from public or private research centers.

L'archive ouverte pluridisciplinaire **HAL**, est destinée au dépôt et à la diffusion de documents scientifiques de niveau recherche, publiés ou non, émanant des établissements d'enseignement et de recherche français ou étrangers, des laboratoires publics ou privés.

Photoinduced structural dynamics of molecular systems mapped by time-resolved x-ray methods

Majed Chergui[*,†] and Eric Collet[*,‡]

[†]Ecole Polytechnique Fédérale de Lausanne, Laboratoire de Spectroscopie Ultrarapide (LSU), ISIC, and Lausanne Centre for Ultrafast Science (LACUS), Faculté des Sciences de Base, Lausanne CH-1015, Switzerland.

[‡] Univ Rennes 1, CNRS, Institut de Physique de Rennes, UMR 6251, UBL, F-35042 Rennes, France.

ABSTRACT:

We review the tremendous advances in ultrafast X-ray science, over the past 15 years, making the best use of new ultrashort x-ray sources including table-top or large-scale facilities. Different complementary x-ray based techniques, including spectroscopy, scattering and diffraction, are presented. The broad and expanding spectrum of these techniques in the ultrafast time domain, is delivering new insight into the dynamics of molecular systems, of solutions, of solids and of Biosystems. Probing the time evolution of the electronic and structural degrees of freedom of these systems on the timescales of femtosecond to picoseconds delivers new insight into our understanding of dynamical matter.

CONTENTS:

1. Introduction

The discovery of the X-rays by William Conrad Röntgen in 1895 sparked off a breath-taking chain of scientific breakthroughs in the first two decades of the XXth century that marked the birth of structural science. The systematic study of the characteristic rays (in emission and absorption) was mainly undertaken by Charles Glover Barkla, who discovered X-ray absorption edges (interestingly, this discovery preceded X-ray diffraction).[1,2] Soon after, the seminal works of Paul Ewald, Max von Laue, William Henry Bragg and William Lawrence Bragg in the period between 1912 and 1913, heralded the birth of a new Era by establishing the laws of X-ray diffraction from crystals and the determination of their structures with atomic resolution.[3-7] The ideal crystal is a highly ordered arrangement of atoms and molecules with perfect periodicity in three dimensions. In the real world this order is always disrupted. At any instant the atoms are displaced from their ideal mean position by thermal motion, even at absolute zero temperature. Soon after the pioneering works of Ewald, von Laue and the Braggs, Debye investigated the effects of thermal motions and disorder showing that they decrease the diffraction intensities of Bragg reflections, especially at high scattering angles.[8] This would lead to the birth of Debye-Scherrer scattering for powder diffraction and diffuse scattering, which applies to disordered media. Further additional discoveries, like electron diffraction and scattering, made it such that by the 1920s, X-ray and electron diffraction techniques had reached the atomic scale resolution of space, i.e. the Å. It can be said that while several spectacular improvements will come in the following decades, the stage was then set for the static structural determination of assemblies of atoms (crystals, molecules, proteins). The advent of computer science with always more powerful calculations made possible the analysis of larger amount of data for pushing such studies toward more complex systems, from the structure of simple crystals (like Na^+Cl^-) to the structure of proteins or viruses.

In parallel to the discoveries concerning scattering of X-rays, work was pursued to understand and interpret X-ray absorption and emission spectra, as the development of quantum mechanics was unfolding. Manne Siegbahn[9-12] developed new apparata and methods to rigorously analyse X-ray spectra. However, X-ray spectroscopy would remain limited to chemical identification of elements and analysis of electronic structure. As a structural tool, X-ray absorption spectroscopy would have to go through several decades of theoretical developments (beautifully described in the historical review by Stumm von Bordwehr[13]) aimed at describing the modulations that appear in the above-edge region of the spectrum of an atom, when it is embedded in a molecular or crystalline edifice. These modulations, called X-ray absorption near-edge structure (XANES) and extended X-ray absorption fine structure (EXAFS) finally received a consistent interpretation through the works of Sayers, Stern and Lytle.[14] Several improvements of the theoretical tools will ensue,[15] making EXAFS in particular (whose treatment is easier), an important element-selective tool in Materials Science, Biology and Chemistry.

Although, the awareness that resolving atomic motion was implicit in Debye's work, several decades would be required before this will become possible, in particular, with the advent of the laser in the early 1960, thanks to the works of Ali Javan,[16,17] Nikolai G. Basov, Alexander M. Prokhorov,[18] Charles Townes and Arthur Schawlow. Soon after the birth of the laser, pulsed nanosecond, then picosecond lasers appeared, but to reach the atomic scale of time, i.e. the femtosecond, laser technology had to wait the mid-1980, thanks to the works of Charles Shank.[19-24]

The time scales of chemical and physical transformation in matter span several decades and the required time resolution depends on the scientific question one needs to address (Figure 1). Animal motion requires typically millisecond resolution, and the first snapshots with such a resolution were taken by the French anatomist and physiologist, Etienne-Jules Marrey,[25] who developed the first shutter camera. Large amplitude protein motion requires ms to μs, which can be monitored by NMR or optical techniques. As the length scale of processes decreases, e.g. acoustic waves, molecular rotation, molecular vibrations, there is need for higher and higher temporal resolution spanning the range from nanoseconds (ns) to femtoseconds (fs). For the description of processes occurring at the atomic scale of length, i.e. the chemical bond, fs-resolution is required. This is the time scale of nuclear motion or vibration in molecules, crystals and biosystems, and has, for that matter been coined the atomic scale of time by A. H. Zewail, who pioneered Femtochemistry, by demonstrating the power of fs pump-probe spectroscopy to describe chemical processes. He was awarded the Nobel Prize for Chemistry in 1999 for his seminal contributions.[26-30]

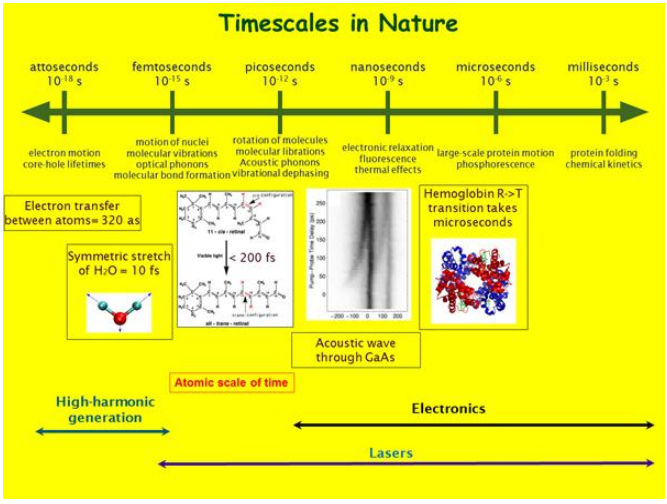

Figure 1: Time scales of fundamental processes in Nature and (below) types of devices to probe them in real-time. The atomic scale of time is the femtosecond and that of length is the Angström.

Indeed, for the first time it became possible to probe in real-time the motion of atoms inside molecules, via their wavepacket dynamics, and monitor chemical reactions and the transition state. This major development and that of others in the growing community of ultrafast scientists,[31-37] were all carried out using optical pulses in the IR, visible and ultraviolet. Yet from the beginning it was clear to many in this community that optical-domain radiation does not deliver structural information, except in a few rare cases, i.e. small molecules whose energy topology (i.e. potential energy curves) is known. This does not apply to assemblies of more than 3 atoms and therefore early on in the 1990s, were there suggestions to replace the optical probe pulse by ultrashort pulses of electrons or of X-rays. A. H. Zewail was the sole to adopt the route with electron pulses,[38-41] while most of the community adopted X-rays.[42-54] The main challenge in this endeavour was the development of sources of ultrashort electron or X-ray pulses and the mastering of data acquisition schemes which differed greatly depending on whether one carries out diffraction, scattering or spectroscopic measurements. The common technical preoccupation of scientists coming from very different scientific backgrounds (Chemistry, Biology, Solid state physics, Materials Science, Engineering) has created a convergence of interests towards instrumentation that is used equally by different communities.

The pioneering work of the Zewail group on ultrafast electron diffraction and more recently, microscopy and Electron Energy Loss Spectroscopy has been reviewed in several excellent papers and is beyond the scope of this review.[55-60] Rather, here we focus more specifically on the studies using X-ray pulses that have been undertaken in the last 15 years to probe the photoinduced structural changes in molecular systems, either in solutions or in crystalline forms. While several reviews have already been published on the X-ray probing of molecular systems,[56,61-71] this is the first that binds together the solution and crystalline phases.

Probing the nuclear dynamics of molecular systems requires both the atomic-scale resolution of space (the Å) of structural methods such as X-ray or electron diffraction and X-ray absorption spectroscopy, with the atomic resolution of time, the femtosecond. The principle of all these approaches consists in exciting the sample with an ultrashort laser pump pulse and probing it with a second ultrashort X-ray (or electron) probe pulse, whose time delay with respect to the first is tuned by optical delay lines in the femtosecond to picosecond range, or even longer times.

When an X-ray beam is incident on a sample, several processes can occur as schematically depicted in Figure 2. The beam can be scattered with a change of the incident wave vector. This forms the basis of scattering and diffraction methods, which over the past century have been refined to a high degree of sophistication to study molecules in crystals or in solution. Most of the incident beam is however absorbed creating a photoelectron extracted from a core orbital by the high energy incident beam. This X-ray absorption process is the basis of structural methods described below. The core hole can be refilled by an electron from a higher core orbital leading to X-ray emission, which contains extremely valuable information about the electronic and spin structure of the system. Finally, either the photoelectron or electrons resulting from Auger processes may be detected, providing valuable electronic structure information. These various approaches will be discussed in detail in §§ 3.

Central to the methods discussed here are ultrashort X-ray pulses. Thereafter, we describe the available sources delivering such pulses.

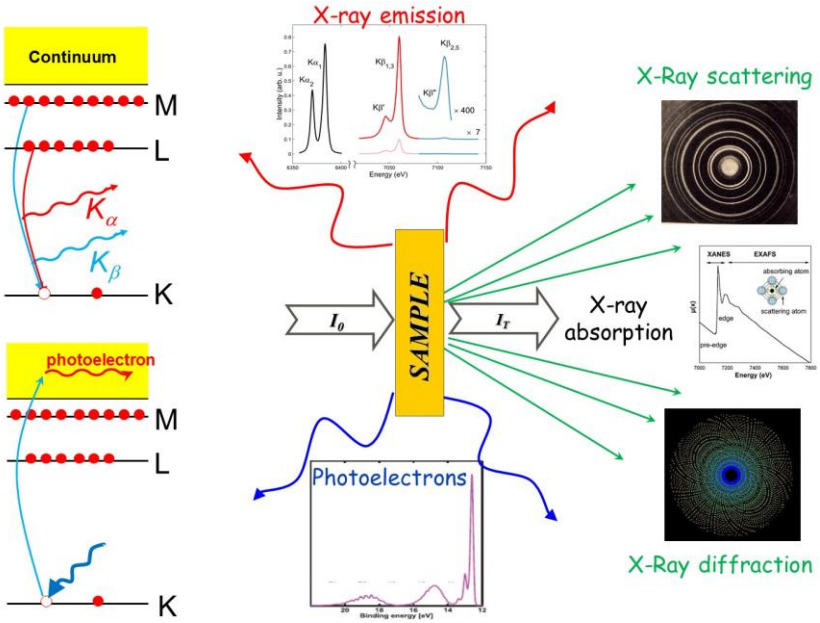

Figure 2: Processes that are triggered when an X-ray beam intensity (I_0) is incident on a sample. Different types of core-level spectroscopies are possible: X-ray absorption spectroscopy (XAS), photon-in/photon-out spectroscopies which are broadly classified as X-ray emission (XES) and Photoelectron spectroscopy (photo-in/electron-out). X-ray scattering is used to probe structures of molecules in solution and X-ray diffraction for crystalline systems.

2. Sources of Ultrashort X-ray pulses

Performing time-resolved X-ray experiments with picosecond to femtosecond time resolution requires ultrashort X-ray pulses, as there are no detector capable of picosecond to femtosecond resolution. Thus the time resolution has to rely on the source and on the use of optical delay lines, just as in ultrafast optical spectroscopy. There are several classes of sources of ultrashort X-ray pulses, which can be broadly classified as table-top or large scale installations. Within these two categories, sources also differ in pulse duration, energy range, energy tunability, etc. The commonly used table-top sources include: (i) laser-driven table-top plasma sources, which can generate 100 fs hard X-ray pulses;[72] (ii) high harmonic generation (HHG) sources that can reach attosecond pulse durations but are limited to the vacuum ultraviolet (VUV) to soft X-ray range.[73] The large scale installations are all accelerator-based facilities such as synchrotrons, which can generate 100 ps X-ray pulses that can be shortened to 100 fs using the slicing scheme,[74-77] or X-ray free electron lasers (X-FELs), which can generate intense X-ray pulses of few fs.[78] In the following we will give a brief description of ultrashort pulsed hard X-ray sources based on table-top and large-scale installations, as several detailed reviews on each type can already be found in the literature.[61,67,72,78-80] The most commonly used sources for ultrafast X-ray studies to date have been the plasma based ones (table-top), synchrotrons and X-ray free electron laser, on which we concentrate hereafter.

2.1 Plasma-based sources

In laser-driven plasma sources,[81] a femtosecond laser pulse with peak intensity higher than 10^{16} W/cm^2, is used to irradiate a metal target, resulting in creation of a plasma. The thus generated free electrons are accelerated by the very high electric field of the laser pulse and their interactions with target atoms leads to emission of soft and hard X-ray radiation. However, the emitted X-ray pulse is isotropic and it fluctuates in intensity on a pulse-to-pulse basis, requiring special optics to collect the radiation and special set-up designs to correct for the fluctuations. Usually, the collected radiation amounts to only a small part of the typically 10^9 X-ray photons emitted per pulse, because of constraints on time resolution.[72] For a target thickness of the order of 10 µm, the characteristic emission has duration of the order of 100 fs. An interesting intrinsic property of this technique is that time zero is very well defined, as the same optical laser is used to excite the sample and generate the plasma. It is with this technique that Rischel *et al* reported the first fs X-ray diffraction study of the ultrafast melting of molecular layers.[82]

Recent developments in laser and target technologies have allowed the generation of hard X-ray pulses at kHz repetition rates and much reduced intensity fluctuations. Because, the irradiated target is damaged irreversibly, it is moved to refresh it after for each laser pulse. Furthermore, a highly stable spatial position of the target area with fluctuations of less than 20 μm is needed. Some hard X-ray plasma sources with Cu tape targets are driven by sub-50 fs pulses and work at 1 kHz repetition rate[83] and the collimated hard x-ray flux on the sample reaches up to 10^7 photons/s. It was shown that by using intense mid-IR sub-100-fs pulses allows for accelerating electrons from the Cu target due to much higher kinetic energies comparably long optical period, thus generating a 25 times higher X-ray flux than with 800 nm laser pulses.[84]

2.2 Large-scale facilities: Synchrotrons

The X-ray pulses generated by third generation synchrotrons are of the order of 50-150 picosecond, and can be used to probe photoinduced structural changes on time scales of >100 ps, either by X-ray diffraction, scattering or spectroscopy. The pioneering development of the X-ray scattering technique with 100 ps time resolution was performed on the ID09B beam-line by the Wulff group at the European Synchrotron Radiation Facility (ESRF, France).[85,86] It is now available in several places around the world, such as the APS (Argonne, USA) and the KEK-AR (Tsukuba, Japan).[87] For example, during experiments performed at the ESRF in the 16-bunch mode, the different bunches from the synchrotron generate X-ray pulses separated by about 176 ns. In the 1 kHz repetition rate mode, the X-ray flux is decreased by a factor of ≈ 6000, as a mechanical chopper selects one X-ray pulse every ms. Nevertheless, the X-ray flux in the 1 kHz time-resolved mode is comparable with the one of a conventional X-ray tube. Such a technique has been successfully utilized to perform structural investigations of chemical or biochemical photoinduced phenomena occurring on 100 ps time scale.[88]

X-ray absorption spectroscopy with 50-100 ps resolution was pioneered by the Chergui group at synchrotrons.[54,56,61,62,67,68,71,89-97] Parallel to the latter, developments driven by L. Chen and her group were also taking place.[64,65,98-100] Time-resolved X-ray spectroscopy quickly emerged as an important tool for studying solution phase photoinduced electronic and structural changes in chemical systems at synchrotrons in the USA,[101,102] Japan,[87,103,104] and by several groups worldwide using the US, Swiss and Japanese synchrotrons.

Until about 2010, time-resolved X-ray absorption experiments were carried out using a 1 kHz femtosecond laser, while synchrotrons operate at MHz repetition rates, so that at least 10^3 of the X-ray pulses remained unused. A major development was introduced by the Chergui group, which consisted in using a ps pump laser (rather than a fs one) whose repetition rate is half or an integer fraction of that of the synchrotron.[105] Keeping all other parameters fixed, this leads to an increase of the signal by the root square of the laser repetition rate compared to the same signal recorded with a 1 kHz laser. This scheme also opens the possibility to perform photon-in/photon-out experiments (including scattering and diffraction), which require a high incident flux per second.[106] This development was followed by similar ones at the APS[107] and Elettra.[108]

In order to extract femtosecond X-ray pulses from synchrotrons, in particular with energy tuneability, the slicing scheme was proposed by Zholents and Zholterev[109] and its experimental validation was reported at the ALS.[74] It consists in co-propagating an intense fs laser pulse (100 fs) with the electron bunch (100 ps) in the storage ring, and the interaction between the two slices out wedges that have the same time structure as the laser pulse. The first “slicing” beamlines were developed at the ALS[110,111] and at BESSY-Germany[112] and were operating in the soft X-ray range. The first hard X-ray slicing source was implemented at the Swiss Light Source,[77] where a fs laser beam is split to "pump" and "probe" branches. The "probe" branch modulates the energy of the electrons in the modulator where electrons in the magnetic device interact with the femtosecond laser. The slice of electrons passing through the undulator generates a femtosecond X-ray pulse used to probe the sample at a variable time delay with respect to the pump pulse which is intrinsically synchronized to the sliced beam. This is a great advantage of the slicing scheme, but the photon flux in the X-ray pulse is very low (typically 1/1000 of the 50-100 ps pulse), even more so, when performing X-ray absorption spectroscopy experiments, which require a narrow energy band pass. Nevertheless, it was with the slicing scheme that the first fs X-ray experiment on a molecular system was achieved on a large facility by Chergui and co-workers.[113] The new generation of machines, X-ray free electron lasers, overcomes this limitation as discussed hereafter.

2.3 Large-scale facilities: X-ray Free Electron Lasers (XFEL)

X-ray Free Electron Lasers are linear accelerators with insertion devices (undulators) at their end, so that the electron bunches are used only once (Figure 3). The magnetic structure used to generate X-rays are linear sections hundreds of meters long. Such long interaction volumes force the electrons in the bunch to interact constructively via the generated X-ray field, giving rise to the so-called microbunching, which shortens the X-ray pulse duration tremendously (≤ 100 fs), enhances coherence, emittance and importantly flux, with values of 10^{12} photons/pulse in 0.1% bandwidth. This self-amplified spontaneous emission (SASE) of hard X-rays was generated for the first time in the hard X-ray range at the Linac Coherent Light Source (LCLS) at SLAC (Stanford, USA)[114] and later at SACLA (Sayo, Japan).[115] New machines will be inaugurated in 2017: the European X-FEL (Hamburg, Germany) and the SwissFEL at the Paul Scherrer Institute (Villigen, Switzerland), while another machine is under construction in Korea.

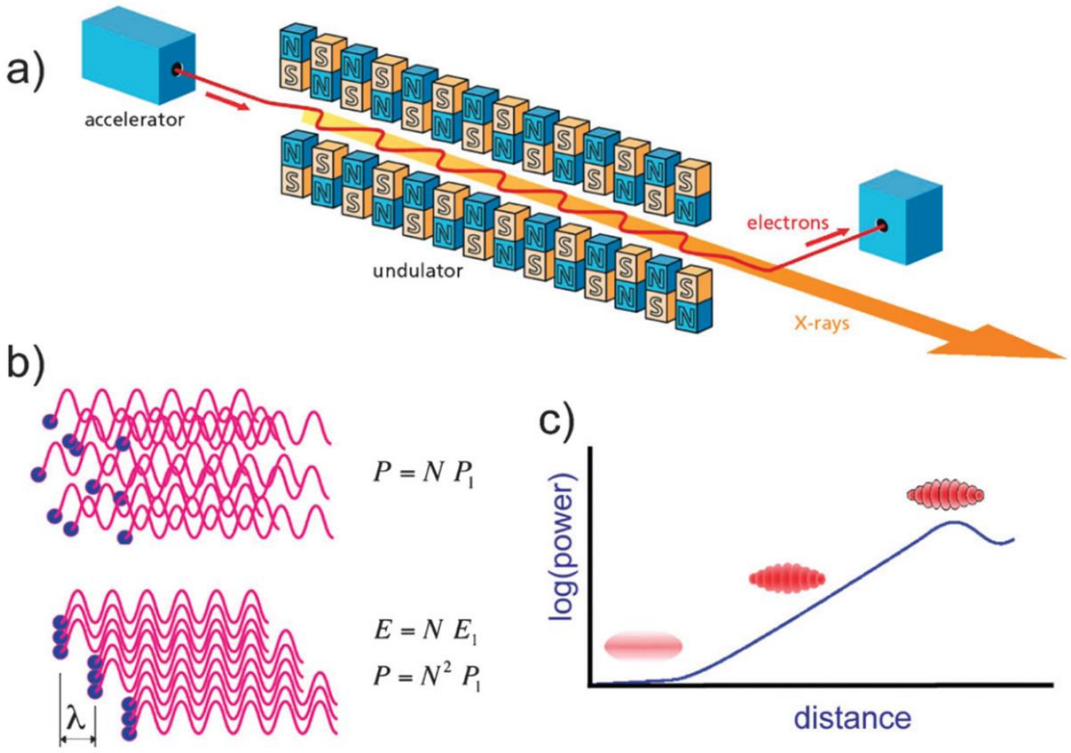

Figure 3: Operation principle of the Free Electron Laser. Electrons are accelerated close to the speed of light. As the beam passes through the undulator (a), which is an array of magnets, the electrons are forced to wiggle transversely along a sinusoidal path about the axis of the undulator, leading to emission of light. When the latter becomes sufficiently strong, interaction between the transverse electric field of the light and the transverse electron current causes some electrons to gain and others to lose energy to the optical field. This energy modulation leads to a microbunching (b) of the electrons, which are separated by one optical wavelength along the axis, and to an increase in radiated power and coherence (c). Reprinted with permission from Reference [116]. Copyright 2017 Royal Society of Chemistry.

The LCLS and SACLA deliver up to 10^{14} photons/second on the sample and the time duration of the X-ray pulses can be decreased down to a few fs. Because of the fluctuating initial conditions of the SASE, the spectral and the time structures of the X-ray pulses fluctuate on a shot-to-shot basis. However, it is now possible to correct for these fluctuations using monochromators and normalization methods for better characterizing the X-ray spectrum, while the use of the timing-tool allows achieving few-fs time sorting.[117]

While the hard X-ray FELs are all based on the principle of SASE, one machine, FERMI@Elettra (Trieste, Italy), operates as a seeded FEL and therefore as a real laser.[118-121] It generates soft X-ray pulses up to about 300 eV, and work is in progress to increase this limit to the Oxygen K-edge.

3. Structural dynamics with X-rays: Methods

3.1 X-ray spectroscopies

3.1.1 X-ray absorption spectroscopy

An X-ray absorption spectrum (XAS) consists of absorption edges, which represent ionisation thresholds of the various core orbitals (Figure 4). An edge spectrum can be divided in three energy parts: the pre-edge region, the edge and the region up to about 50 eV above it, or so-called X-ray near-edge absorption structure (XANES), and the region at higher energy, called the extended X-ray absorption fine structure (EXAFS). These have been described in several textbooks and review articles,[15,61,122-125] so that here, we only repeat the main characteristics of each region and what type of information they contain.

In pre-edge transitions, the core electron is excited to unoccupied or partially filled valence orbitals just below the ionization potential (E_0 in figure 4). Therefore, these atomic transitions contain element-specific information about the occupancy of valence orbitals, which are the ones involved in chemical bonding and chemical transformations. Once above E_0, in the XANES region, the atom is ionized and the photoelectrons (PE) that are generated have low kinetic energy, i.e. a high scattering cross-section. For this reason, they undergo multiple scattering (MS) processes, giving rise to strong modulations of the absorption coefficient, which dominate the signal. These processes contain information about the three-dimensional structure around the absorbing atom, i.e. coordination numbers, bond distances and bond angles, as discussed in several publications.[15,68,122,124,126-128] In the EXAFS region, the PEs have a large kinetic energy (i.e. smaller scattering cross-section) and the signal is dominated by single scattering (SS) events, giving rise to weak modulations of the absorption coefficient. This region delivers information about coordination numbers and bond distances to the nearest neighbours of the absorbing atom.

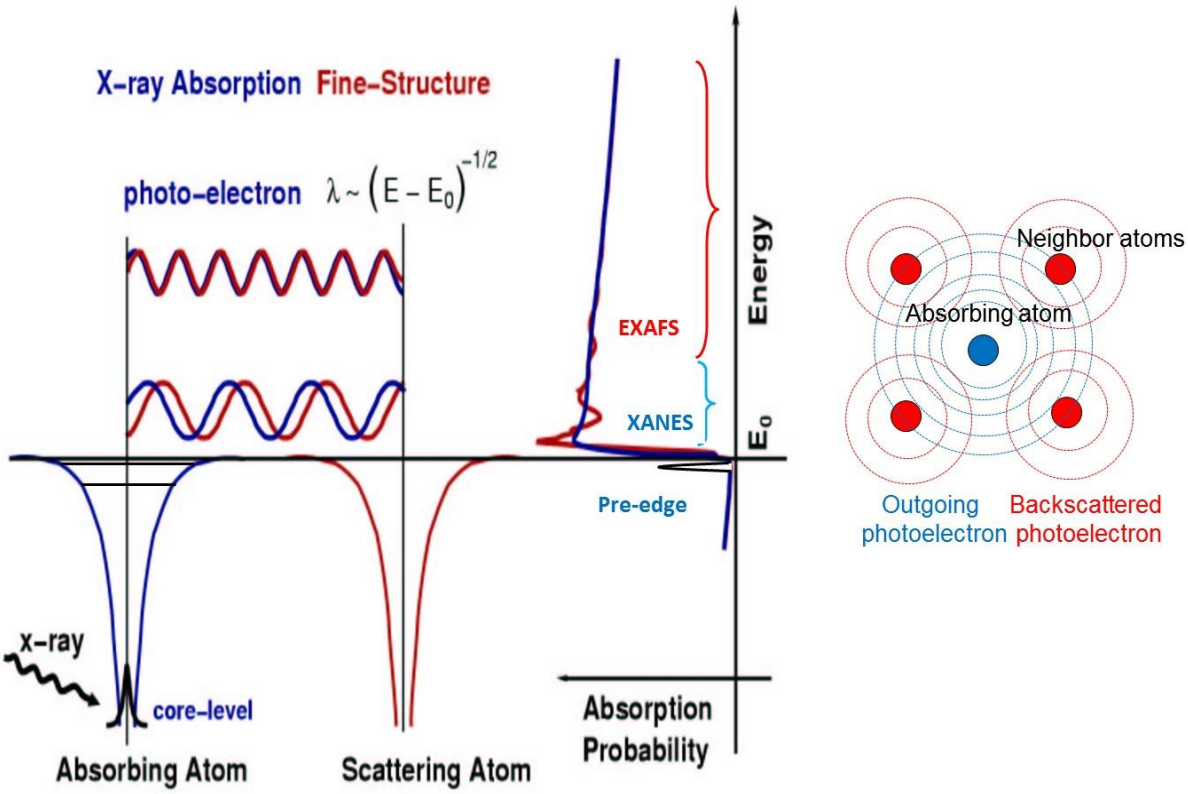

Figure 4: X-ray absorption spectroscopy. Excitation of a core orbital to the orbitals below the ionization potential (E_0) gives rise to pre-edge transitions, which probe the unoccupied density of states. Above E_0, there is a jump in the absorption cross-section giving rise to an edge and a photoelectron is generated whose de Broglie wavelength depends on its excess energy ($E-E_0$). Low energy electrons have high scattering cross sections, so if the absorbing atom is embedded in an assembly of atoms, multiple scattering events occur (right panel), giving rise to modulations of the spectrum in the above ionization region, called the X-ray absorption near edge structure (XANES). As the kinetic energy of the electrons increases, the cross section decreases and weaker modulations appear which form the Extended X-ray absorption fine structure (EXAFS).

The descriptions of the pre-edge region (bound-bound transitions) and the above-edge region (bound-to-continuum transitions) call for different theoretical treatments, which have been described in detail in ref. [70] and will not be repeated here.

The key feature of XAS is its ability to probe both the electronic structure of an absorber and the nuclear structure around it in the same measurement. In particular, it is important to stress that one interrogates the valence orbitals of the system, which are those entering in the formation and transformation of chemical bonds. In this respect, XAS is unique compared to all other X-ray diffraction tools, where accurate determination of the electron density can only be retrieved by time consuming high-resolution measurements and topological analysis.

For extending XAS into the time-domain, the now commonly adopted strategy was developed by the Chergui group and it consists in recording transient XAS by taking the difference at a particular X-ray energy and pump-probe time delay (Δt) of the transmission signal from the excited sample (pumped) minus that from the unexcited sample (unpumped) on a pulse-to pulse basis.[61,62,92,95] This requires that the laser operates at half or an integer fraction of the repetition rate of the X-ray source. The advantage of the pulse-to-pulse data acquisition scheme is that it corrects for short term fluctuations and long-term drifts of the source, such that the transient signals can be acquired at the shot noise of the synchrotron source, which is very stable. A measurement of the background in the gap where no X-rays are present is also made. It is then subtracted of the corresponding X-ray signal to compensate for any drifts over time of the data acquisition baseline. The transient spectrum is then:

$$\Delta I(\Omega, t) = f \cdot \left[\varphi(t) I_{pumped}(\Omega) - I_{unpumped}(\Omega)\right]$$

where f is the photolysis yield and φ (t) represents the quantum yield of the photogenerated product, whose time dependence reflects decay processes. This general methodology also applies to the second-order spectroscopies described in the next section.

3.1.2 Photon-in/photon-out X-ray spectroscopies

Photon-in/photon-out X-ray spectroscopies[129] involve the detection of emitted X-ray photons after X-ray absorption (Figure 2). While XAS provides insight into the unoccupied valence orbitals, just as in optical spectroscopy, X-ray emission spectroscopy (XES) provides information about the occupied and partially occupied density of states (DOS). These spectroscopies are treated within second-order perturbation theory and are therefore also called second-order spectroscopies.[130] Their theoretical description in relation to time-resolved studies was discussed in ref. [70] and will not be repeated here.

Photon-in/photon-out spectroscopies with incoming hard X-rays span a wide variety of approaches, which allow retrieving soft X-ray (L- or M-edges), low-energy excitations, perform site selective and/or range-extended EXAFS[131-133] and record high-resolution XAS spectra.

Because the X-ray scattering and fluorescence cross-sections are low thanks to the advent of more intense X-ray sources and high-resolution detectors, it has become possible to record steady-state X-ray emission (XES) or X-ray Raman spectroscopy in a routine way. Their extension in time domain experiments has become possible thanks to the increased photon flux brought about by the high repetition rate schemes at synchrotrons[105,107] or the X-FELs are making time-resolved second-order spectroscopies new tools in chemistry, condensed matter physics and biology.

Photon-in/photon-out spectroscopies are described by the Kramers-Heisenberg equation.[134] Just as in the optical domain, this equation describes the absorption of a photon from the ground state i to an intermediate state n, that decays to a final state f, which can be seen as coherently coupled absorption and emission events. This implies that interference between different intermediate states can affect the spectral weights. However, in the hard X-ray range, the weights are generally small and interference terms can be neglected.

In a non-coherent process, the absorption matrix elements from initial state i to intermediate state n are weighed by the emission matrix element. An example is XAS in total fluorescence yield (TFY) detection mode, where the fluorescence from the sample is collected with no energy resolution, as a function of the incident photon energy. This is equivalent to integrating over the XES matrix elements and consequently, it turns the emission matrix elements into a constant.[135] This approach is advantageous when the signal of interest contributes only a small fraction to the total absorption, or when the sample transmission is very large, e.g. dilute samples.

3.1.2.1 Non-resonant X-ray emission (NXES)

X-ray emission can be triggered by absorption of a core electron either into a resonant state or non-resonantly. For non-resonant X-ray emission (NXES), the incident photon energy is much above the Fermi energy for a core transition, and the PE is ejected into the continuum (Figure 2). The spectral weights are largely independent of the incident photon energy and the lifetime broadening of the spectrum corresponds to $\Gamma_n + \Gamma_f$.[136]

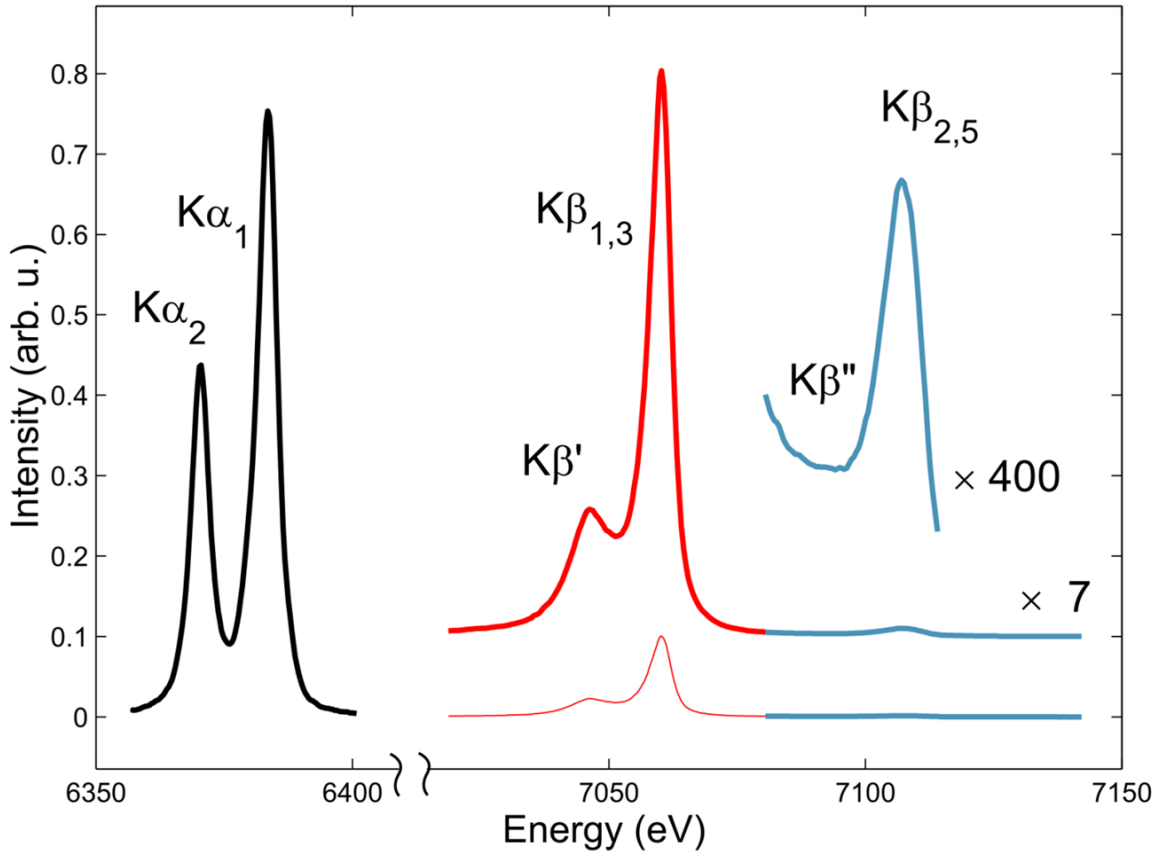

Figure 5: Typical K-edge emission spectrum of Fe showing the characteristic emission lines. Courtesy G. Vanko.

Figure 5 shows the K emission spectrum of an Fe(II) complex, i.e. after creation of a hole in the Fe 1s-orbital is characterized by a number of spectral lines: the strongest of which are the $K\alpha_1$ and $K\alpha_2$ lines, due to transitions from the $2p_{3/2}$ and $2p_{1/2}$ levels (making up the L-shell), respectively. These core-to-core transitions are commonly employed to retrieve TFY XAS (§ 3.1.2). At higher energies lie the $K\beta_{1,3}$ lines ($3p \rightarrow 1s$) transitions, which are nearly one order of magnitude weaker than the $K\alpha$ ones. Still higher in energy are the so-called valence-to-core $K\beta_{2,5}$/ Kβ" lines. These are much weaker due to a poorer overlap of initial (valence orbital) and final (core orbital) wave functions. They are the emission equivalent of the pre-edge transition in XAS (Figure 4). Because they stem from the valence orbitals, the $K\beta_{2,5}$/ Kβ" lines are very sensitive to the chemical environment of the emitting atom, in particular the ligand orbitals, and, to a certain extent, bond distances.[129,137,138] In time-domain experiments, they will yield important information about the valence electron density change resulting from an ultrafast chemical process.

3.1.2.2 Resonant X-ray emission (RXES)

Resonant X-ray emission (RXES) occurs when the incident X-ray photon energy excites an unoccupied orbital, occurs. The signals are more intense than in NXES and are incident energy-dependent.[139-141] This is also called resonant inelastic X-ray scattering (RIXS). Thereafter, this term will be used. RIXS combines XAS and X-ray diffraction in one single experiment. The X-ray direction yields spatial information, while the spectroscopic part, through the anomalous scattering amplitude, provides information about the electronic states of the system.[142] In case the initial and final states are different, an energy transfer to the system occurs.[143] In RIXS maps, the incident and emitted (or energy transfer) photon energies are displayed on a 2D correlation plot. Figure 6 shows the Pt L_3 ($2p_{3/2}$-$3d_{5/2}$) RIXS plane of the di-platinum complex $[Pt_2(P_2O_5H_2)_4]^{4-}$ (abbreviated PtPOP) measured in solution in the two most commonly used presentation formats: XAS vs XES and XAS vs Energy transfer.[70] It was obtained using a dispersive X-ray spectrometer in von Hamos geometry that detected the L_1 X-ray emission (9.44 keV), and scanning the incident X-ray energy across the L_3-edge.[144] By resolving both the incident and emitted photon energies, one simultaneously measures the occupied and unoccupied density of states around the resonant core excitation. In addition, the transferred energy corresponds to elementary excitation of the final state of the material, which can include low-energy excitations such as charge-transfer or ligand-field excitations in the case of metal complexes.[145,146]

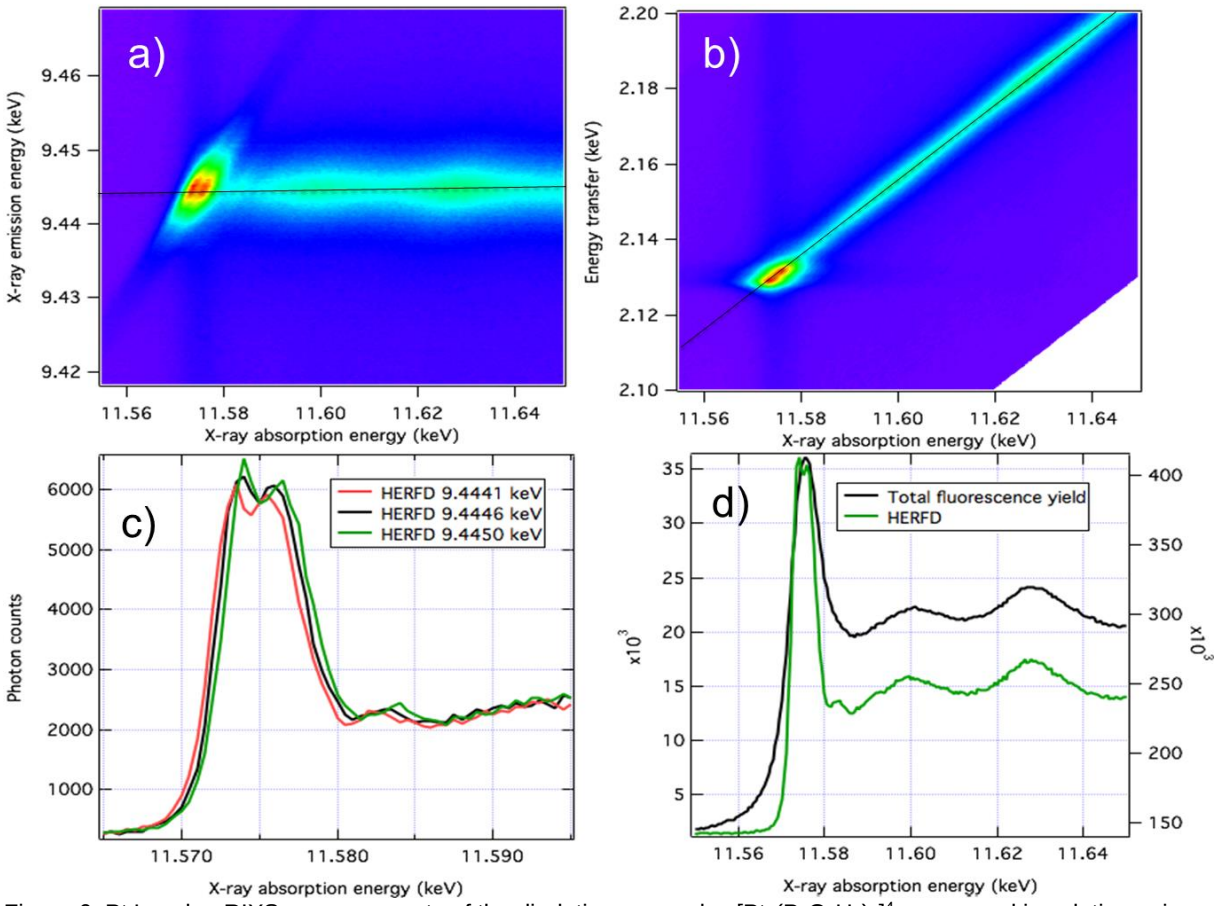

Figure 6: Pt L_3-edge RIXS measurements of the di-platinum complex $[Pt_2(P_2O_5H_2)_4]^{4-}$ measured in solution using a dispersive von Hamos spectrometer.[144] (a) and (b) present the $2p_{3/2}$–$3d_{5/2}$ resonant inelastic X-ray scattering (RIXS) plane as XAS vs XES and XAS vs Energy transfer plots, respectively, where Energy transfer = XAS − XES. (c) shows high-energy resolution fluorescence detection (HERFD) signals at three X-ray emission energies, corresponding to horizontal slices in (a) and diagonal slices in (b). Note the sensitivity of the HERFD signal to the chosen emission energy. (d) Comparison between the total fluorescence yield (TFY) and HERFD signals, illustrating the increased energy resolution possible with the HERFD technique. Reprinted with permission from Reference [70]. Copyright 2017 Elsevier.

3.2 X-ray Scattering

Scattering techniques of X-rays, as well as of neutrons and electrons, represent a fundamental tool to investigate structural aspects of matter and its transformations.[147,148] Hereafter we highlight the some important features and the X-ray scattering and diffraction and the extension of these methods to time-resolved techniques, which open the possibilities to observe how matter rearranges in real-time.[88] The scattering of monochromatic X-rays (wavelength λ), through the interaction with electrons contained in atoms, changes the direction of the incident radiation. This process is described through the momentum transfer $\vec{Q}$ between the incident $\overrightarrow{k_i}$ and diffracted $\overrightarrow{k_d}$ (or scattered) wave vectors.

$$\vec{Q} = \overrightarrow{k_d} - \overrightarrow{k_i}.$$

This change of direction is also measured by the angle $2\theta = (\widehat{\overrightarrow{k_d}, \overrightarrow{k_i}})$. The resulting scattering of the X-ray wave by an assembly of atoms forming a molecule gives rise to interferences along $\vec{Q}$. This scattering process can be described in the case of disordered molecules in solution for example, with random position and orientation, or in the case of highly ordered molecules paving a 3D crystalline lattice. In the first case, the scattered signal will be shaped by the dephasing of the waves scattered by the different atoms of the molecules, whereas in the second case additional interferences from the different nodes of the lattice will give rise to constructive interferences around the Bragg peaks only.

3.2.1 Scattering of molecules from disordered media

Molecules in solution (or in gas phase) show a statistical distribution of positions and orientations. The Curie symmetry principle explains why the scattered X-ray signal $S(\vec{Q})$ from such an ensemble of disordered molecules

is isotropic and only depends on the modulus $Q=(4\pi/\lambda)\sin(\theta)$. This isotropic signal observed with bi-dimensional detectors is translated to one-dimensional intensity curves, *S(Q)*, obtained by the radial integration of the signal. The Debye description, which holds for isolated molecules in gas-phase, is a simple approach to analyze scattering patterns from liquids:

$$S(Q) = \sum_{i,j} f_i(Q) f_j(Q) \frac{\sin(Q.r_{ij})}{Q.r_{ij}}$$

where $f_i(Q)$ denotes atomic form factors and r_{ij} are the distances between the atoms *i* and *j*. This description basically reproduces the scattering pattern by molecules through a set of atoms with interatomic distances. More detailed analysis for molecules in solution also includes the bulk solvent contribution and the solvation shell.[149] Tracking the molecular structural change in the time domain is easier through:

$$\Delta S(q,t) = S(q,t) - S(q),$$

whereby the ground state scattered signal *S(q)* is subtracted from the scattered signal *S(q,t)* at a time delay *t* after photoexcitation. From this change of the scattering pattern, the structural modification is refined. Behind this very simple description of the process, it should be underlined that the solvent response can be the dominating part of the measured signal and that it in most cases it is far from trivial to extract the solute contribution.[150] More details on the X-ray data processing can be found in e.g., ref. [151].

3.2.2 Diffraction by molecules in crystal lattices

In molecular crystals, the molecules adopt well-defined positions and/or orientations. A perfect 3D crystal is built with a periodical repetition, over the unit cells, of a molecular motif along 3 lattice vectors $\vec{a}$, $\vec{b}$ and $\vec{c}$, forming the unit cell.[147] The unit cell is also described by the length of three axes: *a, b, c* and the angles α, β and γ between them. As in the case for isolated molecules, an incident X-ray is scattered by the electrons around atoms. The different atoms within the unit cell scatter X-rays with different amplitudes (atomic form factors) and phases (atomic positions $\vec{r_j}$ in the unit cell). However, since atoms in a crystal are arranged in a regular pattern, the scattering by a crystal gives rise to constructive interferences for specific directions $\vec{Q}$, corresponding to the nodes of the reciprocal lattice (defined by $\vec{a}^*,\vec{b}^*,\vec{c}^*$). Each of these directions $\vec{Q} = h\vec{a}^*+k\vec{b}^*+l\vec{c}^*$ is associated with integer values of the *(hkl)* coordinates and corresponds to the so-called Bragg peaks. The intensity of every Bragg peak is proportional to the square modulus of the amplitude $F(\vec{Q})$ scattered by all the electrons of a unit cell and the structure factor of the unit cell is given by:

$$F(\vec{Q}) = F(hkl) = \sum_j f_j(Q) \exp(-\vec{Q}.\vec{r_j}) = \sum_j f_j(Q) \exp(-2i\pi(hx_j + ky_j + lz_j))$$

The integrated intensity of a Bragg peak on the *(hkl)* node corresponds to $I(hkl)=|F(hkl)|^2$. Thus the information about the position of atoms within the unit cell is distributed in the structure factors of the different Bragg peaks on the nodes of the reciprocal lattice. Solving and refining a structure is possible through the measurement of the position and intensities of the Bragg peaks.

There are different techniques to perform X-ray diffraction measurements.[147] Monochromatic X-ray radiation on a single crystal requires to mount it on a goniometer. During small rotation of the sample (≈1°), different Bragg peaks cross the Ewald sphere, i.e. when $\vec{Q} = h\vec{a}^*+k\vec{b}^*+l\vec{c}^* = \overrightarrow{k_d}-\overrightarrow{k_i}$ and X-rays are scattered along different directions $\vec{Q}$ and collected on a 2D detector. The images measured with 1° step are converted into a three-dimensional model of the diffracted intensity on the nodes of the reciprocal lattice $I(\vec{Q})=I(hkl)$. Then, a three-dimensional map of the scattering atoms is obtained by comparing calculated intensities for a given structure to the measured ones. This is made possible with different software's like SHELX[152] or JANA.[153] Solving the structure of a molecular crystal, made of 100 independent atoms in the unit cell for example, means finding 9 parameters for each atom *j* in the unit: its coordinates x_j, y_j, z_j, cell and the 6 anisotropic thermal motion parameters. Accurate structures are obtained when thousands of Bragg peaks are collected. Extremely accurate data and analysis make it possible to obtain precise 3D electronic density.

When single crystals are too small, X-ray scattering can be collected from a powder, made of many and statistically disoriented small crystals. The resulting diffraction rings are converted in scattered intensity $I(|\vec{Q}|)$. If the data collection is simple, as with the Debye-Scherrer method, the structural and symmetry analysis is more difficult. Indeed, the diffracted intensity of some Bragg peaks with different $\vec{Q}$ but same $|\vec{Q}|$ superpose, even if these are not equivalent by symmetry.

Another option is to use the Laue technique, where a continuous radiation (white or pink beam, with continuous $|\vec{k}|$) impacts a stationary crystal. A set of diffracted beams are diffracted at different $\vec{Q}$ corresponding to different $|\vec{k}|$. Contrary to monochromatic measurements, where the diffracted beams intersect a single Ewald at $\overrightarrow{k_d}$, different (hkl) can cross the distribution of Ewald's spheres related to the distribution of $|\vec{k}|$ and collecting X-ray scattering

does not require a sample rotation. This technique is appropriate for biocrystals, made of large unit cells, as many nodes of the reciprocal lattice give rise to diffraction. Coppens and co-workers used this technique on molecular crystals for tracking diffracted intensity changes in the time domain (see § 5.2.2).

One problem for time-resolved photo-crystallography is the difficulty to achieve a homogeneous excitation of the molecular crystals. For single crystals the laser penetration depth may be smaller than the sample thickness, or it may depend on the sample orientation. For powdered samples, some grains may be more exposed to laser radiation than others. Finally, on long timescales the strains in the crystal induced by light can also broaden the Bragg peaks and this inhomogeneous structure makes the interpretation of intensity changes more difficult.

3.2.3 Symmetry and broken symmetry

Since the structure factor is written as the contribution of individual atoms within the unit cell, the symmetry existing in real-space translates into reciprocal space, as stated again by the Curie symmetry principle. The spatial distribution of atoms is associated with a spatial distribution of the electron density ρ(x, y, z), and therefore a spatial distribution of $f_j(Q)$. The diffraction pattern, which is the effect of X-ray scattering by atoms in a crystal, has the same (or a higher) symmetry than its cause. For example, when a 2-fold symmetry axis along $\vec{b}$ exists in the crystal structure, any spatial density ρ follows this symmetry ρ(x, y, z) = ρ(-x, y, -z). This gives the relationship between different structure factors *F(hkl) = F(-h k -l)*. The symmetry operators of the space group, which are relating the different symmetry-equivalent atomic positions in the unit cell, translates in the symmetry equivalence of the intensities of different Bragg peaks with different *(hkl)*. In addition, for specific symmetry operators including fractional translation (such as non-primitive unit cell or non-symmorphic symmetry elements like screw axes or glide planes), the intensity of some Bragg peaks vanishes by symmetry on specific nodes. For example, in the case of crystals with 2_1 screw axis along $\vec{b}$ the density follows ρ(x y z)=ρ(-x y+1/2 -z). Then their structure factors:

$$F(0k0) = 0 \text{ for } k = 2n + 1.$$

Ordering phenomena and more generally broken symmetry in chemistry, physics and materials science are responsible for the emergence of physical properties, such as ferromagnetism and ferroelectricity, for example. The ordering of groups of atoms in different electronic states is often associated with a structural reorganization sometimes manifested by the appearance of regular patterns in real-space, as is the case for charge-density waves (CDW), spin-density waves (SDW) or superconductors, for instance.

A phase transition between two phases of high and low symmetry is described in the generalized framework of the Landau theory of phase transitions through the evolution from the high symmetry space group.[154] In the high symmetry space group G_0, the density is totally symmetric and invariant under the symmetry operators of G_0. The electron density in this space group is the same for different positions (x,y,z) and (x',y',z') symmetry equivalent and therefore ρ_0 (x,y,z) =ρ_0(x',y',z'). When a phase transition drives the system to a lower symmetry phase, with space group G being a sub-group of G_0, Landau proposed to decompose the density observed in G as a sum of two components:

$$\rho = \rho_0 + \eta.\Delta\rho$$

ρ_0 is a totally symmetric spatial density described above with respect to the high-symmetry phase, $\Delta\rho$ describes the symmetry lowering of the density towards the low-symmetry phase. The deviation of the low symmetry phase from the high symmetry phase is measured by the amplitude of the order parameter η. In a crystal, the translation symmetry $\vec{T}$ on the lattice is written as

$$\vec{T} = m\vec{a} + n\vec{b} + p\vec{c} \text{ with m, n, p integers.}$$

Therefore $\rho_0(x, y, z) = \rho_0(x + m, y + n, z + p)$. There are many examples of molecular materials showing phase transitions associated with loss of translation symmetry.[155,156] Let us consider a system associated with a cell doubling along $\vec{c}$ axis. $\vec{c'}$=2$\vec{c}$ is the new translation vector along the direction $\vec{c}$ and we have to consider now the new lattice with translational symmetry

$$\vec{T'} = m\vec{a} + n\vec{b} + p\vec{c'}$$

where the density is invariant with $\vec{T'}$ and so $\rho_0(x, y, z) = \rho_0(x + m, y + n, z + p)$. However, the density is no more invariant with $\vec{c} = \frac{\vec{c'}}{2}$ in the low symmetry phase $\rho_0(x, y, z) \neq \rho_0(x + m, y + n, z + p + 1/2)$. Figure 7 illustrates schematically how the (electronic) density changes for a cell doubling: in the low symmetry phase the spatial density is modified with respect to the high symmetry. The doubling of the translational symmetry in real space gives rise to additional Bragg peaks: since $c'^* = \frac{1}{2}\, c^*$, the Bragg peaks of the low symmetry phase are located on the nodes of the lattice $\vec{Q} = h\overrightarrow{a^*} + k\overrightarrow{b^*} + (l + \frac{1}{2})\overrightarrow{c^*}$. Since h, k and l' are integers, the superstructure peaks appear at the boundaries of the Brillouin zone along c*.

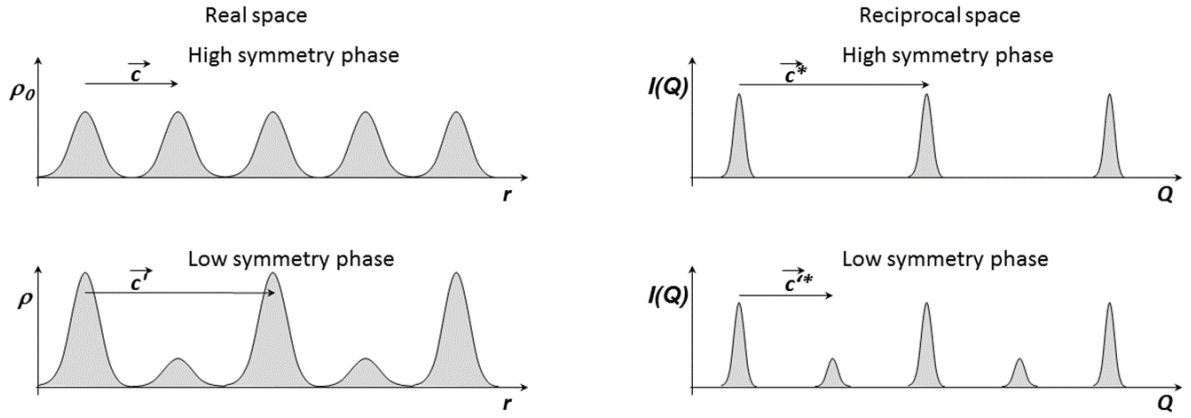

Figure 7: (left) Schematic representation of the structure factor on the crystalline sites, through the electronic density $\rho_0(r)$. In the high symmetry phase the crystal periodicity is $\vec{c}$. In the lower symmetry phase where a cell doubling occurs, the density $\rho(r)$ alternatively increases and decreases on the sites and the new perdiodicity is $2\vec{c}$. (Right) Corresponding diffracted intensity in the reciprocal space with periodicities $\vec{c}^*$ and $\vec{c}'^* = \frac{1}{2}\vec{c}^*$.

3.2.4 Local order and diffuse scattering

Molecular packing in crystals is not perfectly periodic: atoms move and molecular states may fluctuate in time and space. The instantaneous structure factor $F_m(\vec{Q})$ of a unit cell *m* at position $\vec{R}_m$ on the lattice, can be decomposed into two terms: the average value in space and time $< F(\vec{Q}) >$ of the crystal and the deviation $\Delta F_m(\vec{Q})$ of this unit cell m :

$$F_m(\vec{Q}) = < F(\vec{Q}) > + \Delta F_m(\vec{Q})$$

The X-ray scattering intensity by a crystal can then be decomposed in two terms:

$$I(\vec{Q}) = N^2 \left| \langle F(\vec{Q}) \rangle \right|^2 \sum_{h,k,l} \left| \delta(\vec{Q} - \vec{Q}_{hkl}) \right|^2 + N' \sum_{m} \langle \Delta F_n^*(\vec{Q}) \Delta F_{n+m}(\vec{Q}) \rangle \, e^{-i\vec{Q}.\vec{R}_m}$$

The first one is associated with the Bragg diffraction by the average 3D periodic crystalline structure (structure factor $< F(\vec{Q}) >$), which was described above and is located on the nodes $\vec{Q}_{hkl}$ of the reciprocal lattice. The second term is the diffuse scattering, which is more or less spread out within the reciprocal space, depending on the spatial extension of the local deviations $\Delta F_m(\vec{Q})$ over the different cells m. This diffuse scattering is located in the reciprocal space on the Fourier-transforms of the spatial correlations function of $\Delta F_m(\vec{Q})$. Figure 8 shows how correlations extending only along a single direction ($\vec{a}$, 1D correlation) modulate the intensity of the diffuse scattering in the reciprocal space located in planes perpendicular to $\vec{a}$. If $\vec{R}_m = n\vec{a}$ the diffuse scattering is observed around $\vec{Q}$ with h integer.[157,158] If $\vec{R}_m = 2n\vec{a}$ the diffuse scattering is observed $\vec{Q}$ with coordinates h=n+1/2. The spatial extension of the correlation along $\vec{a}$, the correlation length ξ, is inverse proportional to the width of the diffuse planes along $\vec{a}$.

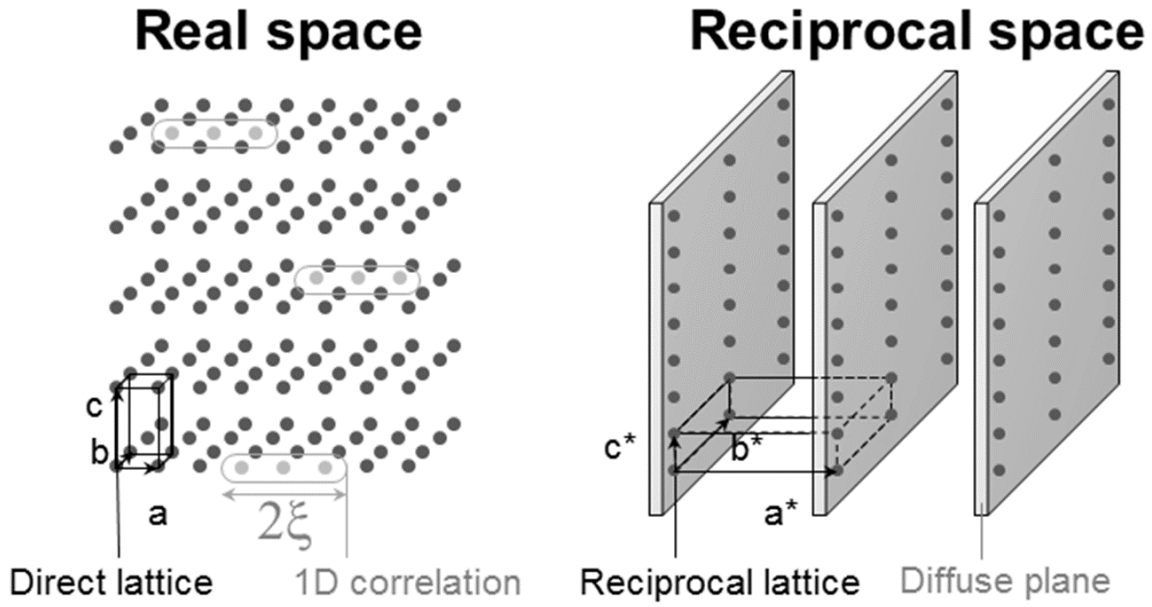

Figure 8: (left) Schematic crystalline structure with an average structure factor *F* (black spheres in real space) repeating on a 3D periodic lattice, resulting in X-ray diffraction at the node of the reciprocal space (spheres, right). Fluctuation of the structure factor modifies the diffraction pattern and when local deviations (grey spheres) extend along one direction with a characteristic correlation length ξ, diffuse planes are observed (light grey, right).

4. Structural dynamics of transition metal complexes in solution

Most of this section will be devoted to transition metal (TM) complexes because they have been and still are the most commonly investigated molecular systems by time resolved hard X-ray methods. Indeed, the presence of heavy elements (the metal atom) makes the use of hard X-ray for spectroscopic studies (XAS, XES, RIXS) necessary, but also an advantage as there is no need for vacuum. At the same time, these elements have large scattering cross-section making them also preferable for XRS or XRD.

Photoexcitation of a TM complex in solution triggers a wide range of phenomena that include: intramolecular electronic-vibrational relaxation, spin transitions, bond breaking and forming, reactivity with the solvent species, solvation dynamics, etc., all of which bear electronic and structural signatures. In the following, we will dwell with examples of systems that have been carried out using the methods described in §§ 3. Whenever possible, emphasis will be placed on those processes and phenomena that have been simultaneously investigated using both X-ray scattering and X-ray spectroscopic methods.

4.1 Intramolecular Charge Transfer

Photoinduced electron transfer (ET) is among the most common process in metal-based molecular complexes, and its understanding is essential for efficient storage and conversion of solar energy into chemical or electrical energy. The doorway to these processes are often the metal-to-ligand-charge-transfer (MLCT) or Ligand-to-metal-charge-transfer (LMCT) states, whose absorption bands dominate the visible spectrum. Because of the intramolecular charge transfer, there is significant change of the electronic structure of the constituents of the molecule, especially, the metal atom that becomes oxidised or reduced. This clearcut (from the point of X-ray spectroscopy) change is the reason why these processes were the first to be investigated by time-resolved X-ray absorption spectroscopy. Indeed, the first example of the sort was a XAS study with 70 ps time resolution at the Ru $L_{2,3}$-edge of the photoexcited aqueous Ruthenium(II)-tris-2,2'-bipyridine ($[Ru^{II}(bpy)_3]$).[91,159] In the ground state spectrum of the complex, the predominantly octahedral field of the complex splits the d-orbitals into a lower t_{2g} orbital and an upper e_g orbital (Figure 9 left). All six 4d electrons of Ru^{2+} are in the lower t_{2g} orbital while the e_g orbital is empty. Upon excitation of the ^{1}MLCT state, an electron is transferred from the metal t_{2g} orbital to the bpy ligand, populating the long-lived (~600 ns) ^{3}MLCT state[160] and opening up a new channel for a (2p-4d(t_{2g})) core transition. In refs [91,159], all the features of the electronic structure changes were observed: i) the blue shift of the 2p-4d(e_g) transition due to

the oxidation state change from Ru^{2+} to Ru^{3+}; ii) the appearance of a new resonance at the 2p-4d(t_{2g}) transition, due to the hole created in the t_{2g} orbital. These features were analysed by the ligand field multiplet theory,[159] in very good agreement with the experimental data. From the change of ligand field splitting between ground and excited state and using an electrostatic model that relates the octahedral ligand field splitting to the metal-ligand distance,[161] a Ru-N bond contraction of ~0.02 Å in the excited state was derived, while the analysis of the EXAFS region[122] delivers a value of the Ru-N bond contraction of ~0.04 Å, treating all Ru-N distances equally (i.e., in D_3 symmetry). These were later further supported by the analysis of the XANES.[162] These results are in line with the low temperature spectroscopic studies of the MLCT state.[163] These results about the excited state structure are confirmed by Quantum chemical calculations.[164,165] Later, several picosecond Ru L- and K-edge studies upon excitation of the ^{1}MLCT state of different Ru polypyridyl complexes reported similar trends.[166-170]

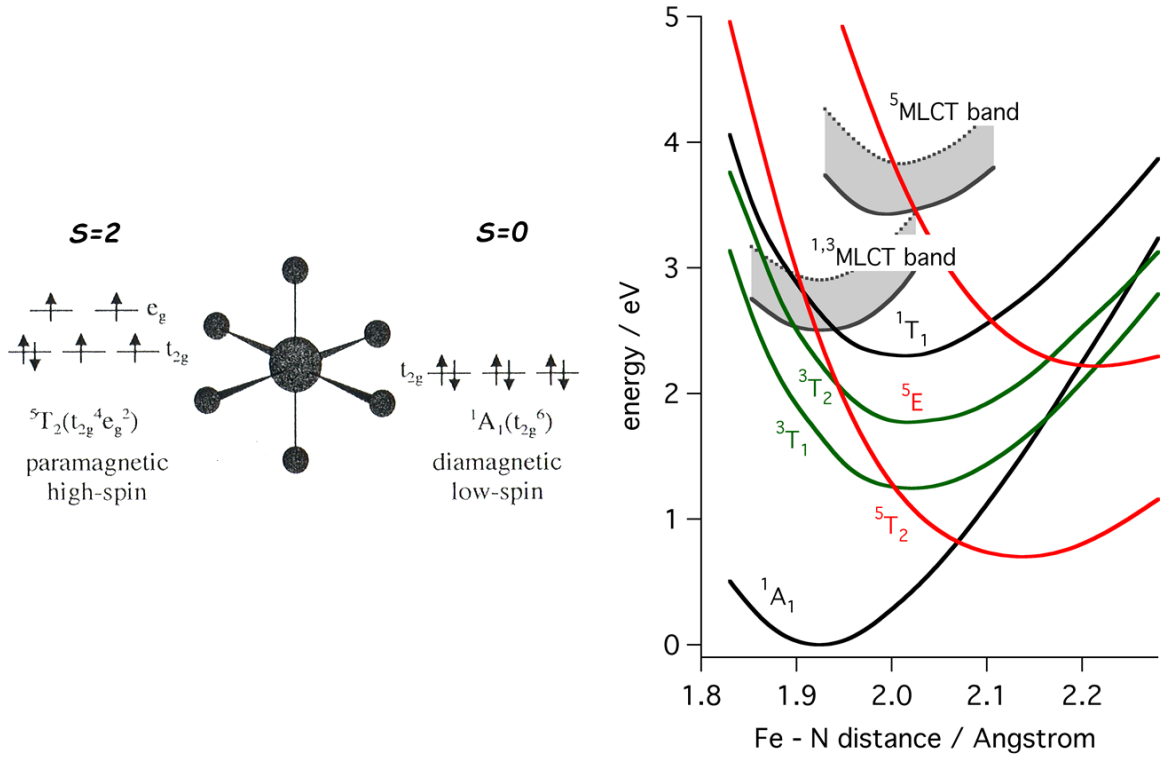

Figure 9: (left) Representation of the occupancy of ligand-filed split d-orbitals for a d^6 octahedral complex. (right) Schematic potential curves of [$Fe^{II}(bpy)_3$] along the Fe-N bond. Reprinted with permission from ref. [171]. Copyright 2010 John Wiley and Sons.

More significant in terms of dramatic nuclear structure changes upon a photoinduced intramolecular CT is the case of Cu(I)-diimine complexes. Indeed, upon transfer of an electron to the ligand, a significant structural change from a tetrahedral geometry to a flat one occurs (Figure 10a). Chen and co-workers[172-174] investigated the structure of the MLCT states of such complexes, in particular ([$CuI(dmp)_2$]$^+$ (dmp=2,9-dimethyl-1,10-phenanthroline)), by ps XAS. Upon 400 nm photoexcitation, one reaches the S_2 state, which decays on an ultrafast time scale to the S_1 state[172,175-177] followed by relaxation to the T_1 state. Chen and co-workers observed the photoinduced electronic and structural changes by ps XANES and EXAFS and concluded that: (i) the excitation of the MLCT state induces an electronic configuration change from Cu^I ($3d^{10}$) to Cu^{II} ($3d^9$); (ii) the inner-sphere reorganization changes the coordination number of the MLCT state from four to five in toluene, which is presumed to be non-coordinating; (iii) the average Cu-ligand bond lengths increased in the MLCT state in toluene, but decreased in acetonitrile, reflecting the difference in the interactions of the copper with the fifth ligand. The conclusion of solvent coordination was supported by simulations of the XANES spectra.[178]

An interesting question that arises in certain complexes, with strong mixing of metal-halogen orbitals, such as halogenated Rhenium ones, is the issue of the charge transfer from the metal to the ligand, do the halogen orbitals also take part in the electronic rearrangement? While time-resolved Raman and IR data do point to it being the case,[179 180], a direct proofs of a 2-centre electron transfer has been lacking. With the unambiguous sensitivity of XAS to oxidation states, the Chergui group confirmed the scenario of electron density being transferred from both the halogen and the Rhenium atom to the bpy ligand in the case of Rhenium-halogen carbonyl polypyridine complexes.[181] The experiment was carried out with 70 ps resolution and fs experiments or maybe also attosecond ones, are needed to demonstrate if the process is simultaneous or sequential.

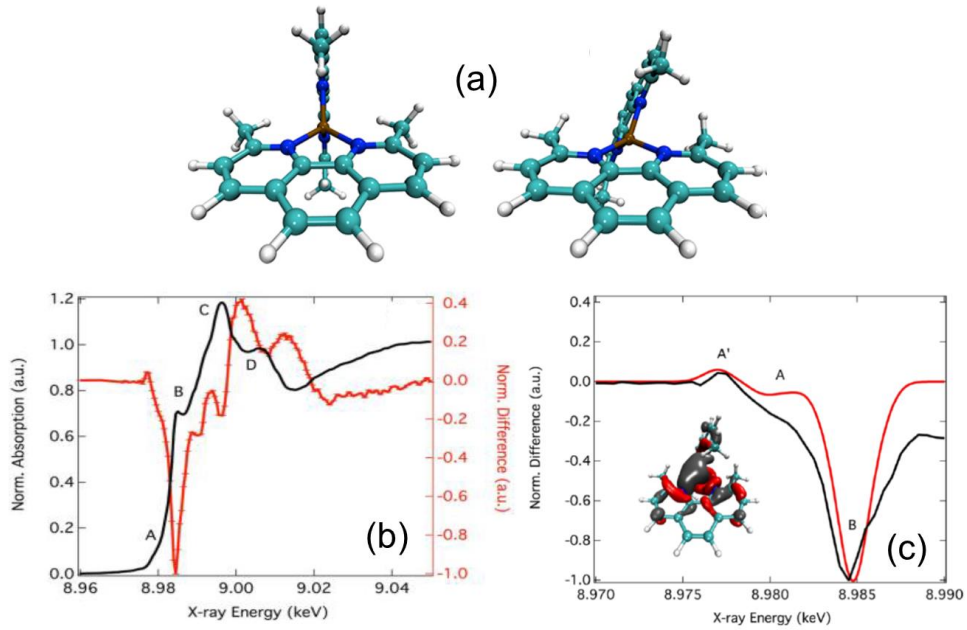

Figure 10: (a) ground state structure (left) and ^{3}MLCT excited state structure (right) of $[Cu(dmp)_2]^+$. An acetonitrile molecule pointing towards the Cu atom is added on top of the molecule. (b) static (black) and transient Cu K-edge spectrum of the molecule recorded at 50 ps time delay. (c) Simulated pre-edge transient spectrum (red, singlet minus triplet) using TD-DFT in comparison with the experimental transient (black). Inset is the molecular orbital for the transitions with the largest oscillator strengths for A′. Reprinted with permission from Reference [182]. Copyright 2013 American Chemical Society.

The issue of solvent coordination dates back to the works of McMillin and co-workers who studied the luminescence lifetimes of such complexes and found it to be significantly shortened in donating solvents (i.e., those behaving as Lewis bases), such as acetonitrile (MeCN), compared to non-donating solvents, such as dichloromethane (DCM) that showed one to 2 orders of magnitude longer lifetimes (~100 ns).[183] They attributed this quenching to complexation of a solvent molecule, most likely at the metal centre of the molecule. In order to further investigate this hypothesis, the Chergui group undertook a ps XAS study of $[Cu(dmp)_2]^+$ in MeCN and DCM along with optical and theoretical studies.[182,184,185]

Figure 10b (black line) shows the steady-state Cu K-edge XANES of the complex in MeCN. The weak A feature just below 8.98 keV is a quadrupole 1s-3d pre-edge transition but it also contains a ligand contribution, as explained below. The B band is assigned to the 1s→4p transition. The C and D features are above-ionization potential (IP) XANES features, due to multiple scattering. The transient signal in MeCN at a time delay of 50 ps for $[Cu(dmp)_2]^+$ solvated is also shown in Figure 10b. A weak positive feature appears near the position of the A due to the hole that is created in the highest occupied molecular orbital (HOMO) by photoexcitation.[186] At higher energies there are strong negative and positive features in the region of the B to D features. Also, the transients turned out to be very similar MeCN and DCM. In fact, the intensity loss of the B feature, which was taken as evidence of exciplex formation,[177,178] can simply be explained in terms of the oxidation shift of the system from Cu(I) to Cu(II),[182] as in the case of Ruthenium complexes discussed above.

In ref. [182], the A and B features of the ground state spectrum were analyzed using TD-DFT. The A feature is dominated by transitions into the lowest unoccupied molecular orbital (LUMO) and LUMO+1 orbitals. These are mainly (~97%) comprised of electron density located on the ligand atoms, which explains its weak intensity, as this transition draws its oscillator strength via a weak mixing with the Cu 4p orbitals. In contrast, the B feature corresponds to excitations into molecular orbitals and due to their proximity to the continuum, they are rather diffuse, but this feature contains a larger 4p (dipole-allowed) contribution. Figure 10c compares the pre-edge experimental transient at 50 ps and results of the TD-DFT calculated difference spectrum of the triplet electronic structure minus the ground-state spectrum. The features present in the experimental transient are reproduced both in terms of energy and relative intensity. In particular, the new (positive) A′ feature arises, as expected, from a transition into the electron hole at the HOMO created by photoexcitation. Since the HOMO is dominated by the Cu 3d-character,[182] this feature has previously been attributed to a 1s→3d quadrupole transition.[186] The lack of solvent coordination

was supported by calculations of the radial distribution functions (RDFs) from a classical molecular dynamics simulation for both the ground and lowest ^{3}MLCT states of the complex in both solvents. Further support came from a QM/MM simulation, showing that no bound exciplex forms between the solvent molecules and the complex. Rather, the solvent-dependent lifetimes of $[Cu(dmp)_2]^+$ were rationalized in terms of the energy gap between the ground and ^{3}MLCT states.[182] The lifetime also depends on the spin−orbit-coupling, which itself is affected by the dihedral angle, and on the energy gap between the ^{1}MLCT and ^{3}MLCT states.

This system turned out to be an ideal one to investigate the correlated charge, nuclear and spin dynamics in TM complexes. Indeed, ultrafast optical studies by the Tahara group have revealed a rich vibrational wave packet pattern upon excitation of the singlet MLCT state.[187,188] In this respect, Tavernelli and co-workers have carried detailed quantum dynamical[184] and wave packet dynamics simulations[185] that could be translated into fs XAS signals for future XFEL experiments.

4.2 Photoinduced spin cross-over dynamics

One of the fascinating features of Fe^{2+}-, Fe^{3+}- and Co^{2+}-based molecular complexes is their ability to change from the low (LS) to the high (HS) spin state at thermal equilibrium under the effect of temperature, pressure or irradiation, and have for that matter been named spin cross-over complexes (SCO).[189,190] The light induced SCO has been coined Light-Induced Excited Spin-State Trapping (LIESST),[191] and the HS to LS process, reverse-LIESST.[192] These dramatic (ΔS=2) spin transitions are interesting for applications in magnetic data storage/optical reading but also of direct relevance to biology, since the active site of hemoproteins are Fe(II)- or Co(II)-based porphyrins that undergo similar spin change during their biological functions (see § 6).

In the predominantly octahedral field due to the ligands (Figure 9), all electrons are in the lower t_{2g} sub-shell in the low spin (LS) ground state, while transferring electrons to the e_g orbitals increases the spin state. Because the e_g orbitals derive from the d_{x2-y2} and d_{z2} orbitals, they are antibonding in 6-fold coordinated complexes, which leads to a striking metal-ligand bond elongation in the high spin (HS) state. Studies of the LS to HS photoswitching were intensely carried out in solution using optical methods. McGarvey and Lawthers reported that the equilibrium between the spin states of iron(II) spin-crossover complexes in solution near RT can be photophysically perturbed via irradiation into the strong spin and parity allowed metal-ligand charge transfer (^{1}MLCT) absorption bands of the low-spin (LS) species.[193] The intersystem crossing (ISC) dynamics was then explored with the use of complementary probes, sensitive to different degrees of freedom, which strongly help investigating both ultrafast electronic and structural dynamics.[97,113,192,194-198]

A generic diagram of the potential energy curves of the various states of Fe(II)-based complexes is shown in Figure 9, as a function of the Fe-N bond length, which is supposed to be the reactive coordinate of the spin transition.[171] The MLCT states have nearly the same equilibrium distance as the ground state, in agreement with the results on Ru(II) complexes discussed above,[159] while the ligand field states ^{1,3}T, ^{5}T and ^{5}E have their equilibrium distances elongated by ~0.1 Å, ~0.2 Å, and ~0.3 Å, respectively, relative to the ground state bond distance. Light excitation into the singlet Metal-to-Ligand-Charge-Transfer (^{1}MLCT) state or to the lower-lying ligand field states leads to population of the lowest quintet state $^5T_2$ with unity quantum yield.[189] The lifetime of the latter varies by several orders of magnitude as a function of ligand and temperature[189] with $[Fe^{II}(bpy)_3]$ having the shortest lived quintet state lifetime (650 ps) at RT. Structural studies by X-ray diffraction or X-ray absorption spectroscopy under quasi steady-state conditions, confirmed the ~0.2 Å elongation of the Fe-N bond for Fe(II)-based complexes with long-lived HS states[199-201] but the question arose if this applies to the shortest lived HS state of $[Fe^{II}(bpy)_3]$, as predicted by theory.[202]

Khalil et al[203] and Gawelda et al[96] captured the structure of the quintet state after laser excitation using 70 ps hard X-ray pulses probing the structure changes at the K edge of Iron. In the first case, the system was $[Fe^{II}(tren(py))_3]$ in acetonitrile, which has a quintet state lifetime of 60 ns, while in the second case, it was $[Fe^{II}(bpy)_3]$, onto which we hereafter focus our discussion as this system has emerged as the test bed for all new ultrafast X-ray methods on molecular systems. Figure 11 shows the Fe K-edge XANES of the molecule in the LS ground state (a), the transient (difference) spectrum at 50 ps time delay (b) and the XAS spectrum of the HS quintet state (a), as retrieved from the ground state and the difference spectra and from the photolysis yield determined in laser-only experiments (and convoluted to match the much longer x-ray probe width). The structural analysis of the excited state was based on fitting both the transient XANES[96] and the transient EXAFS spectra.[62,204] These confirmed that the Fe-N bond elongation is ΔR_{Fe-N}=0.20 Å, and is nearly the same in the HS state of all Fe(II) complexes, regardless of the HS lifetime,[199,203] implying that the latter is not determined by the Fe-N bond distance. Rather, the adiabatic energy and the coupling parameters between LS and HS state are the crucial parameters. Indeed, of all Fe(II)-SCO complexes, $[Fe^{II}(bpy)_3]$ has the highest lying quintet state and as a matter of fact, the shortest HS lifetime.

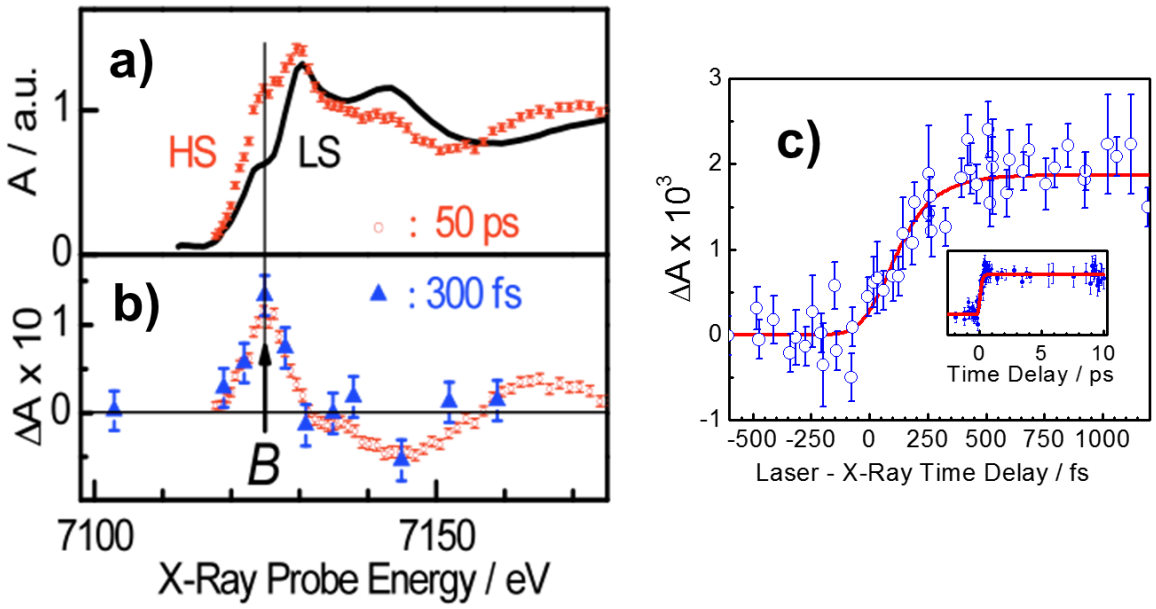

Figure 11: (a) static (black) Fe K-edge absorption spectrum of $[Fe^{II}(bpy)_3]$ and the spectrum in the high spin state (red data points) at 50 ps time delay, retrieved using the transient (red) in (b) and the ground state spectrum. (b) Fe K-edge transient at 50 ps time delay (red data points) and at 300 fs time delay (blue triangles) measured using the slicing source at the Swiss Light Source. (c) time scans at the B-feature. The inset shows a time scan up to 10 ps. Reprinted with permission from Reference [113]. Copyright 2017 The American Association for the Advancement of Science.

In the above studies using Fe K-edge spectroscopy,[96,203] information about the electronic structure was contained in the pre-edge region which is characterized by weak 1s-3d transitions. The Fe $L_{2,3}$-edges are more advantageous in this respect because the 2p-3d transitions are dipole allowed and the core-hole lifetime broadening is smaller, which makes the spectral lines narrower. Huse et al[101] carried out a picosecond L-edge spectroscopic study of $[Fe^{II}(tren(py))_3]$ for the first time, using a liquid cell equipped with SiN membrane windows. Their results showed a significant reduction in orbital overlap between the central Fe(3d) and the ligand N(2p) orbitals, consistent with the expected ~0.2 Å increase in Fe-N bond length upon formation of the high-spin state. Another important development came with the first implementation of a ps X-ray emission spectroscopy measurements on $[Fe^{II}(bpy)_3]$, fully demonstrating the power of XES to identify spin states of metal complexes.[205] Because XES uses a single incident energy, it is a technique that can be combined with X-ray scattering (XRS) in solutions. This unique combination of techniques was demonstrated by Bressler and co-workers, allowing them to correlate the formation of the HS state with changes in the surrounding solvent, as discussed in § 4.4 below.[106,206] These exciting developments also prepared the ground for the femtosecond experiments at XFELs.

Indeed, femtosecond resolution is needed if one wants to follow the ultrafast structural dynamics of photo-excited systems in real-time, and thus answer a host of questions that have escaped femtosecond optical spectroscopies or ps XAS. In particular, the mechanism and relaxation pathways of the photo-induced HS-LS conversion in Fe(II) complexes were still unknown until a few years back.[189,207,208] One of the reasons for this situation was the fact that the intermediate $^{1,3}T$ states (Figure 10) are optically silent, while the HS quintet state had no known spectroscopic signature in the visible. Although it was established[96] that departure from the ^{3}MLCT state occurs in ~130 fs, the population time of the HS state needed to be measured directly. To that purpose, the Chergui group[113] exploited the fact that the XANES spectrum contains a marker of the HS state, via the multiple-scattering[209] B-feature that appears on the edge and increases in intensity upon elongation of the Fe-N bond in the HS state (Figure 11). Using hard X-ray fs pulses generated by the slicing scheme at the SLS, the evolution of the B-feature could be probed as a function of pump-probe delay,[113] and a population time of the HS state of 150±50 fs was measured (Figure 11).

Soon after, the same group developed and used broad-band deep-Ultraviolet (UV) spectroscopic observables of the HS state, confirming this population time.[97,195]

Further studies were performed using fs soft X-ray pulses from the slicing source at the ALS to probe the Fe $L_{2,3}$-edges transient absorption.[210] This first femtosecond soft X-ray experiment of a molecular system in solution confirmed the findings of the fs hard X-ray[113] and the deep-UV[195] studies. When the LCLS XFEL came into operation, the fs hard X-ray absorption experiment was repeated, yielding the same result[211] but with a much reduced data acquisition time due to the orders of magnitude larger flux compared to the slicing scheme. Finally, more recently, several new fs X-ray studies on SCO complexes have been carried out in the solid phase, which are discussed in §5.

The above studies, while revealing a remarkably fast SCO for the first time, left a question open as to the pathway leading from the ^{1}MLCT state to the HS state and whether it bypasses the intermediate ^{1,3}T states (Figure 11) or not. In ref. [113], this option was considered and it was suggested that if this were to be the case, then the transit time via the intermediate states would have to be <60 fs. To verify the hypothesis of intermediate states, having different spin and/or oxidation states, XES is ideal as discussed in § 3.1.2.[212] Building on the experience from ps XES experiments,[106,205,206] the first study of this sort in the femtosecond time domain was carried by Zhang et al[197] on photoexcited $[Fe^{II}(bpy)_3]$ in solution. The time-resolved K_β fluorescence spectra provided the sensitivity to spin dynamics needed to address the above question. Figure 12 shows the transient XES at 50 fs and 1 ps time delay. In this figure, the identification of the quintet state is straightforward using the K_β fluorescence spectrum. The significant difference between the spectra in Figures 12c and d suggests the presence of excited-state species other than the $^5T_2$ state. With kinetic modelling, the authors could distinguish between the ^{1,3}MLCT, ^{3}T and $^5T_2$ states in the relaxation cascade probed with K_β fluorescence. They thus concluded that the system goes via the intermediate ^{3}T state during the SCO dynamics. The resolution of the experiment (~125 fs) was however not sufficient to unambiguously identify the intermediate step, although the spectral signatures were clearly suggesting them. In order to address further this point, a transient deep-UV absorption study at high time resolution (<60 fs) was carried out,[198] concluding that the SCO is much faster (< 50 fs) than previously measured, and that the depopulation time of the MLCT state and the population time of the quintet state are the same. While this result still does not discard the passage via an intermediate state, it makes its transit time extremely short (< 20 fs).

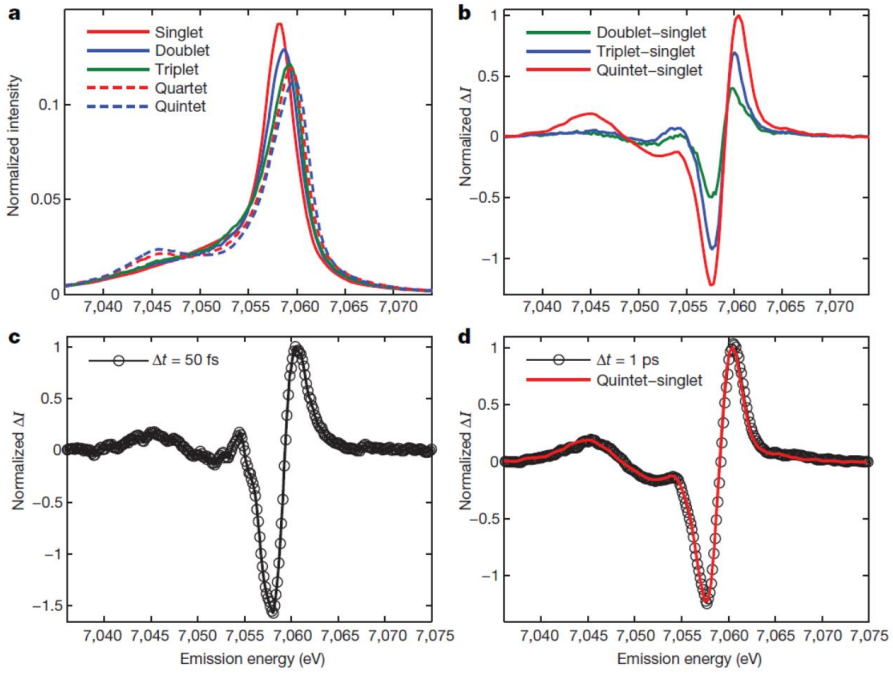

Figure 12: Spin-dependent iron Kβ fluorescence spectra: a) The Kβ fluorescence spectra of ground state model iron complexes with different spin moments: singlet ($[Fe(2,2'\text{-bipyridine})_3]^{2+}$, red), doublet ($[Fe(2,29\text{-bipyridine})_3]^{3+}$, blue), triplet (iron(II) phthalocyanine, green), quartet (iron(III) phthalocyanine chloride, red dashed), and quintet ($[Fe(phenanthroline)_2(NCS)_2]$, blue dashed); b) Model complex difference spectra for the ^{1,3}MLCT, ^{3}T and $^5T_2$ excited states constructed by subtracting the singlet model complex spectrum from the doublet, triplet and quintet model complex spectra shown in (a); c) Kβ transient difference spectra obtained at 50-fs time delay for $[Fe(2,2'\text{-bipyridine})_3]^{2+}$ (black circles). d) Kβ transient difference spectra obtained at 1-ps time delay for $[Fe(2,2'\text{-bipyridine})_3]^{2+}$ (black circles), which closely matches the model complex difference spectra (red) obtained when subtracting the singlet from the quintet spectra shown in a. Reprinted with permission from reference [197]. Copyright 2017 Nature Publishing Group.

More recently, Lemke, Cammarata et al used femtosecond XANES at the LCLS X-FEL to track electronic and structural change of $[Fe^{II}(bpy)_3]$ in solution and found that the HS state is populated within 120 fs and that the process is accompanied by the activation and damping of coherent vibrations.[213] This mode is associated with the totally symmetric Fe-ligand bond elongation during LS to HS conversion, which was previously reported by optical pump-probe spectroscopy.[195,198] This first example of coherent vibrational wave packet motion observed by ultrafast X-ray spectroscopy in the case of a molecule in solution is an exciting development and was soon followed by the demonstration of wave packets probed by ultrafast X-ray scattering in solution as described now.

Biasin et al[214] studied the structural dynamics upon SCO in photoexcited $[Co^{II}(terpy)_2]$ in an aqueous solution with femtosecond X-ray scattering at LCLS. Their analysis showed that photoexcitation leads to elongation of the Co-N bonds, followed by coherent Co-N bond length oscillations arising from the displacive excitation of a vibrational mode dominated by the symmetrical stretch of all six Co-N bonds (Figure 13). The mode has a period of 0.33 ps and decays on a sub-picosecond time scale. It was found that the equilibrium bond-elongated structure of the high spin state is established on a single-picosecond time scale and that this state has a lifetime of ~7 ps. This first demonstration of vibrational wave packets by fs XRS in solution opens the way to more systematic studies on molecular systems, as the tools are refined and the data treatment becomes more routine. Among these is the possibility to exploit the polarization properties of the pump and probe pulses as explored in a simulation by Penfold *et al* on a model system consisting of di-iodine in solution.[215]

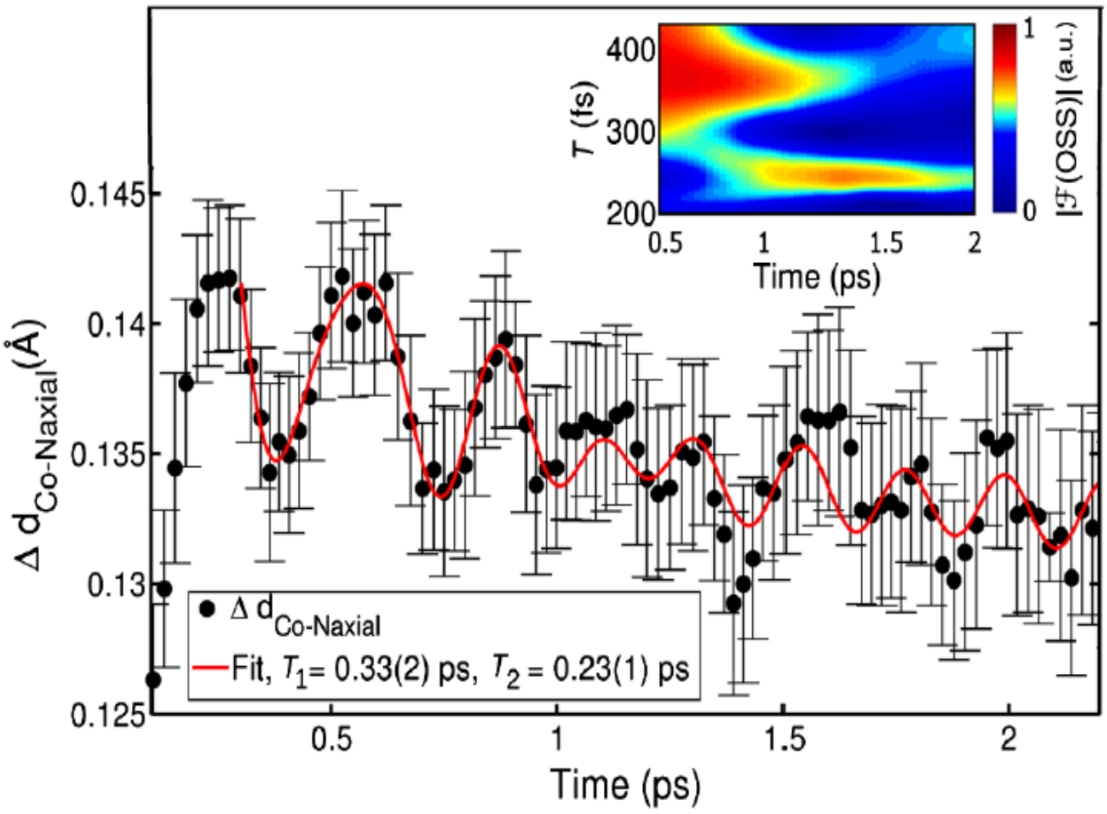

Figure 13: Femtosecond X-ray scattering of $[Co^{II}(bpy)_3]$. Time evolution of the Co-N bond lengths (black dots) retrieved from the fs XRS data. The insert shows a time-resolved Fourier transform of the oscillatory part of the difference scattering signal indicating sequential activation of two vibrational modes. The red line shows a heuristic fit, incorporating sequential activation of first a $T_1 \sim 0.33$ ps mode and then a $T_2 \sim 0.23$ ps mode identified as, respectively, breathing- and pincer-like by direct comparison with our DFT calculations. Reprinted with permission from reference [214]. Copyright 2017 American Physical Society.

Finally, a development worth mentioning is the recently demonstrated ability to record ultrafast XES with a table top plasma source. The experiment was carried out on $[Fe^{II}(bpy)_3]$ showing that the method is not limited to large scale installations.[216]

4.3 Bond forming dynamics

The triplet excited states of dinuclear d^8-d^8 platinum, rhodium, and iridium complexes (bridged by various ligands) exhibit remarkable photophysical and photochemical properties, which are strongly determined by their structure.[217] The unusually high photocatalytic activity of these complexes are a manifestation of the newly formed bond in the lowest excited singlet and triplet $^{1,3}A_{2u}$ states, owing to the promotion of an electron from the antibonding $d\sigma^*$ (d_z^2-derived) to the bonding $p\sigma$ (p_z-derived) orbitals, which should therefore lead to a contraction of the metal-metal bond (Figure 14).

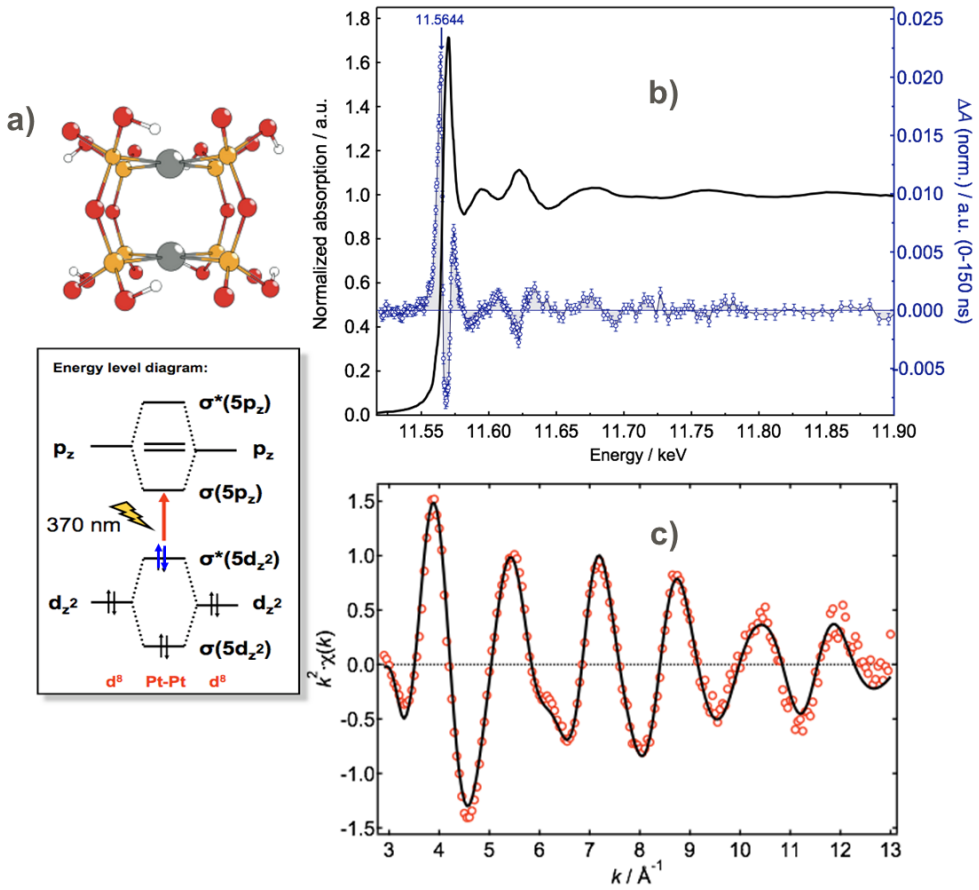

Figure 14: a) structure of the $[Pt_2(P_2O_5H_2)_4]^{4-}$ molecule and orbital scheme involving the excitation of a d to p orbital; b) Static Pt L_3 XAS spectrum of in solution (black line, left axis) and the transient (excited–unexcited) XAS spectrum (blue circles, right axis, same units as left) integrated up to 150 ns after excitation; c) Transient EXAFS data (circles; binned from the data in (b)) and best fit (solid line) with the following results: a Pt-Pt contraction of 0.31(5) Å, a platinum–ligand elongation of 0.010(6) Å. The error bars represent the standard error of the measurement. Courtesy of R. M. van der Veen.

The $[Pt_2(P_2O_5H_4]^{4-}$ (PtPOP) molecule is among the most intensely studied d^8-d^8 dinuclear metal complexes. In solutions, excitation into the first singlet state in the near UV region around 370 nm leads to formation of the long lived (~1 μs) triplet state with unity quantum yield. van der Veen et al[218] resolved its structure using picosecond XAS. Figure 14b shows the ground state Pt L_3-edge XAS spectrum (black trace) as well as the transient spectrum (blue dots), integrated from 0 to 150 ns to improve the signal-to-noise ratio. The XANES region exhibits a new absorption band at 11.564 keV below the absorption edge, which is due to the creation of a hole in the $5d\sigma^*$ orbital upon laser excitation, that can then be accessed from the $2p_{3/2}$ core orbital (L_3 edge).[219] Clear changes are also visible in the EXAFS region (Figure 14b,c), reflecting structural modifications between the ground and excited triplet states.

From the transient EXAFS spectrum (Figure 14c), the magnitude of the Pt-Pt bond contraction as well as, for the first time, the changes affecting the Pt-P bonds were extracted,[220] and the best fit is shown in Figure 14c. It was found that while the Pt-Pt bond contracts by 0.31(5) Å, in good agreement with the X-ray photocrystallography data (see below),[221] the Pt-P bonds slightly elongate (by ~20 mÅ), in agreement with theoretical predictions.[221] This work underscores the ability to retrieve details of the excited state structure of a rather complex molecular system in liquid solution, due to the high sensitivity of the experiment, coupled to a rigorous structural analysis based on fitting the transient EXAFS spectra directly in energy space.[204]

Soon after the above work, Christensen et al[222] reported a picosecond solution X-ray scattering study of the same system, deriving generally similar results as in ref. [220]: a Pt-Pt bond contraction of ~ 0.24 Å and a slight elongation of the Pt-P bond. This was followed by a ps XAS study on another diplatinum comple by Chen and co-workers,[223] who also showed bond formation in the excited state with a contraction of the Pt-Pt distance by ~ 0.2 Å.

PtPOP is a remarkable molecule in the sense that its ground and excited potentials are highly harmonic and that the optical spectrum is only sensitive to the Pt-Pt coordinate.[224,225] It is therefore easy to retrieve the excited state structure from a Franck-Condon analysis, which shows a Pt-Pt bond contraction in the triplet state 0.1 Å smaller than that derived by ps XAS.[218,220] The origin of the discrepancy lies, in the fact that the Pt atoms are directly exposed to the solvent and the EXAFS analysis neglected the contribution of the solvent, while the optical domain spectroscopy is not sensitive to it. This underscores the importance of including solvent contributions in the analysis of EXAFS and XANES, as was demonstrated in systematic quantum mechanics/molecular mechanics molecular dynamics simulations of PtPOP in three different solvents,[226] showing a clear solvent effect on the Pt L_3-edge spectra. This was also observed in an experimental XAS study of Rhenium-halogen carbonyl complexes showing a strong effect of the environment on the edge spectrum of the solvent-exposed halogen atom, while that of the central Re atom was unaffected.[181]

4.4 Solvation and its dynamics

Most of preparative and natural chemistry and all of biology take place in liquid solutions or in heterogeneous media, such as liquid-solid interfaces. In these cases, the solvent molecules are by no means spectators but they participate in the reactions in a variety of direct or indirect ways. From the outset, since a (photo)chemical implies rearrangement of electrons within the solute, a new field of forces is seen by the solvent molecules, to which they react in order to minimise the free energy of the system. This process, called solvation dynamics, implies rearrangements, which occur on time scales ranging from femtoseconds to much longer.

For many years, the understanding of the solvent response to photoinduced charge redistribution in solutes has been a major field of research in chemical physics, and even more so with the advent of femtosecond spectroscopy some 30 years ago.[31,227] However, all of these studies used optical probes, which do not deliver structure. Therefore, the structural dynamics of the solvation shell was mostly retrieved by simulations of the solute's observables. Furthermore, optical probes cannot distinguish the high frequency response of the solute from that of the solvent. Only in very few peculiar cases, could the response of the solvent directly be monitored by optical spectroscopy in real time, such as in condensed rare gas media or hydrogen,[228-232] but these are not common solvents.

The examples discussed in §§ 4.1 and 4.3 have already stressed the role of the solvents in probing photoinduced processes using X-ray spectroscopy and scattering. Early on, the Chergui group had proposed the study of solvation dynamics using atomic solutes whose electronic structure can be modified by an optical pump pulse, while the solvation shell changes would be monitored at core transitions of the solute, thus providing a direct visualization.[90] This experiment was then successfully carried out on aqueous iodide, both with ps and fs (using the slicing scheme) resolution, probing the Iodine L_1 and L_3 edges.[233,234] They could thus monitor the change from hydrophilic solvation (around iodide) to hydrophobic solvation (around iodine), which was supported by quantum and classical molecular dynamics simulations and DFT calculations.[234-236]

For more complex systems, advanced Hybrid DFT/classical or full ab-initio molecular dynamics simulations of the solvent effect on the excited state dynamics of systems such as $[Ru^{II}(bpy)_3]$,[237] or $[Fe^{II}(bpy)_3]$[238] were reported. With the advent of the high repetition rate scheme for ps experiments (§ 2.2.2), Bressler and co-workers[106,206,212] combined XES, XRS and XAS to observe the interplay between intramolecular dynamics and the intermolecular caging solvent response with 100 ps time resolution in the case of $[Fe^{II}(bpy)_3]$. On this time scale, the initial ultrafast spin transition and the associated intramolecular geometric structure changes, discussed in § 4.2, are long completed as well as the solvent heating due to the initial energy dissipation from the excited HS molecule. Combining information from XES and XRS, the excitation fraction as well as the temperature and density changes of the solvent were followed on the lifetime of the HS state (ca. 0.6 ps), allowing the detection of an ultrafast change in bulk solvent density. The correlation between these three signals is shown in Figure 15-I.

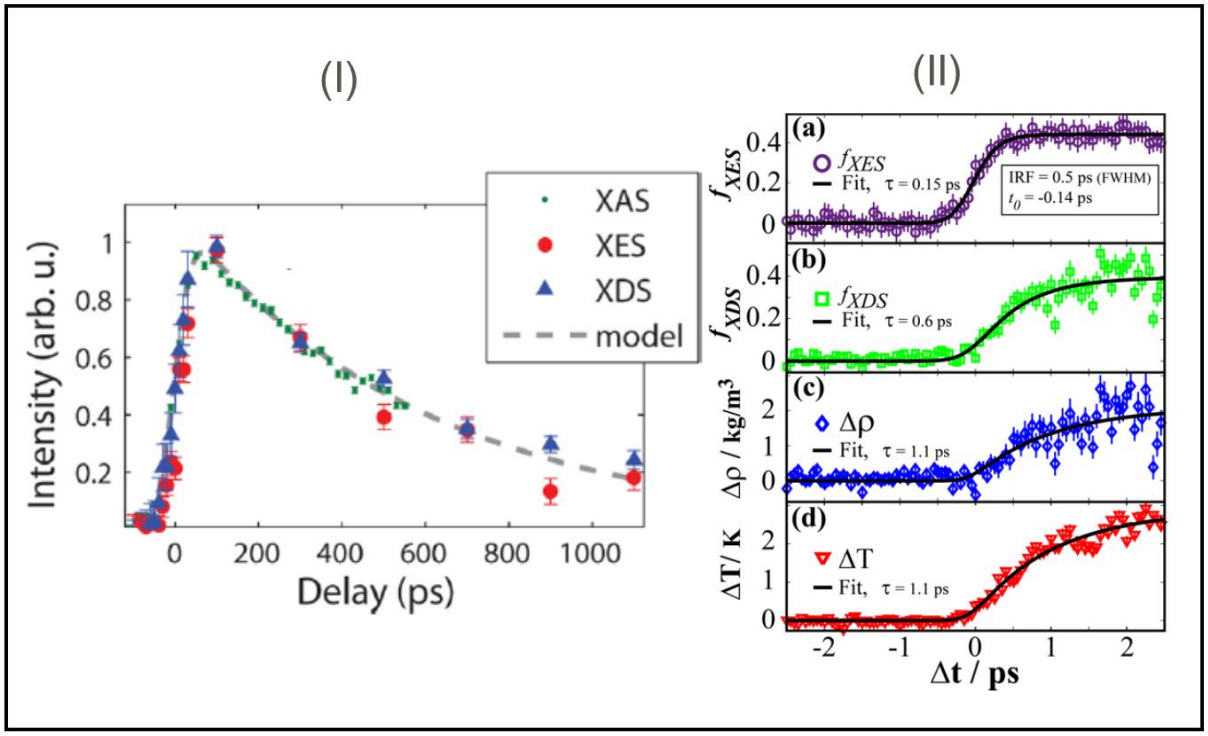

Figure 15: (I) ps resolved evolution of the HS fraction from XAS, XES, and XDS. The XAS data were taken in a separate measurement, while the XES and XRS data were taken simultaneously. Reproduced from ref. [206]. (II) (a) and (b) show the temporal evolution of the fraction of photoexcited solute molecules measured by XES and XRS, respectively. Black lines show fits of kinetic models as described in ref. [239]. The response from the formation of the HS state precedes the structural response, which in turn is faster than the solvent response summarized in (c) and (d). Reproduced from reference [239]. Copyright 2016 American Chemical Society.

An elegant analytical approach directly utilizing the spectroscopic data in the XDS analysis allowed the authors to extract information about the changes in the solvent cage and in particular, to deduce a decrease in the number of water molecules in the first solvation shell, as previously predicted by theory.[238] This type of studies sets a precedent for similar ones with fs resolution at XFELs. It is on sub-ps time scales that the solvent start to respond and monitoring its structural dynamics in real-time delivers invaluable insight into its role in the overall energy redistribution dynamics, as explored theoretically in simulations of fs-XRS of diatomic halogen molecules in solution.[215]

Very recently, a combined fs XRS and XES study of $[Fe^{II}(bpy)_3]$ was reported by Haldrup et al (Figure 15-II).[239] The simultaneously recorded X-ray diffuse scattering patterns reveal slower subpicosecond dynamics triggered by the intramolecular structural dynamics of the photoexcited solute. By simultaneous combination of both methods only, the authors extracted new information about the solvation dynamic processes unfolding during the first picosecond (ps). The measured bulk solvent density increase of 0.2% (Figure 15-II) indicates a dramatic change of the solvation shell around each photoexcited solute, confirming the above mentioned previous ab-initio molecular dynamics simulations.[238] Structural changes in the aqueous solvent associated with density and temperature changes occur with ~1 ps time constants, characteristic of the structural dynamics of water. The slower solvent response time scale allows direct observation of the structure of the excited solute molecules prior to when the solvent contributions become dominant.

4.5 Reactivity to solvent species

The simplest unimolecular reaction, the rupture of an interatomic bond, can become a complex process when the molecule is in a solvent. Indeed, the latter is not just a spectator but it influences the outcome of the reaction in different ways: (i) sterically by caging the fragments, in the so-called "cage effect"[240] or (ii) electronically by providing a field of forces that shifts in a differential way the potential surfaces onto which the dynamics occurs, thus modifying

the exit pathways of the fragments. As a consequence, this facilitates or hinders the release of fragments into the solvent depending on the solute-solvent interactions. Last, the nascent fragment may themselves undergo reactions with the solvent molecules, giving rise to new photoproducts.

Time-resolved X-ray tools provide a way not only to identify the outcome of the photoinduced process, but also to track down the intramolecular pathways leading to bond breaking, provided the temporal resolution is in the femtosecond range, as intramolecular processes are ultrafast in nature.[241]

As far as coordination chemistry complexes are concerned, so far only few examples are available. Furthermore, these examples involve dissociation of the parent molecule and substitution of a ligand by a solvent molecule. Basically only two cases, aqueous $Fe(CN)_6$ and $Fe(CO)_5$ in alcohols have so far been investigated by time-resolved X-ray spectroscopy.

Aqueous $Fe(CN)_6$: it had been found back in the 1970s that for the ferrous complex, the dominant photochemical channel was excitation wavelength dependent: predominantly photoionization for wavelengths < 300 nm and predominantly photoaquation for >300 nm, with a small yield of the other product in both cases.[242,243] For the ferric complex, the situation was less clear-cut. Finally, these optical domain experiments were carried out with 1 ns time resolution and they did not address the mechanisms yielding one or the other product. In order to confirm the photoaquation channel, Chergui and co-workers carried time-resolved XAS studies with 70 ps resolution using the high repetition rate data acquisition scheme described in § 2.1.2.2.[244] These studies also included the ferric complex. Upon 355 nm excitation, the transient spectra for both the ferrous and ferric complexes exhibit a red shift of the edge reflecting an increased electron density at the Fe atom. For the former (Figure 16a), an enhanced pre-edge transition was also observed. These observations reflect the formation of the aquated $[Fe(CN)_5OH_2]^{3+}$ species, which was supported by quantum chemical calculations that in addition, provided its structural parameters (Figure 16a). These first ps XAS studies allowed to establish observables of the aquated species, however because of the limited time resolution they do not deliver information about the mechanism leading to the aquated products. It is not clear if the dissociation of a CN ligand and the binding of a solvent molecule are sequential or concerted. Steady-state Fe L-edge spectra,[245] and Fe K-edge RIXS and XES of the complex in water and ethylene glycol[246] revealed the existence of specific interactions of the solvent molecules with the solute, but the connection to reactivity is still awaiting further studies at high temporal resolution. The results for the ferric complex are shown in Figure 16b, showing a much noisier transient due to the much lower yield for photoaquation.

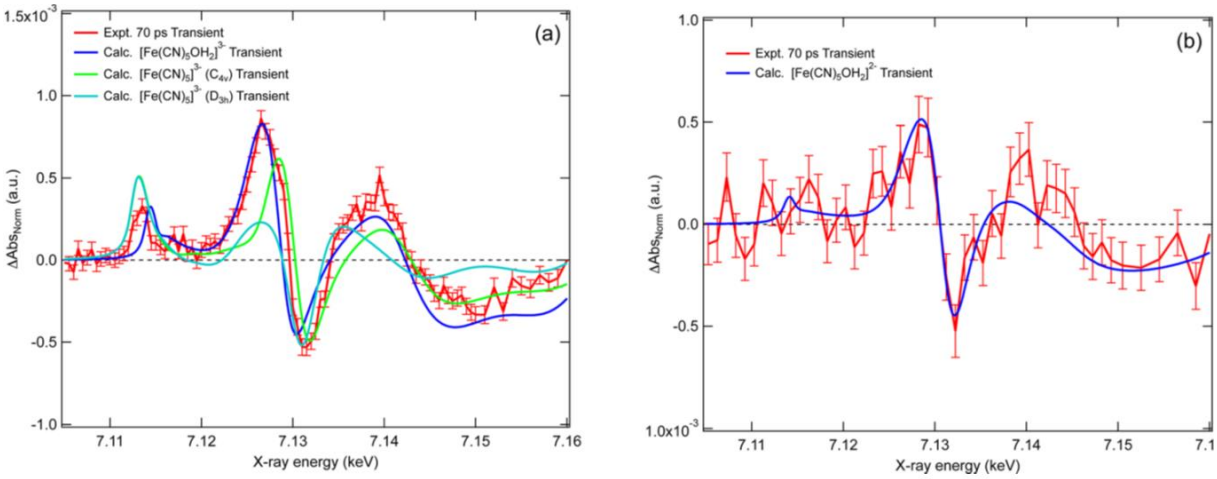

Figure 16: (a) The experimental (red) 70 ps after 355 nm photoexcitation of $[Fe(CN)_6]^{4-}$ and calculated transient spectra of $[Fe(CN)_5]^{3-}$, C_{4v} (green) or D_{3h} (cyan), and $[Fe(CN)_5OH_2]^{3-}$ (dark blue); (b) The experimental transient (red) 70 ps after photoexcitation of $[Fe(CN)_6]^{3-}$ at 355 nm and calculated transient spectra of $[Fe(CN)_5OH_2]^{2-}$ (blue). Reproduced from reference [244]. Copyright 2014 American Crystallographic Association.

$Fe(CO)_5$: In the gas phase, absorption of a 266 nm photon leads to a primary dissociation step of one CO with a quantum yield close to unity.[247,248] $Fe(CO)_4$ then undergoes further fragmentation with a high quantum yield.[248] In solution, depending on the excitation wavelength and the solvent, sequential dissociation can be suppressed,[249,250] though not completely eliminated.[251,252] It is well known that singlet $Fe(CO)_4$ is highly reactive and capable of ligand addition with a number of common organic compounds: alkanes, alkenes, alcohols, alkylphosphines, and alkylsilanes.[251-255] This reactivity arises from the electron deficiency at the metal centre of $Fe(CO)_4$ and the lack of steric hindrance with the solvent, making it a strong electrophile.

Questions arise as to the mechanism of reaction and how the solution affects the excited-state relaxation pathways in $Fe(CO)_5$ and $Fe(CO)_4$. An important aspect of the reactivity of the latter relates to its spin state.[252,253] Using time-resolved Fe K-edge X-ray absorption spectroscopy with a plasma source, Ahr et al[256] investigated $Fe(CO)_5$

photodissociation in ethanol and concluded that due to electronic interaction with the solvent molecules, the removal of CO and the addition of EtOH were concerted processes, although the $Fe(CO)_4EtOH$ product was not resolved directly. Their model was based on the argument that in solution a weak $Fe(CO)_5$-EtOH complex is formed in the ground state.[257]

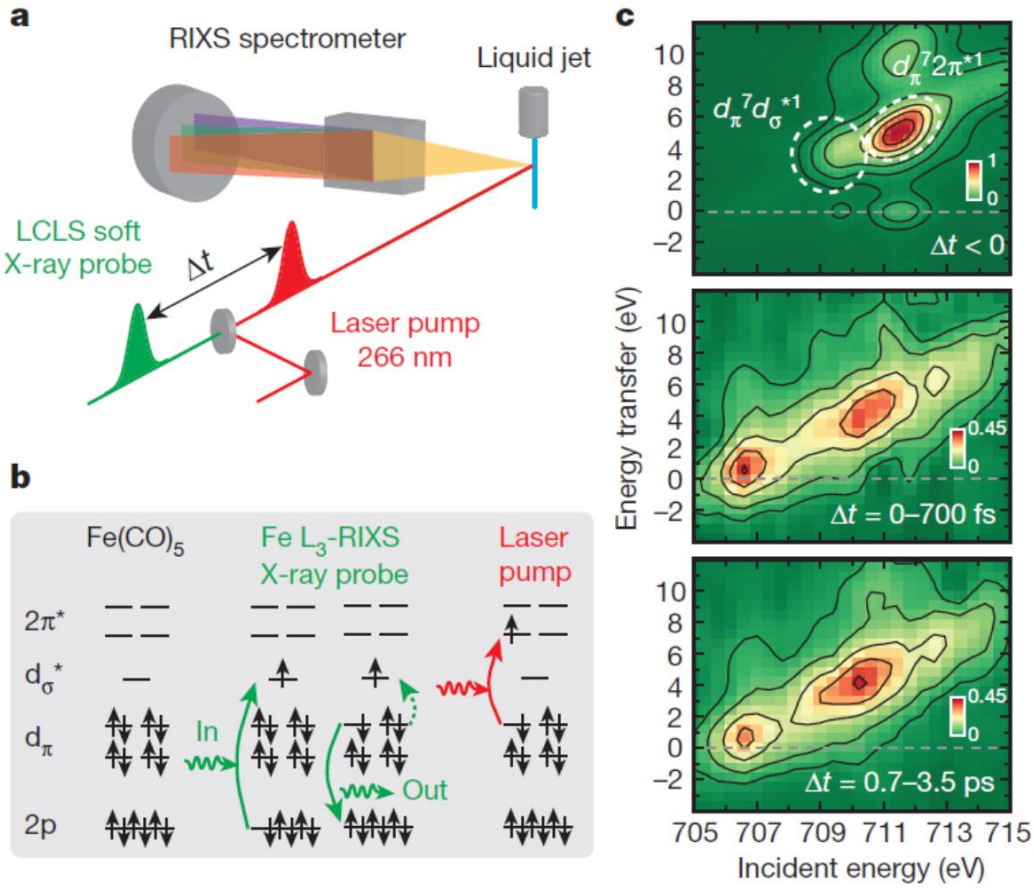

Figure 17: Scheme and results of the fs RIXS experiment on $Fe(CO)_5$ in solution: a) Scheme with optical-laser pump and soft X-ray probe. The intensity of RIXS is measured at the Fe L_3-absorption edge with a dispersive grating spectrometer; b) Electron configuration of ground-state $Fe(CO)_5$ with single electron transitions of X-ray probe and laser-pump processes (orbital assignments according to Fe 2p and 3d or ligand 2p character and according to symmetry along the Fe–CO bonds; the asterisk marks antibonding orbitals). RIXS at the Fe L_3-absorption edge with 2p-dσ* excitation involves scattering to final dp-dσ* ligand-field excited states. Optical dπ-2π* excitation triggers dissociation; c) Measured Fe L_3-RIXS intensities (encoded in colour) versus energy transfer and incident photon energy. Top: ground-state $Fe(CO)_5$ (negative delays, probe before pump). Middle and bottom: difference intensities for delay intervals of 0–700 fs and 0.7–3.5 ps, respectively, isolating transients by subtracting scaled intensities of unpumped $Fe(CO)_5$ from the measured intensities (scaling factor 0.9). Reprinted with permission from reference [258]. Copyright 2017 Nature Publishing Group.

Very recently, Wernet and co-workers[258,259] implemented the first fs-RIXS experiment in the soft X-ray domain to address these questions. An example of RIXS spectra is shown in Figure 17. They found that the photo-induced removal of CO generates the $Fe(CO)_4$ species in a hitherto unreported excited singlet state that either converts to the triplet ground state or combines with a CO or solvent molecule to regenerate a penta-coordinated Fe species on a sub-picosecond timescale. This parallel ultrafast intra-molecular spin crossover and ligation of the $Fe(CO)_4$ is explained by a branching of the reaction pathway likely in its $^1A_1$ state. A sub-picosecond time constant of the spin crossover from $^1B_2$ to $^3B_2$ is rationalized by the proposed $^1B_2$-$^1A_1$-$^3B_2$ mechanism. Ultrafast solvent molecule binding of the $^1B_2$ state of $Fe(CO)_4$ is significantly faster than the spin-forbidden and diffusion limited ligation process occurring from the $^3B_2$ ground state. The authors proposed that the ultrafast ligation (200-300 fs) occurs via $^1B_2$ - $^1A_1$ - $^1A_0$ Fe(CO)4EtOH pathway and it is governed by the solute-solvent collision frequency. This very fast solvent molecule binding is quite surprising.

The issue of solvent coordination was also raised in X-ray absorption studies of photoexcited Copper-phenanthroline complexes,[173,177,178,182] which we discussed in § 4.1.

4.6 Intersite Charge Transfer

Paragraph 4.1 dealt with intramolecular charge transfer, however much of photocatalysis,[260] solar energy conversion[261] and biology[262-264] involve intersite charge transfer, either between molecular entities or in heterogeneous media, e.g. at interfaces between a molecular systems and a solid substrate. Core-level spectroscopies provide unambiguous markers of the oxidation state changes of specific elements and in a time-resolved mode, they emerge as the ideal technique for probing intersite charge transfer. In the following, we concentrate on recent time-resolved XAS studies that have been performed mainly on dye-sensitized solar cells and on molecular assemblies.

Interfacial charge injection: Transition metal oxides, such as Titanium dioxide (TiO_2) or Zinc oxide (ZnO) are the most promising materials for applications in solar-energy conversion and photocatalysis.[265,266] To this aim sensitization of the large band gap semiconductor metal oxide substrate by an adsorbed dye molecules enables the injection of electrons into its conduction band (CB) upon excitation by visible light by the dye.[267] This sensitization, most commonly with ruthenium-based polypyridine complexes, became the basis of dye-sensitized solar cells (DSSCs). The efficiency of solar-related processes depends on the transport and trapping of charge carriers, and although the trapping of electrons in the CB has been known for years, the nature of the traps at room temperature remains unknown,[260,268,269] due to the lack of element- and/or structure sensitive tools to identify them. Optical pump/XAS probe studies at the Fe K-edge were first applied to study electron injection from an adsorbed organic dye into iron oxide NPs.[102,270] By comparing the transient spectra with simulations, it was concluded that reduced metal sites formed small polarons within 150 ps, which was the time resolution of the experiment. As far as metal-based sensitizers are concerned, several groups have investigated the change of oxidation state of the metal upon MLCT excitation of the dye and injection into the substrate.[166,174] but the fate of the electron in the substrate was not investigated. The first study of the electron injection with element-selective probing of both the sensitizer and the substrate was carried out by the Chergui group on Ruthenium dyes adsorbed on anatase TiO_2 nanoparticles (NPs) and compared with the results of band gap excitation of bare NPs.[271,272] These experiments found that a full electron charge is trapped in both cases, but that the traps due to charge injection are different from those resulting from band gap excitation as can be seen from Figure 18.

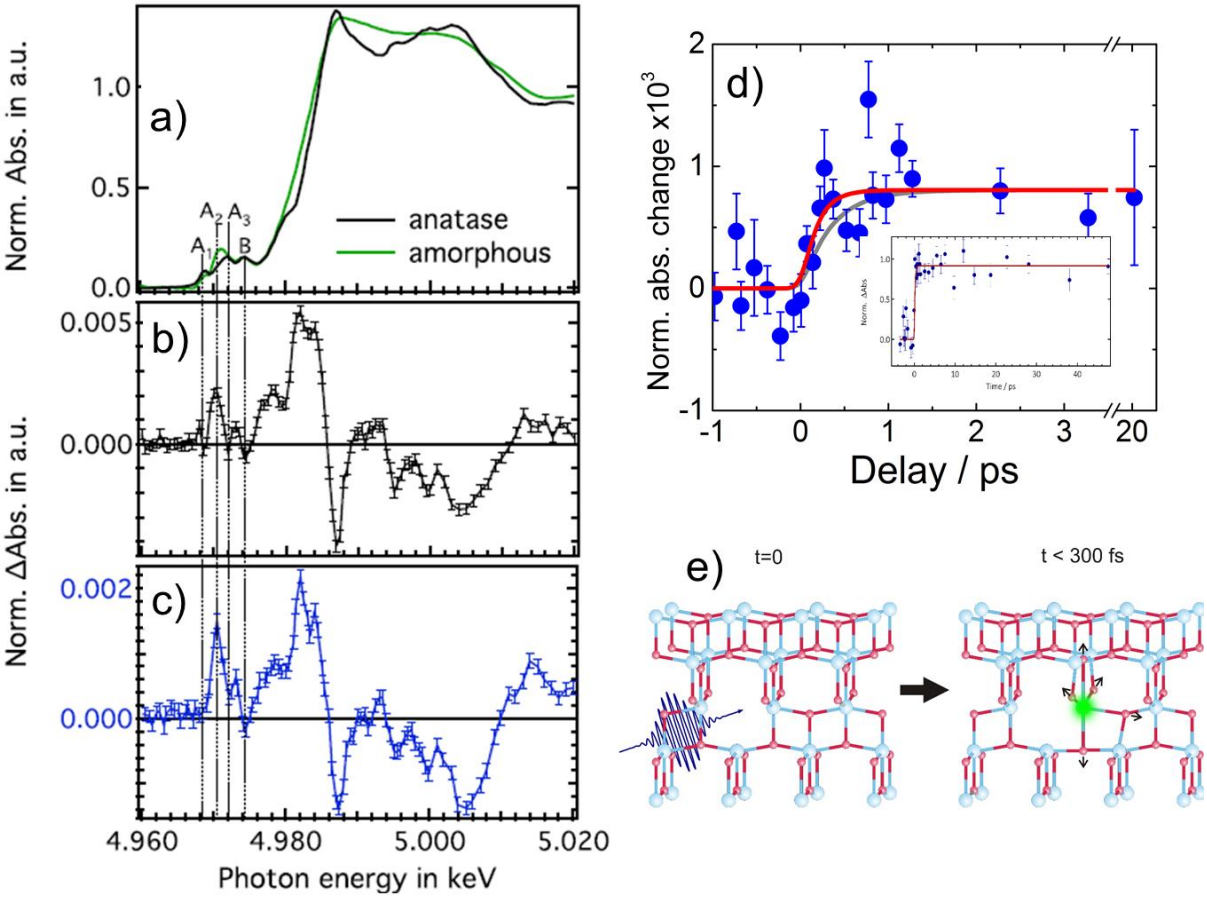

Figure 18: Titanium K-edge spectra of anatase and amorphous TiO_2 nanoparticles (pre-edge peaks A1–3 and B and X-ray absorption near-edge structure): a) steady state Ti K-edge absorption spectra of bare anatase and amorphous TiO_2; b) Transient X-ray absorption spectra of bare anatase TiO_2 nanoparticles at a time delay of 100 ps (black), after excitation at 355 nm above the band gap; c) Transient XAS spectrum of ruthenium N719-dye-sensitized anatase TiO_2 NPs at a time delay of 100 ps (blue) after excitation at 532 nm. The subtle differences

between b) and c) have been discussed in ref. [271,272] and are due to the trapping of electrons deep inside the shell (band gap excitation) of the nanoparticles or on its surface (injection case). Reprinted with permission from ref. [271,272]. Copyright 2014 John Wiley and Sons; d) Femtosecond pump-probe transient recorded at 4.981 keV of bare nanoparticles excited at 355 nm. The rise time is limited by the resolution of the experiment (170 fs, red trace) but not exceeding 300 fs (grey trace); e) this implies that the electron is trapped in the immediate vicinity of where it was created. Reproduced from reference [272].

Panels b) and c) of figure 18 show that while the transients in the bare and the dye-sensitized case are overall similar, there are some subtle differences, especially when it comes to the pre-edge region. Further experimental and theoretical studies are needed to clearly identify the nature of the trapping sites.

Charge injection was also reported in the case of films of TiO_2 NPs sensitized by gold NPs, but the laser and synchrotron sources were used as continuous sources and differences were taken between laser-on and laser-off RIXS spectra.[273]

From these time-resolved XAS studies, it appears that the electron acts as a contrast agent upon trapping. Indeed, this comes from the fact that oxidation state changes of an element show up as a shift of the edge position, which increases or decreases in energy depending, respectively, on whether the atom has been oxidized or reduced. The edge shift may contain additional causes, such as bond distance changes between the atom of interest and its neighbors. In the above-edge region, transitions probe the unoccupied density of states above the Fermi level, and a reduction of intensity right above the edge reflects the filling of unoccupied states, similar to the band filling found in optical studies of semi-conductors. Therefore, an X-ray absorption spectrum should be able to detect both localized charges (typically as small polarons at regular sites or at defects) and delocalized ones, as recently demonstrated in the case of perovskites.[274] It seems however that in the case of TiO_2 (Figure 18), the signal is dominated by charge localization, which we found to occur on an ultrafast time scale of < 200 fs (Figure 18d).[272]

Recently, time-resolved photoemission has been implemented to probe the interfacial dynamics in transition metal oxides. Gessner and co-workers used Vacuum ultraviolet synchrotron pulses to probe the charge injection from the RuN3 dye to the ZnO substrate.[275,276] Photoemission gives element-specific information and probes unambiguously oxidation state changes via the measurement of the binding energy. They focused on the region of the C1s and Ru3d binding energies around 290 eV, implying that only the dye could be probed. The same experiment was then repeated with fs resolution at the XFEL yielding injection times of 500 fs.[277] These developments are adding new methods to the toolbox of ultrafast element-specific techniques for probing electronic and structural changes at interfaces.

Molecular assemblies: Canton et al.[278] combined fs XES and X-ray scattering (XRS) in the hard X-ray range at the XFEL SACLA in Japan to characterize the non-equilibrated electron transfer (ET) dynamics in donor–acceptor molecular assemblies that contain optically dark active sites. The bimetallic complex they studied consists of a light harvesting, ruthenium (Ru)-based chromophore linked to an optically dark cobalt (Co) electron sink by a bridge that mediates the ultrafast ET. This prototypical dyad exemplifies the wide class of synthetic and natural photocatalysts for which the coupled electronic and structural dynamics are only partially understood beyond the decay of the Franck–Condon state. They could thus nail down the dynamics of electron departure from the donor, the transit time via the bridge and the arrival to the acceptor, and finally, the formation time of the high spin state in the latter (Figure 19). The need for an observable such as XES is related to the fact that the Co-complex does not have known optical spectroscopic observables of its high spin state.

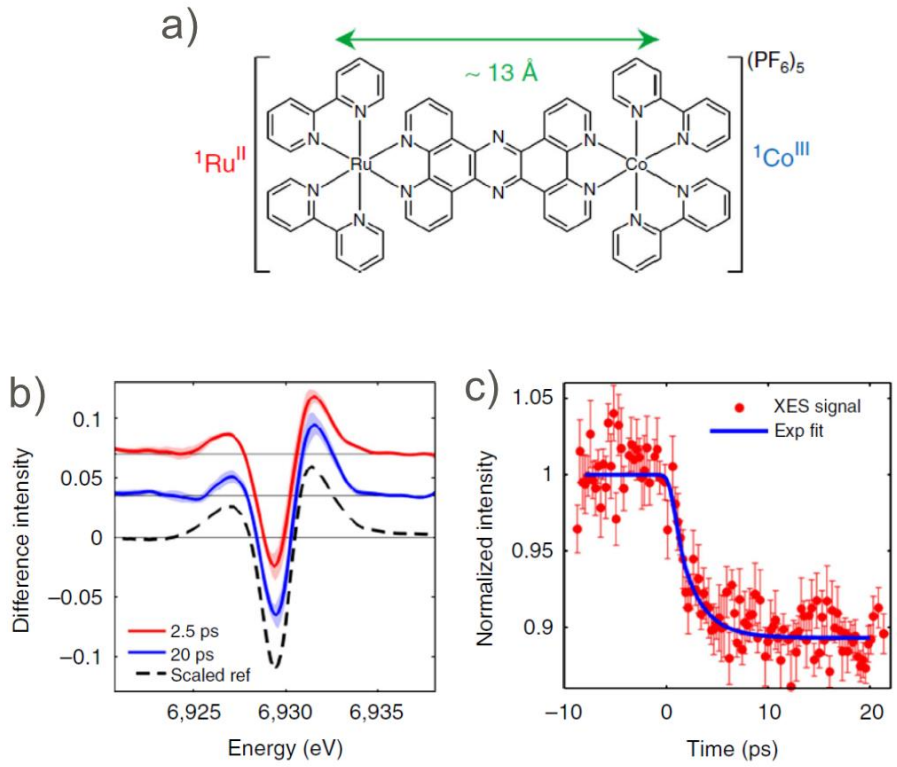

Figure 19: (a) The [1Ru^{II}=Co^{III}] complex. The Ru and Co centres are held 13Å apart by the tpphz rigid bridge. (b) Co Kα1 difference XES at 2.5 (red) and 20 ps (blue) pump-probe delay. The shaded areas indicate the uncertainty level. The dashed black curve is the simulated reference for a ^{1}Co^{III}(LS)-Co^{II}(HS) conversion, scaled to the 20 ps trace. (c) Kinetic trace at 6.93 keV (red dots) and single-exponential fit with a 1.9 ps lifetime, broadened by a 520±410 fs XFEL IRF (blue line). Reproduced from reference [278]. Copyright 2015 Nature Publishing Group.

5. Molecules in crystals

The low reactivity of molecules in the solid state was underlined by the famous sentence “A crystal is a chemical graveyard’’ attributed to Prof. Lavoslav Ružička.[279] If the reactivity is limited by the molecular packing, in terms of forming new molecules, the behaviour of bistable molecules in the solid state may however take advantage of the stronger interactions between them, mediated through the lattice. Photoinduced phenomena in molecular crystals represent a nice opportunity to control physical properties of materials by light or to induce single-crystal-to-single-crystal transformation.[280] The existence of cooperative response to light in molecular solids is one of the most striking examples, as the responses of elementary molecular components of the material add up in a non-linear fashion. This is especially true for photoinduced phase transitions, where the excitation by a light pulse can abruptly generate transformations towards a new macroscopic state.[281] During photoinduced phenomena, several microscopic and macroscopic degrees of freedom play their part on significantly different length and time scales, from microscopic to macroscopic. Then time-resolved studies are of great importance to separate different physical processes on their intrinsic timescale.

5.1 Spin cross-over

The above mentioned LIESST was discovered in SCO crystals more than 30 years ago.[282,283] It arose several questions related to the photoswitching mechanism compared to solutions: Would the crystalline lattice, through the elastic coupling between the volume-changing molecules, favor or not LIESST? Since, contrary to molecules in solution, SCO solids can present collective phase transitions and thermal hysteresis related to LS/HS bistability, is it possible to drive cooperative transformation with photoexcitation? It is only recently that the Collet group demonstrated the possibility to generate and detect transient spin states in crystals by femtosecond optical spectroscopy, opening the possibility to study the ultrafast dynamics in the solid state.[284,285] Single-shot and complete switching were also reported inside the thermal hysteresis of these materials by Raman and X-ray diffraction,[286,287] but a laser heating process was questioned. Indeed, SCO crystals excited by a femtosecond laser pulse undergo a complex out-of-equilibrium dynamics associated with three main steps (Figure 20).[288] First, the

light pulse locally photoswitches an initial fraction $X_{HS}^{h\nu}$ of molecules from LS to HS states within ≈200 fs. Second, the internal lattice pressure due to HS molecular swelling and lattice heating induces lattice expansion on the ns timescale. As the HS state of higher molecular volume is then favored, an additional switching towards HS state occurs, increasing the HS fraction up to X_{HS}^{El} during this so-called elastic step. Third, because of the laser heating, the global temperature of the crystal increases (≈10s K) and drives a third "thermal" step as the higher temperature favors HS state of higher entropy and the HS population thermally equilibrates to X_{HS}^{Th}. The main features associated with these three steps are presented hereafter.

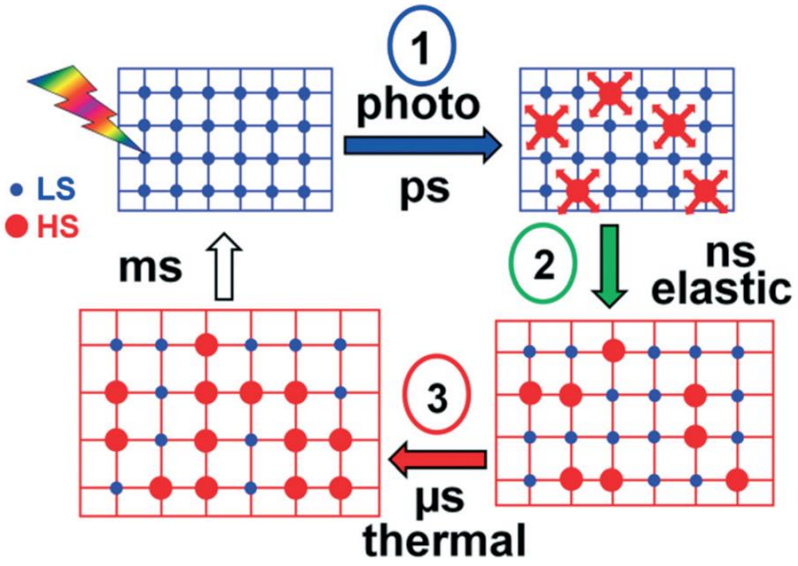

Figure 20: Schematic drawing of the out-of-equilibrium dynamics in SCO crystals. The laser pulse locally photo-switches molecules from LS (blue) to HS (red) states within less than 1 ps (step 1). The molecular swelling and lattice heating induce lattice expansion driving cooperative elastic switching in the ns time window (step 2). The HS state is then thermally populated (μs) and accompanied by another crystal expansion (step 3). Reprinted with permission from reference [289]. Copyright 2017 The Royal Society of Chemistry.

5.1.1 Femtosecond spin-state switching in the solid state

In addition to the femtosecond studies of LS to HS photoswitching performed in solution as described in § 4.1, LIESST was also investigated in molecular solids by Collet & Cammarata with fs optical spectroscopy and with fs XANES at the LCLS X-FEL.[288,290,291] In SCO Fe^{II} molecular solids, X-ray diffraction reveals important changes of the molecular structure, around the FeN_6 octahedron, between LS and HS states at thermal equilibrium but also in the long-lived photoinduced HS state at very low temperature. In the prototype $[Fe(phen)_2(NCS)_2]$ material, the main structural deformation is the increase of the average Fe-N distance from $\langle Fe\text{-}N\rangle_{LS} \approx 1.97$ Å to $\langle Fe\text{-}N\rangle_{HS} \approx 2.16$ Å,[290] as in solutions (see § 4.2), accompanied by a torsion of the octahedron. The XANES spectrum changes around the Fe K-edge between the LS and HS states can be observed at thermal equilibrium and is very similar to that reported in solution (Figure 11). The derived structural change and its time scale are indeed similar to the solution case.[113,211] Similar results were obtained in the derivative SCO material $[Fe(PM\text{-}AzA)_2(NCS)_2]$.[291]

This ultrafast structural dynamic in SCO solids was also investigated by x-ray diffraction by Chergui, Elsaesser and co-workers.[292] They used a laser-plasma source X-ray source delivering ($Cu\ K_\alpha$, λ = 0.154 nm, 100 fs pulse duration) to measure the time evolution of the intensity of several Bragg peaks. The change of the diffracted intensity $\Delta I_{hkl}(t)$ measured in the pump-probe experiment is connected to the time dependent structure factor of the time-dependent photo-excited state $F_{hkl}^{ex}(t)$ and to the one of the ground state F_{hkl}^{0} through:

$$\Delta I_{hkl}(t) = M_{hkl} L P_{hkl} \left(\left| X_{HS} F_{hkll}^{ex}(t) + (1 - X_{HS}) F_{hkl}^{0} \right|^2 - \left| F_{hkl}^{0} \right|^2 \right)$$

where X_{HS} is the fraction of modified cells, M_{hkl} is the multiplicity of the *(hkl)* ring and LP_{hkl} is the Lorentz-polarization factor. From the time evolution of the powder diffraction pattern (Figure 21), three-dimensional differential electron density maps were derived at each delay, providing access to the time evolution of the Fe–N distance among other structural information such as Fe-pyridine ring and ring-ring distances. Here again the structural rearrangements are found to occur within 200 fs but the accuracy of the analysis is limited by the small fraction of photoswitched molecules in the solid (estimated in this experiment at X_{HS}=0.008).

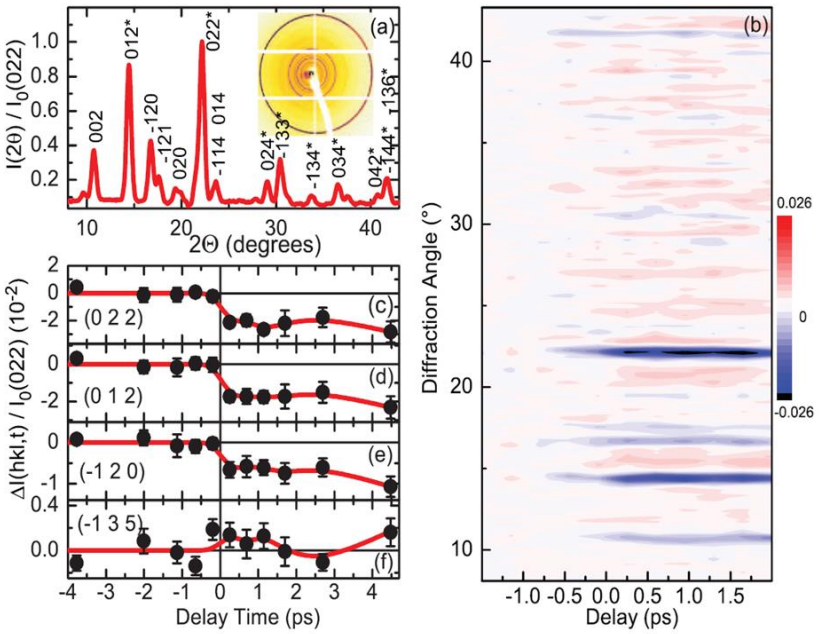

Figure 21: a) Powder diffraction pattern of ([Fe(bpy)$_3$](PF$_6$)$_2$) recorded with the X-ray plasma Source. (b) Transient changes of the X-ray reflections as a function of the delay. (c-f) Change of the diffracted intensity of different Bragg peaks. Reproduced from ref. [292]. Copyright 2013 AIP Publishing.

5.1.2 Multiscale aspect of the out-of-equilibrium dynamics

As mentioned above, both elastic or thermal effects play their part in the out-of-equilibrium process. These two contributions were clearly separated in a recent time-resolved x-ray diffraction study in [Fe(phen)$_2$(NCS)$_2$] single crystals photoexcited by a femtosecond laser flash.[293] The first-order nature of the LS to HS phase transition at thermal equilibrium (180 K) allows disentangling elastic and thermal effects. A single crystal was photoexcited at 140 K and its evolution was probed both by time-resolved optical spectroscopy to track the time evolution of the HS fraction and by time-resolved x-ray diffraction at synchrotron to measure the evolution of the lattice volume (Figure 22). An initial fraction of HS molecules $X_{HS}^{h\nu}$ (typically 0.02) is photo-generated within 200 fs as explained above. This initial photoswitching process occurs at the molecular level and the lattice has no time to expand on this timescale. The lattice expands only after a few ns, as a macroscopic crystal expansion results from the establishment of a mechanical equilibrium within the crystal, because the photoswitched molecules of higher volume exert a negative (or internal) pressure on the lattice. It occurs concomitantly with a second increase of the HS fraction, reaching X_{HS}^{El}=0.04 after ≈20 ns. This elastically driven cooperative response of SCO materials impacted by a laser pulse was recently demonstrated by Collet and Lorenc to be associated with the macroscopic volume change of the crystal both by experiment and theory.[293] It is limited by the propagation of strain waves through the sample (~2000 m.s^{-1}). This self-amplified molecular transformation is reminiscent of a feedback mechanism intrinsic to active media. For SCO solids, the more the volume expands, the more molecules switch, the more the volume expands. Hence, the elastically driven response, resulting from the simultaneous absorption of many photons, is

greater than the sum over individual responses of the constituent molecules. This is a direct manifestation of the cooperative effects induced by a light pulse.

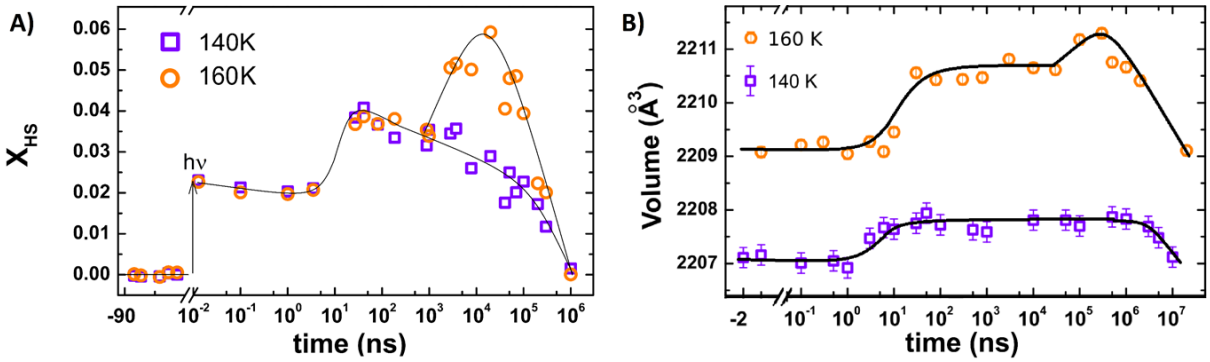

Figure 22: Evolution of the HS fraction X_{HS} (A) and lattice volume (B) after femtosecond laser excitation of LS $[Fe(Phen)_2(NCS)_2]$ at 140 and 160 K. Reprinted with permission from Ref. [289]. Copyright 2016 The Royal Society of Chemistry.

At a higher temperature (160 K) closer to the phase transition temperature, the photoresponse is similar on short time scale. However, on µs timescales a third step occurs, in which the HS fraction reaches X_{HS}^{Th} =0.06 (Figure 23). This effect is associated with the thermal population of the HS state, due to equilibration of the SCO molecules with the hot crystalline lattice. The three main steps in the out-of-equilibrium dynamics of photoexcited SCO crystals have very different characteristic timescales, since photo-switching (<ps) is associated with quantum physics, elastic switching (ns) with mechanics and thermal switching (µs) with thermodynamics.

Zewail et al used four-dimensional electron microscopy to visualize in real and reciprocal- space structural dynamics at the level of a single nanoparticle of Fe(pyrazine)$Pt(CN)_4$ SCO material.[294] Because of the low time resolution (7 ns laser pulse was used as pump) they could not access to the ultrafast photoswitching and elastic steps. However, they could observe anisotropic thermal expansion on the 200 ns timescale at the level of a single particle, which was attributed to the temperature jump induced by light excitation but which may also result from the negative pressure induced by the photoswitching.

5.1.3 Photoresponse of spin-state concentration wave

In SCO materials, the bistability between LS and HS state is associated with thermal, entropy-driven, transition as the HS state has higher entropy. The elastic coupling through the lattice mentioned above between molecules can drive cooperative SCO with hysteretic behaviour. It can also be at the origin of mechanical frustration, generating stepwise conversions of the fraction of HS molecules X_{HS}. Few long-range spatially periodic structures of LS and HS states on the steps have been reported in a vast variety of SCO materials.[295-299] It results from the competition between ferro-elastic and antiferroelastic coupling and the emergence of Devil's staircase-type phenomenon has been pointed out.[300] Such HS-LS long-range ordered structures form spin-state concentration waves (SSCW, Figure 23).

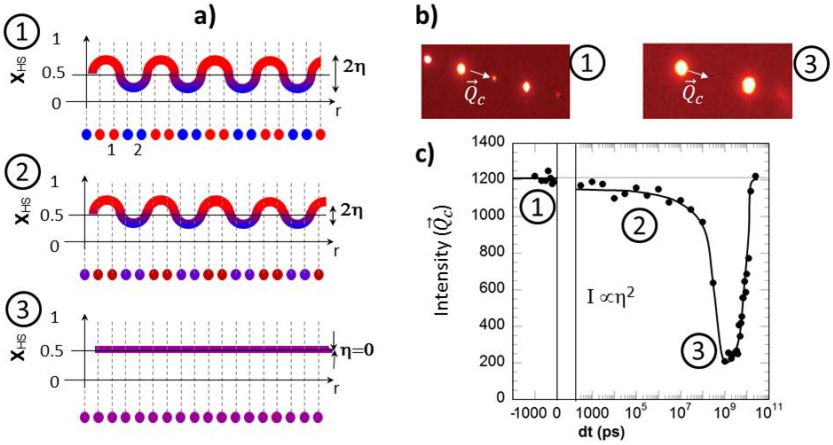

Figure 23: Schematic representation of spin-state concentration wave (a) with a long-range spatial modulation of the HS fraction over the crystalline sites for different amplitude η. (b) The SSCW are associated with new Bragg peaks at Q_c. (c) Time evolution of the intensity of the peaks at Q_c.

The SCO $[Fe^{II}H_2L^{2\text{-}Me}][PF_6]_2$ material undergoes a two-step transition from LS to HS, characterized with an intermediate phase (INT) where X_{HS}=0.5.[301] It is associated with a symmetry breaking due to the long-range ordering of molecules in both HS and LS states resulting in the formation of a spin-state concentration wave (Figure 24), which translates into the spatial modulation of the HS fraction for a lattice site in ***r***:

$$X_{HS}(r)=X_{HS}+(\eta/2)\times\cos(\boldsymbol{Q_c}.\boldsymbol{r}).$$

This is observed by X-ray diffraction through the spatial modulation of <Fe-N> bond-length between crystalline sites. In the case of $[Fe^{II}H_2L^{2\text{-}Me}][PF_6]_2$, $\vec{Q}_c = \frac{1}{2}\vec{c}^*$ corresponds to the doubling of the unit cell along the crystalline $\vec{c}$ axis, along which HS and LS molecules alternate (Figure 23). In the INT phase, the average HS fraction is X_{HS}=0.5 and the order parameter η measures the amplitude of the wave, *i.e.* the difference of the HS fraction on sites 1 (HS) and 2 (LS). This spatial modulation is associated with the appearance of additional Bragg peaks at $\vec{Q} = h\vec{a}^* + k\vec{b}^* + l\vec{c}^* + \vec{Q}_c$ (Figure 23). By considering that site1 (resp. 2) may populate the HS state with a probability X_{HS}^1 (resp X_{HS}^2) and a molecular structure factor F_{HS}, or the LS state with a probability ($1-X_{HS}^1$) and a structure factor F_{LS}, the structure factors of sites 1 and 2 are:

$$F_1(h\ k\ l) = X_{HS_1} \cdot F_{HS} + (1 - X_{HS_1}) \cdot F_{LS}$$
$$F_2(h\ k\ l) = X_{HS_2} \cdot F_{HS_2} + (1 - X_{X_{HS_2}}) \cdot F_{LS_2}$$

Since atoms in site 2 are shifted by ½ $\vec{c}$,

$$F_{HS(LS)_2}(h\ k\ l) = \sum_j f_{HS(LS)_j}\, e^{-2i\pi\left(hx_j+ky_j+l\left(z_j+1/2\right)\right)}$$

$$= \sum_j f_{HS(LS)_j}\, e^{-2i\pi\left(hx_j+ky_j+lz_j\right)} \cdot e^{-i\pi l}$$

Then for $\vec{Q}_c$ where *l* is odd, it comes out that the intensity of the Bragg peaks is:

$$I(\vec{Q}_c) \propto \eta^2 \times |F_{HS} - F_{LS}|^2 \propto \left|X_{HS}^1 - X_{HS}^2\right|^2,$$

since in a first approximation we can consider the structure factor of HS and LS molecular states as constant. The photoresponse of this SSCW to femtosecond light excitation was investigated by time-resolved X-ray diffraction and time-resolved optical spectroscopy.[302] As discussed above for SCO materials, a complex out-of-equilibrium process follows with the local femtosecond molecular switching (<ps), the lattice expansion (ns) and crystal heating (µs). These two last effects are weak on the plateau where X_{HS}=0.5 and the most interesting is the time evolution of the SSCW itself, directly probed through the evolution of $I(\vec{Q}_c)$ as shown and schematically explained in Figure 23. Before laser excitation, state "1", the SSCW with an amplitude η is formed with different HS population on the crystalline sites 1 (mainly HS) and 2 (mainly LS). The femtosecond laser excitation in the band selectively photo-switching of a small fraction of molecules from LS to HS states, state "2", X_{HS}^2 increases within less than 1 ps, as observed by optical spectroscopy, and the intensity of the peak slightly decreases (Figure 23), within the 100 ps time resolution of the X-ray diffraction experiment.[66] On longer timescales, the intensity of all the Bragg peaks at $\vec{Q}_c$ monotonically decreases within 0.1-1 ms and approaches 0, state "3", meaning that on this timescale $X_{HS}^1 \sim X_{HS}^2$. This is a direct evidence that it takes time to destroy the long-range order of the SSCW, since to do so each molecular lattice site needs to reach the same new equilibrium value of X_{HS}. The typical timescale for the molecular system to explore different HS/LS configurations and to reach thermal equilibrium is in the 100 µs-1 ms range. This data also indicates that as the crystal cools down later, the SSCW forms anew within 15 ms, which is the timescale required for the long-range ordering of molecules in HS and LS states.

These different structural aspects in SCO materials represent key points to understand their photoresponse to femtosecond light excitation from molecular to macroscopic response. The different processes in time can be investigated on their intrinsic timescale thanks to time-resolved techniques, making it possible to disentangle molecular, elastic and thermal effects. The molecular spin-state switching dynamics in solids and solution are found to be similar due to the local nature of the process. On the technical point of view, solids can be easily damaged and experiments in solution phase makes investigation of the molecular dynamics easier. However, measurements on single crystals open the possibility to study light polarization effects and that is how breathing and bending modes, activated during the process, were clearly separated.[288] The great interest of SCO solids is their cooperative response to light excitation, where a single photon can switch several molecules by a single pulse, due to the bistable nature of the SCO lattice.[293] These studies in prototypical photoactive molecular solids illustrate this fact and will be extended to other families of materials in future.

5.2 Time-resolved photocrystallography in molecular solids

As illustrated above for SCO materials, structural dynamics in molecular crystals may occur on very different timescales. Femtosecond-timescale experiments give information on a timescale of instantaneous molecular transformation, whereas slower experiments provide statistically averaged response of an assembly of molecules, where kinetics takes over dynamics. Hereafter we present few photocrystallography studies, highlighting what can be learned on the structural changes triggered by light excitation.

5.2.1 Femtosecond studies of molecular crystals

Femtosecond X-ray diffraction experiments were used to study structural dynamics in hard condensed matter, such as the activation of coherent optical phonons,[77,303,304] or the time evolution of order parameters related to the melting of charge and orbital orders.[305] There are up to now very few studies of structural reorganization in molecular crystals, performed by x-ray diffraction on the 100 fs timescale.

Elsaesser and his group used femtosecond powder diffraction experiments, from a Cu Kα plasma source, to study the photoresponse of the hydrogen-bonded ionic ammonium sulfate [$(NH_4)_2SO_4$] initiated by 3-photon absorption at 400 nm.[72,306] As explained above for SCO materials, the 2θ positions of the diffraction rings remain unchanged on the 100 ps timescale as lattice expansion is much slower. The intensity of about 20 diffraction rings were measured simultaneously for different pump-probe delay and show pronounced changes after photoexcitation, as illustrated in Figure 24-left, exhibiting oscillations with a 650 fs period. Charge density maps change are shown in a plane containing the z axis and the line linking the oxygen atoms 1 and 2. The upper left panel shows the equilibrium charge density $\rho_e(x, y, z)$, the other panels the change of charge density $\Delta\rho_e(x, y, z)$ for different time delays after photoexcitation Figure 24-right.

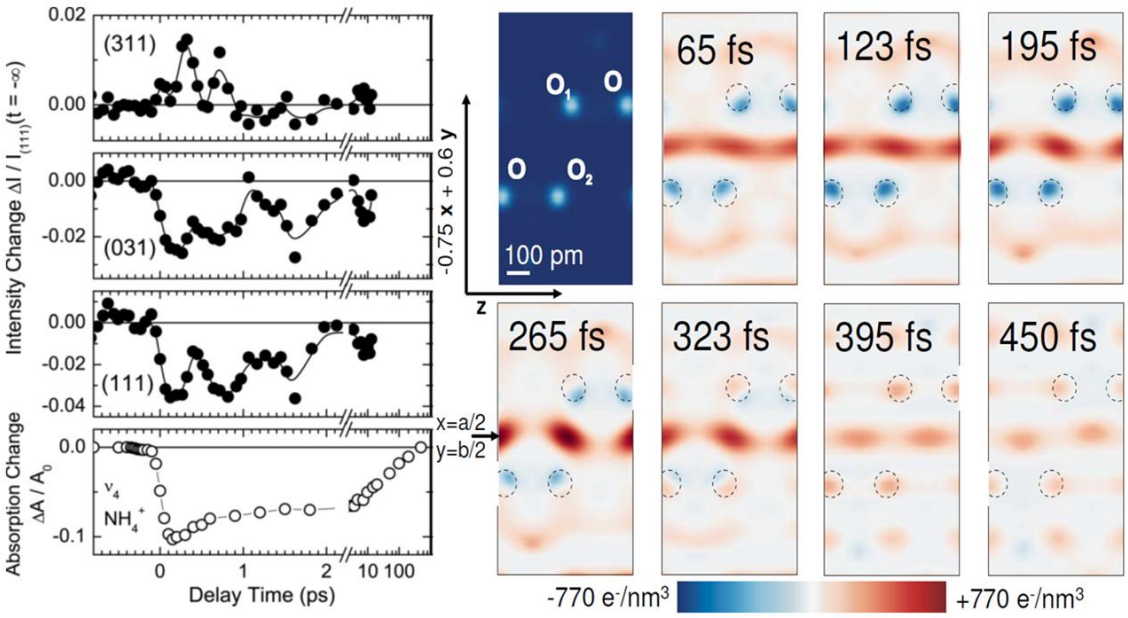

Figure 24: (left) Changes in intensity of diffraction rings of $[(NH_4)_2SO_4]$ after femtosecond laser excitation. Reproduced from Ref. [306]. Copyright 2010 AIPP. (right [72]) time evolution of the electron density. Reprinted with permission from Ref. [72]. Copyright 2010 International Union of Crystallography.

These structural oscillations were connected to the 50 cm^{-1} A_g phonon of $[(NH_4)_2SO_4]$, considering minor changes in the average positions of the heavier atoms S, N, and O in the unit. The changes of diffracted intensity after photoexcitation were connected to the temporal change of the three-dimensional charge density $\Delta\rho_e(x, y, z, t)$, which is extracted from the time-resolved data by reversing the equation of the structure factor given in 2.3.2:

$$x\Delta\rho_e(x,y,z,t) = \frac{x}{abc}\sum_{hkl}\Delta F_{hkl}(t)\cos[(\frac{hx}{a}+\frac{ky}{b}+\frac{lz}{c})]$$

where *x* is the fraction of modified unit cells in the sample.

The main photoinduced change consists in the formation of a channel-like geometry of enhanced electron density along the z axis, where there are no lattice atoms and indicating that protons move from the neighboring $(NH_4)^+$ groups into positions between the oxygen atoms 1 and 2. The formation of this hydrogen bonded new geometry occurs within 65 fs and requires concerted, or collective, motions of charges and protons. The periodic oscillations of the electron density in the channel corresponds to the period of the lattice A_g phonon mode (50 cm^{-1}), which modulates periodically the O_1-O_2 distance and is accompanied by charge and proton transfer between the channel. This is a nice illustration that femtosecond X-ray diffraction can provided 3D maps in the time domain of changes of molecular structure and charge distributions.

5.2.2 Slower dynamics

In addition to the coherent structural dynamics mentioned above, observed on the timescale of elementary atomic or molecular motions, slower timescales are sometimes pertinent in solids to obtain comprehensive insight in dynamical processes involving molecular rearrangements. For example, the lifetime of some photo-induced triplet and singlet excited states can be in the ns-µs range. It is then possible to study their relaxation with the 50-100 ps time-resolution of synchrotron, due to the natural x-ray pulse width.

Techert et al used 100 ps time-resolved X-ray powder diffraction to study the relaxation mechanisms of the molecular charge transfer salt *N, N* -dimethylaminobenzonitrile (DMABN) after photo-excitation [307] using a femtosecond laser pump. The experiment was performed at the ID09-time-resolved beamline at the ESRF

synchrotron. Transient structural changes could be characterized by an ensemble of geometrical rearrangements. The structural refinements evidenced a fast change of the torsion angle after photoexcitation, bringing the system into a quasiplanar configuration, and a relaxation towards the initial state within 520 ps. Latter Braun et al studied a similar process and concluded that an angular rearrangement of molecules around excited dipoles follows the 10 ps kinetics of charge transfer and that transient x-ray scattering is governed by solvation, masking changes of the chromophore molecular structure.[308]

Other time-resolved x-ray diffraction studies with atomic-resolution were about binuclear metalorganic complexes. After photoexcitation, the promotion of an electron to a stronger bonding state drives molecular contraction, as explained in § 4.3. For $[Pt_2(P_2O_5H_2)_4]^{4-}$ the lifetime of the photoexcited states reaches 50 µs at 16 K and the structure of the photoexcited state could be solved by time-resolved diffraction.[221,309] Then this process of bond contraction of binuclear complexes driven by light excitation was observed in several systems [310]. The use of monochromatic X-ray diffraction technique in time-resolved mode makes time dependent studies difficult because of the low X-ray flux. Coppens used the Laue diffraction method based on polychromatic radiation to study the structural reorganization in a photoactive a binuclear Rh complex.[311] The method is based on the RATIO technique, in which the ratios of measured intensities before (off) and after laser irradiation are used and from which photodifference maps are extracted. Two parameters can be used, corresponding to a set of ratios ($R(hkl)$) or response ratios ($\eta(hkl)$), defined as:

$$R(hkl) = I_{on}(hkl)/I_{off}(hkl) \qquad \text{and} \qquad \eta\,(hkl) = (I_{on}(hkl) - I_{off}(hkl))/I_{off}(hkl) = R(hkl)-1$$

In the RATIO method the ON data can be obtained by multiplication of the monochromatic intensities by the synchrotron-determined ratios R,

$$I_{on}(hkl) = R(hkl) * I_{monoc}(hkl)$$

As mentioned in previous examples, the structure factor is weighted by the population of the ground and excited states. Figure 25 shows the photodifference map and the main features observed are a sideward displacement of Rh1 and a displacement of Rh2 towards Rh1, suggesting both a rotation and a shortening of the Rh—Rh vector. Such improved Laue method, capable of producing excited-state structures at atomic resolution of high quality is very promising for the development of dynamical structural science. Other examples are discussed in the review by Coppens.[312]

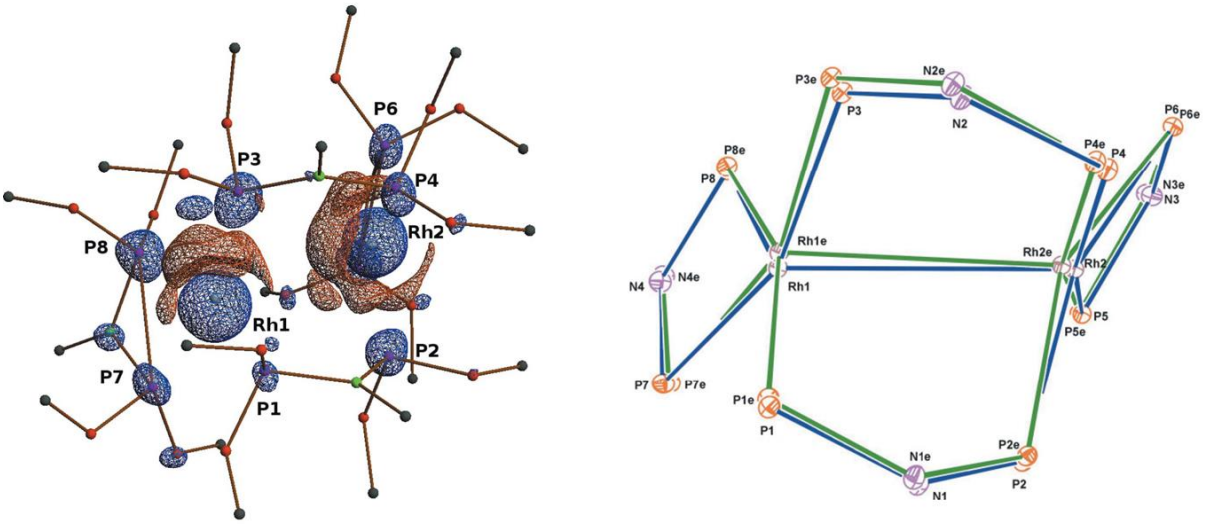

Figure 25. Photodifference maps calculated at isosurfaces of ± 0.25 e Å^3 (left) and molecular diagram indicating

atomic shifts on laser excitation (right), the excited-state atoms are marked with 'e'. Reprinted with permission from ref. [312]. Copyright 2011 International Union of Crystallography.

Another peculiarity of crystals is that the asymmetric unit can contain more than one molecule. Such chemically equivalent, but crystallographically independent molecules can show different structural rearrangements on excitation. This can be associated with different ligand field or environment in the unit cell. This is the case of the highly luminescent Cu(I) dimethyl-phenanthroline photosensitizer complexes studied Makal et al,[313] for which differences in wavelength and lifetime of their luminescence was reported. It was then observed by time-resolved X-ray diffraction that the intramolecular metal-to-ligand charge transfer induced by light for the two independent molecules in the crystal induces different distortions for each site, both in terms of magnitude and direction.

5.3 Cooperative charge-transfer and photoinduced ferroelectricity

The light-induced ferroelectric order in tetrathiafulvalene-p-chloranil (TTF-CA) and derivatives[314] is another nice example of light-activated functions in molecular solids. In this system, the electron donor (D) and electron acceptor (A) molecules alternate along stacks. Above 80 K, the system is in the neutral (N) phase where donor and acceptor molecules alternate in a sequence … $D^0A^0D^0A^0D^0A^0$…. D-A and A-D distances are equivalent because molecules are located on inversion symmetry.[156,315] At low temperature a charge-transfer takes place accompanied by a symmetry breaking due to dimerization, with two possible I states, …$(D^+A^-)(D^+A^-)(D^+A^-)$…or …$(A^-D^+)(A^-D^+)(A^-D^+)$… It is possible to trigger the charge transfer with a laser pulse to photoinduce this neutral-to-ionic transformation.[314,316] Again the mechanism is another example of multiscale phenomena since the initial response induces cooperative electron transfer inside the chains, followed by the ferroelectric 3D ordering between the stacks.

The photo-induced phase transition from neutral to ionic states in TTF-CA is discussed in the literature as resulting from collective excitations, the so-called 1D lattice-relaxed charge-transfer exciton-strings.[157] These nano-scale objects, represented by trains of ionized and dimerized DA pairs extending along the crystalline stacking axis *a* and represented by …$D^0A^0(D^+A^-)(D^+A^-)(D^+A^-)D^0A^0$… The condensation of diffuse scattering in planes perpendicular to the stacking axis *a* after femtosecond laser excitation, by time-resolved experiments performed by Guérin[158] constitutes a direct evidence of the photo-generation 1D lattice-relaxed charge-transfer exciton-strings (Figure 26).

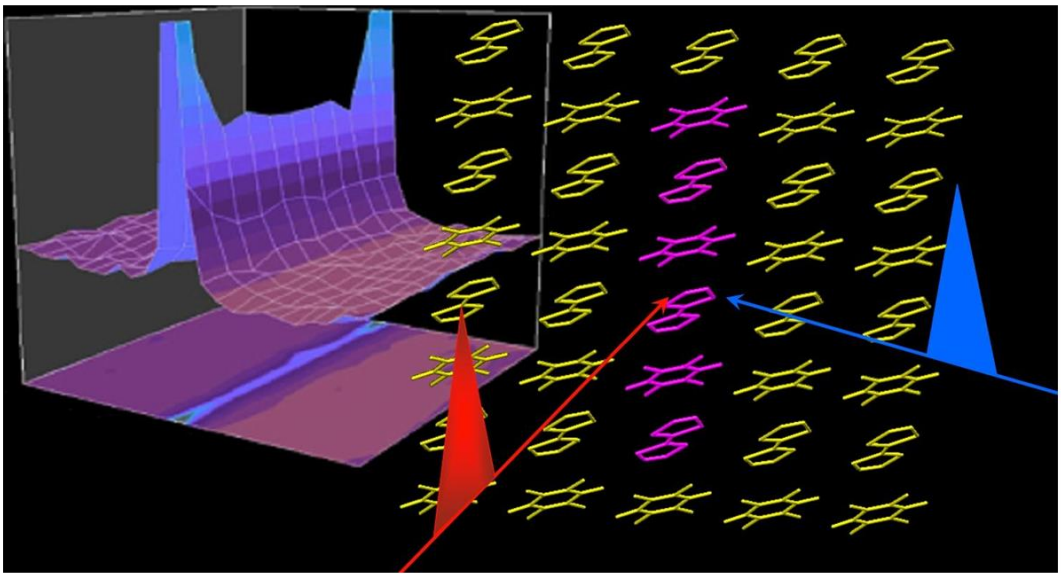

Figure 26. Diffuse scattering located in planes between Bragg peaks (left)(left) related to the photo-excitation of 1D cluster along the stack, as schematically indicated on the right.

The interstack coupling favors 3D ordering of these 1D polar object objects and their ferroelectric order. The symmetry-breaking associated with the generation of the ferroelectric phase with dimerized stacks is characterized by the change of space group. The space group of the paraelectric N phase is *$P2_1/n$*. Molecules lie on inversion symmetry and the intensity of the Bragg peaks *(0k0) : k=2n+1* is zero due to the presence of the *2_1* screw axis, as measured 2 ns before laser excitation (Figure 27). After photoexcitation, the space group of the photoinduced ionic phase changes towards *Pn* and this symmetry breaking is directly evidenced by the appearance of *(0k0) : k=2n+1* Bragg reflections, measured here 1 ns after photo-excitation.[317] As inversion symmetry is lost, a 3D ferroelectric order of (D^+A^-) dimers forms.

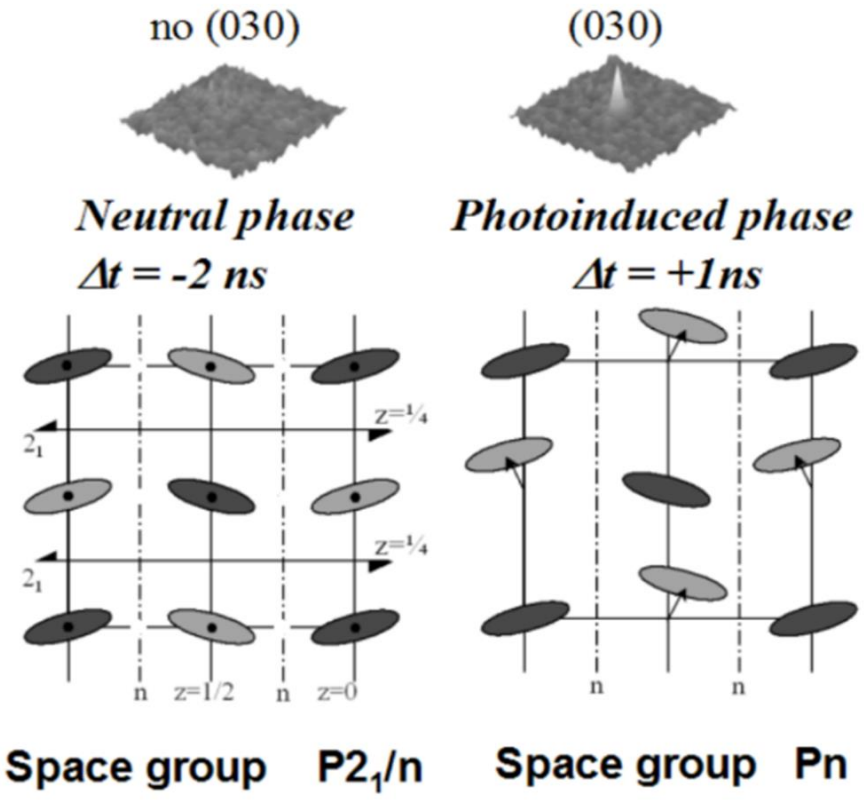

Figure 27. (Top) Reconstructed intensity in the reciprocal (a,b) planes before and after laser irradiation (Δt = -2 ns and +1 ns respectively). Appearance of (030) reflection signs the ferroelectric nature of the 3D photo-induced phase of TTF-CA. (Bottom) Schematic drawing of the space groups in both thermal equilibrium ($P2_1/n$) and photo-induced (Pn) states. Reprinted with permission from ref. [317]. Copyright 2003 The American Association for the Advancement of Science.

6. Biological systems

6.1 Picosecond studies

The huge success of X-ray crystallography for the structural determination of biological systems has been one of the reasons why it was time-resolved crystallography that was mostly considered for studying structural dynamics of biological functions.[318] Interestingly though, the first time-resolved X-ray study on biological systems was not carried out using X-ray diffraction but rather X-ray absorption spectroscopy. Mills and co-workers investigated the ligand dynamics of Myoglobin-CO upon excitation with a laser pulse and probed the evolution of the system at the Fe K-edge.[319] Because, they have been among the first ones to be studied and still represent benchmark systems for testing ultrafast X-ray diffraction or spectroscopic methods on Biosystems, metalloproteins will be the main focus of our attention in the following.

The above mentioned pioneering work of Mills and co-workers showed the sensitivity of Fe K-edge spectroscopy to the CO-ligand dissociation and recombination. This work was carried out with microsecond time resolution and was based on a laser/synchrotron synchronization scheme developed by the authors. Similar studies on Mb-CO were pursued by Clozza et al[320] and mainly by Chance and co-workers.[321] However, it would take several years, even after the advent of picosecond XAS to be able to probe metalloproteins with 100 ps time resolution. One of

the limitations being that biological systems are usually dilute (few mMol concentration or less), making the signal weak. The Chen group could however report studies of metalloporphyrines (the active centre of heme proteins) and detect electronic structure changes[322-324] and more recently they revisited MbCO, the system first investigated by Mills and co-workers, and carried out a detailed structural analysis.[325] The system had previously been used to test the performances of the high repetition rate scheme (§ 2.2) for ps XAS.[105] This is an ideal system because the kinetics of ligand recombination is very slow (msec). However, probing faster (sub-ns) ligand kinetics with XAS was first carried out on myoglobin-NO (Mb-NO) by the Chergui group.[326] This system is known to undergo a multiexponential ligand recombination spanning up to about 200 ps. In ref. [326], the recombination was measured with 70 ps resolution, implying that only the long components could be probed. This work showed that the long-time recombination kinetics is due to NO ligands that are far away from the heme procket, as previously suggested,[327] and that a domed ligated heme form upon recombination.

Probing structural dynamics in protein crystals is particularly tricky due to the photostability of the systems and the difficulty of retrieving the structural information at the atomic scale out of crystals where a few percent of the centres are excited. This challenge was overcome by Anfinrud and co-workers in a beautiful study of the MbCO protein crystals excited in the visible and probed by 150 ps X-ray pulses.[328-331] They could retrieve the whole structural dynamics of the system stretching out to ns's and visualize the docking site of the dissociated CO ligand.

The natural medium of proteins is water and it is desirable to be able to follow the structural changes in this medium. Ihee, Cammarata and co-workers actively investigated the case of MbCO in solutions with XRS at 100 ps time resolution.[86,332-336] Later, the same groups embarked in the study of dimeric hemoproteins,[337,338] with the aim to investigate cooperativity. Solution ps XRS is ideal when looking at conformational changes, large amplitude side chain motions and folding-unfolding processes and the above studies revealed several hitherto unknown details of the large scale protein dynamics. This type of experiments will be pursued, despite the advent of XFELs, because synchrotrons can fill the gap between 100 ps and infinite times, which is crucial in biology. However, with XFELs it becomes possible to investigate the short time dynamics that precede the long-time ones.

6.2 Femtosecond studies

As far as metalloproteins are concerned, the status of fs X-ray studies has recently been reviewed by Kern et al.[339] Here we focus on the more recent developments of the last few months. Because local structural changes (i.e. at short distances) scale with short time scales, fs XAS can provide valuable information about the changes in the immediate vicinity of the Fe or Co atoms, which are the bioactive centres in hemoproteins. Levantino et al[340] carried out an Fe K-edge fs study of MbCO, and found that photoinduced structural changes at the heme occur in two steps, with a faster (similar to 70 fs) relaxation preceding a slower (similar to 400 fs) one. They tentatively attributed the first relaxation to a structural rearrangement induced by photolysis involving essentially only the heme chromophore and the second relaxation to a residual Fe motion out of the heme plane that is coupled to the displacement of myoglobin F-helix. This work contained only time traces at fixed probe energies and therefore a structural analysis was not possible, which requires energy scan of the fs XAS transients.

This was recently achieved by Sension and co-workers[341] who investigated the Co-containing Vitamin B12 hemoprotein (cyanocobalamin, CNCbl), demonstrating for the first time the use of fs polarised XANES to probe the photochemistry of the system and reveal sequential structural evolution of CNCbl in the excited electronic state. This study is heralding the use of fs X-ray spectroscopy to probe the active centres of Biosystems. Indeed, short distance scales correspond to short time scales,[61] and therefore probing the initial events of biological functions is more convenient with a local electronic and structural probe such as X-ray spectroscopy.

Nevertheless, solution fs XRS was used by Levantino et al[342] to probe the light-induced structural rearrangements of photoexcited MbCO reporting evidence of the so-called 'proteinquake' through femtosecond X-ray solution scattering measurements. An ultrafast increase of the myoglobin radius of gyration was found to occur within 1 picosecond and to be followed by a delayed protein expansion. As the system approached equilibrium, damped oscillations with a ~3.6-picosecond time period were observed. The authors concluded that their results demonstrate the propagation of a chemical change from a local scale to the global protein in picoseconds.

This first study was followed by another fs XRS study by Barends et al[343] who carried out a detailed analysis of the fs and ps data supported by computational results. Refs [342] and [343] are consistent with the conceptual view of Mb dynamics, in which ultrafast modes of the heme couple with lower-frequency protein modes and, ultimately, with large-scale motions such as the displacements of the E and F helices. This notion that functional protein dynamics are governed by a network of coupled modes spanning a broad range of frequencies and length scales is emerging as a general model for the explanation of protein function.

In addition to studies on hemoproteins, there is intense activity aimed at describing the early time dynamics of proteins such as the Photoactive Yellow Protein (PYP),[344,345] bacteriorhodopsin (bR)[346] and the Photosystem II (PSII) reaction centre,[347] using femtosecond resolved X-ray diffraction. However, sub-ps structural dynamics was only reported for PYP nanocrystals. The structural changes of the p-coumaric acid chromophore and the protein were recorded down to 100 fs.[348] These measurements probed the motions of the early Franck-Condon (FC) excited state that has recently been also studied by time-resolved Raman spectroscopy at high temporal resolution (<7 fs)[349] showing that a rapid weakening of the hydrogen bond that anchors the chromophore is the primary event out of the FC region.

7. Perspectives and Conclusions

The recent years have witnessed tremendous progress thanks to the development of new data acquisition schemes at synchrotrons (slicing, high repetition rate scheme) and the advent of XFELs. This in turn has broadened the range of methods that can be implemented to characterise molecular systems, in particular photon-in/photon-out and photon-in/electron-out methods. In parallel, the ability to combine methods such as XRS and XES in a single measurement is boosting the capabilities to gather new insight into molecular dynamics, through the simultaneous probing of structural and electronic degrees of freedom dynamics. For example, the combination of fs resolution X-ray spectroscopies with solution phase scattering is a particularly welcome development as it allows probing electronic and structural changes from the interatomic bond to the entire solvation shell. This is of particular interest for phenomena such as solvation dynamics, protein dynamics or multiscale transformation in materials, where a hierarchy of time and length scales characterise the photoinduced processes. In addition, combining XANES and diffraction in solids will also provide complementary information on local electronic and structural changes, and global structural dynamics.

The stage is set for new opportunities to come, but needless to say that time-resolved X-ray spectroscopies at storage rings will remain vital for several reasons: (i) an XFEL is not needed to investigate phenomena on the 100 ps to several hundreds of ns, nor would it be wise to use the latter for such studies, given the high demand on these single user machines. Indeed, there is a wide variety of important phenomena to study in biology, chemistry and materials science that do not require a high temporal resolution as illustrated above; (ii) for many experiments to be planned at XFELs, it is highly advantageous to perform synchrotron-based experiments that establish observables and the level of signal, to be extrapolated to XFEL experiments; (iii) as already mentioned above, synchrotrons will not only be useful for XAS but also for photo-in/photon-out experiments, as well as scattering and diffraction that do not require a sub-100 ps time resolution.

The future promises several exciting avenues that still are nascent at present. Ultrafast Soft X-ray spectroscopies have been briefly mentioned in this review, but the ability to explore the regions between the Carbon K-edge (ca. 280 eV) and the 1 keV limit opens a window of opportunities for exploring dynamics in molecular systems. Indeed, most light elements such as C, N, O, S, etc. have their K-shells in this region, while several TM atoms, such as Fe, Co, Cu, Zn, Ni, etc. have their L-shell transitions. All of these elements play a central role in coordination chemistry and in biology and the extension of XFELs into the soft X-ray regime is highly desired. At present, the sole such machine is FERMI@Elettra (Trieste). This, along with the development of new sample delivery strategies under vacuum,[350,351] is opening new possibilities to investigate molecular systems, not only using photon-based detection soft X-ray spectroscopies, but also ultrafast photoelectron core-level spectroscopies of solutions as demonstrated by Abel, Faubel and others in recent years.[352-355]

Table-top HHG sources are making tremendous progress and are constantly increasing the upper energy limit, with constant improvement that promise reaching the N and the O K-edges.[356] With the sample delivery strategies mentioned above, the range below 100 eV is also very exciting to investigate as it is the region where several light elements (N, O, etc.) have their L-edges, while TM atoms have their M-edges. The first ultrafast absorption studies on TM oxides in the sub-100 eV range are demonstrating the power of studies in these ranges.[357-359]

New methods keep being developed at XFELs, which promise to open novel insight into a host of molecular phenomena, such as the High energy resolution off-resonant spectroscopy (HEROS), which records entire edge-spectra in a single shot and was recently demonstrated in static mode.[360] In a time-resolved mode, it would avoid having to scan the energy to record a transient XAS. The high fluxes and coherence properties of XFELs are also opening the field to new nonlinear X-ray spectroscopies, similar to what happened following the birth of the laser decades ago. Four-wave mixing (FWM) processes, based on the third-order nonlinear light–matter interactions, can combine ultrafast time resolution with energy and wave vector selectivity, and enable the exploration of dynamics inaccessible by linear methods.[361] FWM was recently demonstrated by Bencivenga et al[362] using the coherent extreme ultraviolet pulses delivered by the FERMI free-electron laser. The option to extend such studies into the harder X-ray range are presently being explored.[78] Multiphoton X-ray absorption has also become reality.[363] All of these developments are opening the way to extending into the X-ray domain, the rich toolbox of non-linear methods known in the optical domain.

Regarding materials science, femtosecond crystallography studies already reached atomic time and spatial scales for simple systems for which the structural change is refined from few Bragg peaks. For biology, serial femtosecond crystallography with new sample delivery and analysis of x-ray diffraction images is intensively developing and should find similar extension for molecular solids in chemistry and material science. Another important development is the use of resonant inelastic X-ray scattering at XFELs to probe correlated dynamics in solids. RIXS was used to determine the ultrafast magnetic dynamics after photo-doping the Mott insulator Sr_2IrO_4.[364] This technique will be also of great interest to study the ultrafast photoresponse of molecular solids presenting electronic/magnetic order.

New tools need to be assessed with respect to how they can surpass already available ones and deliver new insight. Ultrafast electron-based techniques have made strident progress thanks in particular to the huge contributions of the late Ahmed Zewail[56,58,60] and of others.[365,366] However, ultrafast 1D or 2D IR spectroscopies[367,368] along with ultrafast Raman spectroscopy, offer many features that are found in X-ray based techniques but with the advantage of being lab-based and therefore requiring less technical investment. Processes such as solvent heating (shown in

Figure 15 for the X-ray case) are routinely investigated with IR methods, correlations between various chromophores within a complex system can be detected by 2D IR spectroscopy, provided couplings exist between them. Charge transfer and migration within molecular edifices can also be detected by infrared spectroscopies, given the high sensitivity of certain vibrational dipoles to electric fields.[369] There are many other aspects of vibrational spectroscopies which make them very attractive. However, element-specificity and the ability to grasp global structures is what makes X-ray spectroscopy and scattering, respectively, unique though not superior to other tools. No method is entirely universal and it is only by combining methods that deliver different and complementary observables that one can really solve scientific problems.

The results presented here give an illustration of what can be done and what exciting perspectives are in sight in time domain structural methods as more powerful X-ray or electron sources are being developed. Among the large contributions that this new advanced method may provide, an important goal is to understand and control phase transitions driven by light. A deep understanding of such phenomena at different scales requires the combined use of X-ray or electron diffraction over different time scales (fast and ultra-fast), but also of temporal X-ray absorption and optical spectroscopies. This is the key for elucidating this new kind of coherent manipulation of matter by light and for controlling ultra-fast macroscopic switching of materials. In addition to “high energy” electronic excitation (eV) conventionally used in femtochemistry and photoinduced phase transition to modify the potential energy surface, IR and THz excitation open new possibilities to drive directly correlated lattice motion with low energy photons. This broad spectrum of recent advances in this field set the stage for imminent breakthroughs in the understanding and controlling of our dynamical world.

AUTHOR INFORMATION

Corresponding Authors

* E-mail: majed.chergui@epfl.ch

* E-mail: eric.collet@univ-rennes1.fr

Biographies

Majed Chergui was born in Casablanca (Morocco) in 1956 and grew up in Algeria and Lebanon. After obtaining his BSc in Physics & Mathematics from Chelsea College (later merged with King’s College) London in 1977, he moved to France for his MSc (1978) and PhD (1981) degrees in Molecular Physics at the Université Paris-Sud (Orsay). In 1982, he became research assistant at the CNRS and worked on molecular Rydberg states in condensed phases using vacuum ultraviolet radiation from synchrotrons. After his Habilitation in 1986, he moved to Berlin as an Alexander von Humboldt Fellow and spent 6 years at the Free University. In 1993, he was appointed Full Professor of Condensed Matter Physics at the Université de Lausanne, Switzerland. In 2003, he became Professor of Physics and Chemistry at the Swiss Federal Institute of Technology in Lausanne. His group is known for developing and improving experimental tools to investigate physical phenomena in molecules, proteins and materials. In particular, he pioneered ultrafast X-ray absorption spectroscopy and ultrafast 2-dimensional deep-UV spectroscopy. His contributions have been recognised by several Awards and Prizes among which: the 2009 Humboldt Research Prize (Germany), the 2010 Kuwait Prize for Physics, the 2015 Earle Plyler Prize of the American Physical Society and the 2015 Edward Stern Prize of the International X-ray Absorption Society (IXAS). He is also Head of the Lausanne Centre for Ultrafast Science (LACUS).

Eric Collet was born in Rennes, Région Bretagne, France in 1972. He obtained his BC in 1991 and master degree in Material Science (1996), DEA in Physics (1996), and PhD (1999) degrees from University of Rennes 1. He was postdoc (1999–2001) at Laboratoire Léon Brillouin, the French neutron center, CEA/Saclay (France). He has been working on phase transition at thermal equilibrium in materials where electronic and structural degrees of freedom have to be considered on an equal footing. In 2001 he became an associate professor at the University of Rennes 1 and launched structural studies of photoinduced phase transitions, for which the structural and electronic changes are strongly coupled. Research topics concerned photocrystallography and applying ultrafast time-resolved x-ray diffraction in the investigation of ultrafast photoinduced transition. In 2007, he became a professor and in 2008 he obtained a chair at the Institut Universitaire de France. He is vice-director of the Institut de Physique de Rennes. Since January 2017 he is co-director of the France-Japan international laboratory IM-LED.

ACKNOWLEDGEMENTS

M.C. acknowledges the crucial contributions of his past and present collaborators on the time-resolved X-ray experiments and that of the theoreticians that have been involved in these studies. He also thanks the teams of the SLS and the SwissFEL for constant support and assistance during the elaboration of projects and the running of the experiments. The support by the Swiss NSF is greatly acknowledged, in particular in recent years via the NCCR:Molecular Ultrafast Science and Technology (MUST). E.C. would like to thank his collaborators in the field of ultrafast X-ray science H. Cailleau, M. Buron, M. Lorenc, M. Cammarata, R. Bertoni, H. Lemke, S. Koshihara, M. Wulff, K. Moffat, R. Henning, T. Graber and the Institut Universitaire de France, Rennes Métropole, Région Bretagne (CREATE 4146), ANR (ANR-13-BS04-0002) and Europe (FEDER) for constant support.

REFERENCES

(1) Barkla, C. G.; Sadler, C. A.: The Absorption of X rays. *Nature* **1909**, *80*, 37-37.
(2) Barkla, C. G.; Collier, V.: The Absorption of X-rays and Fluorescent X-ray Spectra. *Philosophical Magazine* **1912**, *23*, 987-997.
(3) Friedrich, W.; Knipping, P.; Laue, M.: Interference Appearances in X-rays. *Ann Phys-Berlin* **1913**, *41*, 971-988.
(4) Friedrich, W.: A new Interference Occurrence with x-Radiation. *Physikalische Zeitschrift* **1913**, *14*, 317-319.
(5) Bragg, W. H.: X rays and Crystals. *Nature* **1913**, *90*, 219-219.
(6) Bragg, W. H.; Bragg, W. L.: The Reflexion of x-Rays through Crystals. *Z Anorg Chem* **1914**, *90*, 169-181.
(7) Bragg, W. H.: The Reflexion of x-Rays through Crystals (II). *Z Anorg Chem* **1914**, *90*, 182-184.
(8) Debye, P.: Interference of x Rays and Heat Movement. *Ann Phys-Berlin* **1913**, *43*, 49-95.
(9) Siegbahn, M.: On the Spectrums of High Frequency. *Comptes Rendus Hebdomadaires Des Seances De L Academie Des Sciences* **1917**, *165*, 59-59.
(10) Siegbahn, M.: Precision-Measurements in the X-ray Spectra. Part II. *Philosophical Magazine* **1919**, *38*, 639-646.
(11) Siegbahn, M.; Jonsson, E.: The Absorption cut-off Frequency of the x-Rays among the Heavy Elements, Especially among the Rare Earths. *Physikalische Zeitschrift* **1919**, *20*, 251-256.
(12) Siegbahn, M.; Lindh, A. E.; Stensson, N.: On a Method of Spectral Analysis using x-Rays. *Zeitschrift Fur Physik* **1921**, *4*, 61-67.
(13) Stumm von Bordwehr, R.: A History of X-ray absorption fine structure. *Ann. Phys. Fr.* **1989**, *14*, 377-465.
(14) Sayers, D. E.; Stern, E. A.; Lytle, F. W.: New Technique for Investigating Noncrystalline Structures - Fourier Analysis of Extended X-Ray - Absorption Fine Structure. *Physical Review Letters* **1971**, *27*, 1204-&.
(15) Koningsberger, D. C.; Prins, R.: *X-ray absorption : principles, applications, techniques of EXAFS, SEXAFS, and XANES*; Wiley: New York, 1988.
(16) Javan, A.: Theory of a 3-Level Maser. *Phys Rev* **1957**, *107*, 1579-1589.
(17) Javan, A.: Transitions a Plusieurs Quanta Et Amplification Maser Dans Les Systemes a Deux Niveaux. *Journal De Physique Et Le Radium* **1958**, *19*, 806-808.
(18) Basov, N. G.; Krokhin, O. N.; Popov, I. M.: Generation, Amplification, and Indication of Infrared and Optical Radiation by Means of Quantum Systems. *Usp Fiz Nauk+* **1960**, *72*, 161-209.
(19) Shank, C. V.; Fork, R. L.; Yen, R.; Stolen, R. H.; Tomlinson, W. J.: Compression of Femtosecond Optical Pulses. *Applied Physics Letters* **1982**, *40*, 761-763.
(20) Shank, C. V.; Fork, R. L.; Beisser, F.: Basic Design Considerations for Femtosecond Pulse Dye-Lasers. *Laser Focus World* **1983**, *19*, 59-62.
(21) Fork, R. L.; Shank, C. V.; Hirlimann, C.; Yen, R.; Tomlinson, W. J.: Femtosecond White-Light Continuum Pulses. *Optics Letters* **1983**, *8*, 1-3.
(22) Shank, C. V.: Measurement of Ultrafast Phenomena in the Femtosecond Time Domain. *Science* **1983**, *219*, 1027-1031.
(23) Fork, R. L.; Shank, C. V.; Yen, R.; Hirlimann, C. A.: Femtosecond Optical Pulses. *Ieee Journal of Quantum Electronics* **1983**, *19*, 500-506.
(24) Yen, R.; Shank, C. V.; Fork, R. L.: Femtosecond Optical Pulses and Technology. *P Soc Photo-Opt Inst* **1983**, *439*, 2-5.
(25) Marrey, E.-J.: Du vol des oiseaux. *La Revue scientifique* **1869**.
(26) Zewail, A. H.: Femtosecond Transition-State Dynamics. *Faraday Discussions* **1991**, *91*, 207-237.
(27) Zewail, A.: *The chemical bond structure and dynamics*; Academic press: Boston San Diego New York [etc.], 1992.
(28) Dantus, M.; Zewail, A.: Introduction: Femtochemistry. *Chem Rev* **2004**, *104*, 1717-1718.
(29) Zewail, A. H.: Femtochemistry: Atomic-Scale Dynamics of the Chemical bond using ultrafast lasers - (Nobel lecture). *Angew Chem Int Edit* **2000**, *39*, 2587-2631.
(30) Zewail, A. H.: Femtochemistry: Atomic-scale dynamics of the chemical bond. *Journal of Physical Chemistry A* **2000**, *104*, 5660-5694.
(31) Fleming, G. R.; Cho, M. H.: Chromophore-solvent dynamics. *Annu Rev Phys Chem* **1996**, *47*, 109-134.
(32) Jung, G.; Ma, Y. Z.; Prall, B. S.; Fleming, G. R.: Ultrafast fluorescence depolarisation in the yellow fluorescent protein due to its dimerisation. *Chemphyschem* **2005**, *6*, 1628-1632.
(33) Pugliano, N.; Szarka, A. Z.; Gnanakaran, S.; Hochstrasser, R. M.: Photodissociation dynamics of solvated small molecules. *Fast Elementary Processes in Chemical and Biological Systems* **1996**, 3-11.
(34) Pugliano, N.; Gnanakaran, S.; Hochstrasser, R. M.: The dynamics of photodissociation reactions in solution. *J Photoch Photobio A* **1996**, *102*, 21-28.
(35) Zewail, A.: *Femtochemistry ultrafast dynamics of the chemical bond*; World scientific: Singapore New Jersey London [etc.], 1994.
(36) Chergui, M.: *Femtochemistry : ultrafast chemical and physical processes in molecular systems : Lausanne, Switzerland, September 4-8, 1995*; World Scientific: Singapore ; River Edge, NJ, 1996.
(37) Sundström, V.: *Femtochemistry and femtobiology : ultrafast reaction dynamics at atomic-scale resolution : Nobel Symposium 101*; Imperial College Press ;
Distributed by World Scientific Pub. Co.: London
River Edge, NJ, 1997.
(38) Williamson, J. C.; Zewail, A. H.: Structural Femtochemistry - Experimental Methodology. *P Natl Acad Sci USA* **1991**, *88*, 5021-5025.
(39) Williamson, J. C.; Dantus, M.; Kim, S. B.; Zewail, A. H.: Ultrafast Diffraction and Molecular-Structure. *Chem Phys Lett* **1992**, *196*, 529-534.
(40) Williamson, J. C.; Zewail, A. H.: Ultrafast Electron-Diffraction .4. Molecular-Structures and Coherent Dynamics. *Journal of Physical Chemistry* **1994**, *98*, 2766-2781.
(41) Dantus, M.; Kim, S. B.; Williamson, J. C.; Zewail, A. H.: Ultrafast Electron-Diffraction .5. Experimental Time Resolution and Applications. *Journal of Physical Chemistry* **1994**, *98*, 2782-2796.
(42) Ma, H.; Lin, S. H.; Rentzepis, P.: Theoretical-Study of Laser-Heating and Dissociation Reactions in Solids Using Ultrafast Time-Resolved X-Ray-Diffraction. *J Appl Phys* **1992**, *72*, 2174-2178.
(43) Anderson, T.; Tomov, I. V.; Rentzepis, P. M.: A High-Repetition-Rate, Picosecond Hard X-Ray System, and Its Application to Time-Resolved X-Ray-Diffraction. *J Chem Phys* **1993**, *99*, 869-875.
(44) Kieffer, J. C.; Chaker, M.; Matte, J. P.; Pepin, H.; Cote, C. Y.; Beaudoin, Y.; Johnston, T. W.; Chien, C. Y.; Coe, S.; Mourou, G.; Peyrusse, O.: Ultrafast X-Ray Sources. *Phys Fluids B-Plasma* **1993**, *5*, 2676-2681.

(45) Petkov, V.; Takeda, S.; Waseda, Y.; Sugiyama, K.: Structural Study of Molten Germanium by Energy-Dispersive X-Ray-Diffraction. *J Non-Cryst Solids* **1994**, *168*, 97-105.
(46) Tomov, I. V.; Chen, P.; Rentzepis, P. M.: Nanosecond Hard X-Ray Source for Time-Resolved X-Ray-Diffraction Studies. *Review of Scientific Instruments* **1995**, *66*, 5214-5217.
(47) Chen, P.; Tomov, I. V.; Rentzepis, P. M.: Time resolved heat propagation in a gold crystal by means of picosecond x-ray diffraction. *J Chem Phys* **1996**, *104*, 10001-10007.
(48) Larsson, J.; Judd, E.; Falcone, R. W.; Asfaw, A.; Lee, R. W.; Heimann, P. A.; Padmore, H. A.; Wark, J.: Time-resolved X-ray diffraction from laser-heated crystals. *Inst Phys Conf Ser* **1996**, 367-371.
(49) Wulff, M.; Ursby, T.; Bourgeois, D.; Schotte, F.; Zontone, F.; Lorenzen, M.: New opportunities for time resolved x-ray scattering at the ESRF. *J Chim Phys Pcb* **1996**, *93*, 1915-1937.
(50) Larsson, J.; Chang, Z.; Judd, E.; Schuck, P. J.; Falcone, R. W.; Heimann, P. A.; Padmore, H. A.; Kapteyn, H. C.; Bucksbaum, P. H.; Murnane, M. M.; Lee, R. W.; Machacek, A.; Wark, J. S.; Liu, X.; Shan, B.: Ultrafast x-ray diffraction using a streak-camera detector in averaging mode. *Optics Letters* **1997**, *22*, 1012-1014.
(51) Raksi, F.; Wilson, K. R.; Jiang, Z. M.; Ikhlef, A.; Cote, C. Y.; Kieffer, J. C.: Ultrafast x-ray absorption probing of a chemical reaction. *J Chem Phys* **1996**, *104*, 6066-6069.
(52) BenNun, M.; Cao, J. S.; Wilson, K. R.: Ultrafast X-ray and electron diffraction: Theoretical considerations. *Journal of Physical Chemistry A* **1997**, *101*, 8743-8761.
(53) Cao, J. S.; Wilson, K. R.: Ultrafast X-ray diffraction theory. *Journal of Physical Chemistry A* **1998**, *102*, 9523-9530.
(54) Bressler, C.; Chergui, M.; Pattison, P.; Wulff, M.; Filipponi, A.; Abela, R.: A laser and synchrotron radiation pump-probe X-ray absorption experiment with sub-ns resolution. *Proceedings of SPIE* **1998**, *3451*, 108-116.
(55) Shorokhov, D.; Zewail, A. H.: 4D electron imaging: principles and perspectives. *Phys Chem Chem Phys* **2008**, *10*, 2879-2893.
(56) Chergui, M.; Zewail, A. H.: Electron and X-Ray Methods of Ultrafast Structural Dynamics: Advances and Applications. *Chemphyschem* **2009**, *10*, 28-43.
(57) Zewail, A.; Thomas, J. M.: *4D electron microscopy imaging in space and time*; Imperial college press: London, 2010.
(58) Yang, D. S.; Baum, P.; Zewail, A. H.: Ultrafast electron crystallography of the cooperative reaction path in vanadium dioxide. *Structural Dynamics* **2016**, *3*.
(59) van der Veen, R. M.; Penfold, T. J.; Zewail, A. H.: Ultrafast core-loss spectroscopy in four-dimensional electron microscopy. *Structural Dynamics* **2015**, *2*.
(60) Shorokhov, D.; Zewail, A. H.: Perspective: 4D ultrafast electron microscopy-Evolutions and revolutions. *J Chem Phys* **2016**, *144*.
(61) Bressler, C.; Chergui, M.: Ultrafast X-ray absorption spectroscopy. *Chem Rev* **2004**, *104*, 1781-1812.
(62) Bressler, C.; Abela, R.; Chergui, M.: Exploiting EXAFS and XANES for time-resolved molecular structures in liquids. *Z Kristallogr* **2008**, *223*, 307-321.
(63) Bressler, C.; Chergui, M.: Time-resolved X-ray absorption spectroscopy. *Actual Chimique* **2008**, 59-61.
(64) Chen, L. X.: Probing transient molecular structures in photochemical processes using laser-initiated time-resolved X-ray absorption spectroscopy. *Annu Rev Phys Chem* **2005**, *56*, 221-254.
(65) Chen, L. X.; Zhang, X. Y.; Lockard, J. V.; Stickrath, A. B.; Attenkofer, K.; Jennings, G.; Liu, D. J.: Excited-state molecular structures captured by X-ray transient absorption spectroscopy: a decade and beyond. *Acta Crystallogr A* **2010**, *66*, 240-251.
(66) Graber, T.; Anderson, S.; Brewer, H.; Chen, Y. S.; Cho, H. S.; Dashdorj, N.; Henning, R. W.; Kosheleva, I.; Macha, G.; Meron, M.; Pahl, R.; Ren, Z.; Ruan, S.; Schotte, F.; Rajer, V. S.; Viccaro, P. J.; Westferro, F.; Anfinrud, P.; Moffat, K.: BioCARS: a synchrotron resource for time-resolved X-ray science. *Journal of Synchrotron Radiation* **2011**, *18*, 658-670.
(67) Bressler, C.; Chergui, M.: Molecular Structural Dynamics Probed by Ultrafast X-Ray Absorption Spectroscopy. *Annual Review of Physical Chemistry, Vol 61* **2010**, *61*, 263-282.
(68) Chergui, M.: Picosecond and femtosecond X-ray absorption spectroscopy of molecular systems. *Acta Crystallogr A* **2010**, *66*, 229-239.
(69) Chergui, M.: In-situ Characterization of Molecular Processes in Liquids by Ultrafast X-ray Absorption Spectroscopy. In *In-situ Materials Characterization*; Ziegler, A., Graafsma, H., Zhang, X. F., Frenken, J. W. M., Eds.; Springer Berlin Heidelberg, 2014; Vol. 193; pp 1-38.
(70) Milne, C. J.; Penfold, T. J.; Chergui, M.: Recent experimental and theoretical developments in time-resolved X-ray spectroscopies. *Coordin Chem Rev* **2014**, *277–278*, 44-68.
(71) Chergui, M.: Time-resolved X-ray spectroscopies of chemical systems: New perspectives. *Structural Dynamics* **2016**, *3*, 031001.
(72) Elsaesser, T.; Woerner, M.: Photoinduced structural dynamics of polar solids studied by femtosecond X-ray diffraction. *Acta Crystallogr A* **2010**, *66*, 168-178.
(73) Pfeifer, T.; Spielmann, C.; Gerber, G.: Femtosecond x-ray science. *Reports on Progress in Physics* **2006**, *69*, 443-505.
(74) Schoenlein, R. W.; Chattopadhyay, S.; Chong, H. H. W.; Glover, T. E.; Heimann, P. A.; Shank, C. V.; Zholents, A. A.; Zolotorev, M. S.: Generation of femtosecond pulses of synchrotron radiation. *Science* **2000**, *287*, 2237-2240.
(75) Heimann, P. A.; Padmore, H. A.; Schoenlein, R. W.: ALS Beamline 6.0 for ultrafast X-ray absorption spectroscopy. *Synchrotron Radiation Instrumentation* **2004**, *705*, 1407-1410.
(76) Khan, S.; Holldack, K.; Kachel, T.; Mitzner, R.; Quast, T.: Femtosecond undulator radiation from sliced electron bunches. *Physical Review Letters* **2006**, *97*, 074801.
(77) Beaud, P.; Johnson, S. L.; Streun, A.; Abela, R.; Abramsohn, D.; Grolimund, D.; Krasniqi, F.; Schmidt, T.; Schlott, V.; Ingold, G.: Spatiotemporal stability of a femtosecond hard-X-ray undulator source studied by control of coherent optical phonons. *Physical Review Letters* **2007**, *99*.
(78) Bostedt, C.; Boutet, S.; Fritz, D. M.; Huang, Z.; Lee, H. J.; Lemke, H. T.; Robert, A.; Schlotter, W. F.; Turner, J. J.; Williams, G. J.: Linac Coherent Light Source: The first five years. *Rev Mod Phys* **2016**, *88*, 015007.
(79) Rousse, A.; Rischel, C.; Gauthier, J. C.: Ultrafast X-ray sources and applications. *Comptes Rendus De L Academie Des Sciences Serie Iv Physique Astrophysique* **2000**, *1*, 305-315.
(80) Von der Linde, D.; Sokolowski-Tinten, K.; Blome, C.; Dietrich, C.; Zhou, P.; Tarasevitch, A.; Cavalleri, A.; Siders, C. W.; Barty, C. P. J.; Squier, J.; Wilson, K. R.; Uschmann, I.; Forster, E.: Generation and application of ultrashort X-ray pulses. *Laser Part Beams* **2001**, *19*, 15-22.
(81) Rousse, A.; Rischel, C.; Fourmaux, S.; Uschmann, I.; Sebban, S.; Grillon, G.; Balcou, P.; Foster, E.; Geindre, J. P.; Audebert, P.; Gauthier, J. C.; Hulin, D.: Non-thermal melting in semiconductors measured at femtosecond resolution. *Nature* **2001**, *410*, 65-68.
(82) Rischel, C.; Rousse, A.; Uschmann, I.; Albouy, P. A.; Geindre, J. P.; Audebert, P.; Gauthier, J. C.; Forster, E.; Martin, J. L.; Antonetti, A.: Femtosecond time-resolved X-ray diffraction from laser-heated organic films. *Nature* **1997**, *390*, 490-492.

(83) Zhavoronkov, N.; Schmising, K. V. K.; Bargheer, M.; Woerner, M.; Elsaesser, T.; Klimo, O.; Limpouch, J.: High repetition rate ultrafast X-ray source from the fs-laser-produced-plasma. *Journal De Physique Iv* **2006**, *133*, 1201-1203.
(84) Weisshaupt, J.; Juve, V.; Holtz, M.; Ku, S. A.; Woerner, M.; Elsaesser, T.; Alisuskas, S.; Pugzlys, A.; Baltuska, A.: High-brightness table-top hard X-ray source driven by sub-100-femtosecond mid-infrared pulses. *Nat Photonics* **2014**, *8*, 927-930.
(85) Wulff, M.; Kong, Q. Y.; Lee, J. H.; Lo Russo, M.; Kim, T. K.; Lorenc, M.; Cammarata, M.; Bratos, S.; Buslaps, T.; Honkimaki, V.; Ihee, H.: Photolysis of Br(2) in CCl(4) studied by time-resolved X-ray scattering. *Acta Crystallogr A* **2010**, *66*, 252-260.
(86) Cammarata, M.; Levantino, M.; Schotte, F.; Anfinrud, P. A.; Ewald, F.; Choi, J.; Cupane, A.; Wulff, M.; Ihee, H.: Tracking the structural dynamics of proteins in solution using time-resolved wide-angle X-ray scattering. *Nat Methods* **2008**, *5*, 881-886.
(87) Nozawa, S.; Adachi, S. I.; Takahashi, J. I.; Tazaki, R.; Guerin, L.; Daimon, M.; Tomita, A.; Sato, T.; Chollet, M.; Collet, E.; Cailleau, H.; Yamamoto, S.; Tsuchiya, K.; Shioya, T.; Sasaki, H.; Mori, T.; Ichiyanagi, K.; Sawa, H.; Kawata, H.; Koshihara, S.: Developing 100 ps-resolved X-ray structural analysis capabilities on beamline NW14A at the Photon Factory Advanced Ring. *Journal of Synchrotron Radiation* **2007**, *14*, 313-319.
(88) Collet, E.: Dynamical structural science. *Acta Crystallogr A* **2010**, *66*, 133-134.
(89) Bressler, C.; Saes, M.; Chergui, M.; Abela, R.; Pattison, P.: Optimizing a time-resolved X-ray absorption experiment. *Nuclear Instruments & Methods in Physics Research Section a-Accelerators Spectrometers Detectors and Associated Equipment* **2001**, *467*, 1444-1446.
(90) Bressler, C.; Saes, M.; Chergui, M.; Grolimund, D.; Abela, R.; Pattison, P.: Towards structural dynamics in condensed chemical systems exploiting ultrafast time-resolved x-ray absorption spectroscopy. *J Chem Phys* **2002**, *116*, 2955-2966.
(91) Saes, M.; Bressler, C.; Abela, R.; Grolimund, D.; Johnson, S. L.; Heimann, P. A.; Chergui, M.: Observing photochemical transients by ultrafast x-ray absorption spectroscopy. *Physical Review Letters* **2003**, *90*, 047403-1.
(92) Saes, M. G., W.; Kaiser, M.; Tarnovsky, A.; Bressler, Ch.; Chergui, M.; Johnson, S. L.; Grolimund, D.; Abela, R.: Ultrafast Time-Resolved X-Ray Absorption Spectroscopy of Chemical Systems. *Synchrotron Radiation News* **2003**, *16*, 12.
(93) Chergui, M.; Bressler, C.; Abela, R.: The Fast show with X-rays and Electrons. *Synchrotron radiation News* **2004**.
(94) Saes, M.; Bressler, C.; van Mourik, F.; Gawelda, W.; Kaiser, M.; Chergui, M.; Bressler, C.; Grolimund, D.; Abela, R.; Glover, T. E.; Heimann, P. A.; Schoenlein, R. W.; Johnson, S. L.; Lindenberg, A. M.; Falcone, R. W.: A setup for ultrafast time-resolved x-ray absorption spectroscopy. *Review of Scientific Instruments* **2004**, *75*, 24-30.
(95) Gawelda, W.; Bressler, C.; Saes, M.; Kaiser, M.; Tarnovsky, A. N.; Grolimund, D.; Johnson, S. L.; Abela, R.; Chergui, M.: Picosecond time-resolved X-ray Absorption Spectroscopy of solvated organometallic complexes. *Physica Scripta* **2005**, *T115*, 102-106.
(96) Gawelda, W.; Pham, V. T.; Benfatto, M.; Zaushitsyn, Y.; Kaiser, M.; Grolimund, D.; Johnson, S. L.; Abela, R.; Hauser, A.; Bressler, C.; Chergui, M.: Structural determination of a short-lived excited iron(II) complex by picosecond x-ray absorption spectroscopy. *Physical Review Letters* **2007**, *98*, 057401.
(97) Cannizzo, A.; Milne, C. J.; Consani, C.; Gawelda, W.; Bressler, C.; van Mourik, F.; Chergui, M.: Light-induced spin crossover in Fe(II)-based complexes: The full photocycle unraveled by ultrafast optical and X-ray spectroscopies. *Coordin Chem Rev* **2010**, *254*, 2677-2686.
(98) Chen, L. X.: Probing transient molecular structures with time-resolved pump/probe XAFS using synchrotron X-ray sources. *Journal of Electron Spectroscopy and Related Phenomena* **2001**, *119*, 161-174.
(99) Chen, L. X.; Jager, W. J. H.; Jennings, G.; Gosztola, D. J.; Munkholm, A.; Hessler, J. P.: Capturing a photoexcited molecular structure through time-domain X-ray absorption fine structure. *Science* **2001**, *292*, 262-264.
(100) Jennings, G.; Jager, W. J. H.; Chen, L. X.: Application of a multi-element Ge detector in laser pump/x-ray probe time-domain x-ray absorption fine structure. *Review of Scientific Instruments* **2002**, *73*, 362-368.
(101) Huse, N.; Kim, T. K.; Jamula, L.; McCusker, J. K.; de Groot, F. M. F.; Schoenlein, R. W.: Photo-Induced Spin-State Conversion in Solvated Transition Metal Complexes Probed via Time-Resolved Soft X-ray Spectroscopy. *Journal of the American Chemical Society* **2010**, *132*, 6809-6816.
(102) Katz, J. E.; Zhang, X. Y.; Attenkofer, K.; Chapman, K. W.; Frandsen, C.; Zarzycki, P.; Rosso, K. M.; Falcone, R. W.; Waychunas, G. A.; Gilbert, B.: Electron Small Polarons and Their Mobility in Iron (Oxyhydr)oxide Nanoparticles. *Science* **2012**, *337*, 1200-1203.
(103) Sato, T.; Nozawa, S.; Ichiyanagi, K.; Tomita, A.; Chollet, M.; Ichikawa, H.; Fujii, H.; Adachi, S.-i.; Koshihara, S.-y.: Capturing molecular structural dynamics by 100 ps
time-resolved X-ray absorption spectroscopy. *Journal of Synchrotron Radiation* **2009**, *16*, 110–115.
(104) Nozawa, S.; Sato, T.; Chollet, M.; Ichiyanagi, K.; Tomita, A.; Fujii, H.; Adachi, S.; Koshihara, S.: Direct Probing of Spin State Dynamics Coupled with Electronic and Structural Modifications by Picosecond Time-Resolved XAFS. *Journal of the American Chemical Society* **2010**, *132*, 61-+.
(105) Lima, F. A.; Milne, C. J.; Amarasinghe, D. C. V.; Rittmann-Frank, M. H.; van der Veen, R. M.; Reinhard, M.; Pham, V. T.; Karlsson, S.; Johnson, S. L.; Grolimund, D.; Borca, C.; Huthwelker, T.; Janousch, M.; van Mourik, F.; Abela, R.; Chergui, M.: A high-repetition rate scheme for synchrotron-based picosecond laser pump/x-ray probe experiments on chemical and biological systems in solution. *Review of Scientific Instruments* **2011**, *82*, 063111.
(106) Bressler, C.; Gawelda, W.; Galler, A.; Nielsen, M. M.; Sundstrom, V.; Doumy, G.; March, A. M.; Southworth, S. H.; Young, L.; Vanko, G.: Solvation dynamics monitored by combined X-ray spectroscopies and scattering: photoinduced spin transition in aqueous [Fe(bpy)3]2+. *Faraday Discussions* **2014**, *171*, 169-178.
(107) March, A. M.; Stickrath, A.; Doumy, G.; Kanter, E. P.; Krassig, B.; Southworth, S. H.; Attenkofer, K.; Kurtz, C. A.; Chen, L. X.; Young, L.: Development of high-repetition-rate laser pump/x-ray probe methodologies for synchrotron facilities. *Review of Scientific Instruments* **2011**, *82*, 073110.
(108) Stebel, L.; Malvestuto, M.; Capogrosso, V.; Sigalotti, P.; Ressel, B.; Bondino, F.; Magnano, E.; Cautero, G.; Parmigiani, F.: Time-resolved soft x-ray absorption setup using multi-bunch operation modes at synchrotrons. *Review of Scientific Instruments* **2011**, *82*, 123109.
(109) Zholents, A. A.; Zolotorev, M. S.: Femtosecond x-ray pulses of synchrotron radiation. *Physical Review Letters* **1996**, *76*, 912-915.
(110) Steier, C.; Robin, D.; Sannibale, F.; Schoenlein, R.; Wan, W.; Wittmer, W.; Zholents, A.: The new undulator based fs-slicing beamline at the ALS. *Ieee Part Acc Conf* **2005**, 1645-1647.
(111) Heimann, P. A.; Glover, T. E.; Plate, D.; Lee, H. J.; Brown, V. C.; Padmore, H. A.; Schoenlein, R. W.: The advanced light source (ALS) slicing undulator beamline. *Aip Conf Proc* **2007**, *879*, 1195-1197.
(112) Holldack, K.; Khan, S.; Mitzner, R.; Quast, T.: Femtosecond terahertz radiation from femtoslicing at BESSY. *Physical Review Letters* **2006**, *96*, 054801

(113) Bressler, C.; Milne, C.; Pham, V. T.; ElNahhas, A.; van der Veen, R. M.; Gawelda, W.; Johnson, S.; Beaud, P.; Grolimund, D.; Kaiser, M.; Borca, C. N.; Ingold, G.; Abela, R.; Chergui, M.: Femtosecond XANES Study of the Light-Induced Spin Crossover Dynamics in an Iron(II) Complex. *Science* **2009**, *323*, 489-492.
(114) Emma, P.; Akre, R.; Arthur, J.; Bionta, R.; Bostedt, C.; Bozek, J.; Brachmann, A.; Bucksbaum, P.; Coffee, R.; Decker, F. J.; Ding, Y.; Dowell, D.; Edstrom, S.; Fisher, A.; Frisch, J.; Gilevich, S.; Hastings, J.; Hays, G.; Hering, P.; Huang, Z.; Iverson, R.; Loos, H.; Messerschmidt, M.; Miahnahri, A.; Moeller, S.; Nuhn, H. D.; Pile, G.; Ratner, D.; Rzepiela, J.; Schultz, D.; Smith, T.; Stefan, P.; Tompkins, H.; Turner, J.; Welch, J.; White, W.; Wu, J.; Yocky, G.; Galayda, J.: First lasing and operation of an angstrom-wavelength free-electron laser. *Nat Photonics* **2010**, *4*, 641-647.
(115) Ishikawa, T.; Aoyagi, H.; Asaka, T.; Asano, Y.; Azumi, N.; Bizen, T.; Ego, H.; Fukami, K.; Fukui, T.; Furukawa, Y.; Goto, S.; Hanaki, H.; Hara, T.; Hasegawa, T.; Hatsui, T.; Higashiya, A.; Hirono, T.; Hosoda, N.; Ishii, M.; Inagaki, T.; Inubushi, Y.; Itoga, T.; Joti, Y.; Kago, M.; Kameshima, T.; Kimura, H.; Kirihara, Y.; Kiyomichi, A.; Kobayashi, T.; Kondo, C.; Kudo, T.; Maesaka, H.; Marechal, X. M.; Masuda, T.; Matsubara, S.; Matsumoto, T.; Matsushita, T.; Matsui, S.; Nagasono, M.; Nariyama, N.; Ohashi, H.; Ohata, T.; Ohshima, T.; Ono, S.; Otake, Y.; Saji, C.; Sakurai, T.; Sato, T.; Sawada, K.; Seike, T.; Shirasawa, K.; Sugimoto, T.; Suzuki, S.; Takahashi, S.; Takebe, H.; Takeshita, K.; Tamasaku, K.; Tanaka, H.; Tanaka, R.; Tanaka, T.; Togashi, T.; Togawa, K.; Tokuhisa, A.; Tomizawa, H.; Tono, K.; Wu, S. K.; Yabashi, M.; Yamaga, M.; Yamashita, A.; Yanagida, K.; Zhang, C.; Shintake, T.; Kitamura, H.; Kumagai, N.: A compact X-ray free-electron laser emitting in the sub-angstrom region. *Nat Photonics* **2012**, *6*, 540-544.
(116) Patterson, B. D.; Abela, R.: Novel opportunities for time-resolved absorption spectroscopy at the X-ray free electron laser. *Phys Chem Chem Phys* **2010**, *12*, 5647-5652.
(117) Harmand, M.; Coffee, R.; Bionta, M. R.; Chollet, M.; French, D.; Zhu, D.; Fritz, D. M.; Lemke, H. T.; Medvedev, N.; Ziaja, B.; Toleikis, S.; Cammarata, M.: Achieving few-femtosecond time-sorting at hard X-ray free-electron lasers. *Nat Photonics* **2013**, *7*, 215-218.
(118) Allaria, E.; Callegari, C.; Cocco, D.; Fawley, W. M.; Kiskinova, M.; Masciovecchio, C.; Parmigiani, F.: The FERMI@Elettra free-electron-laser source for coherent x-ray physics: photon properties, beam transport system and applications. *New J Phys* **2010**, *12*.
(119) Zangrando, M.; Cudin, I.; Fava, C.; Gerusina, S.; Gobessi, R.; Godnig, R.; Rumiz, L.; Svetina, C.; Parmigiani, F.; Cocco, D.: First results from the commissioning of the FERMI@Elettra free electron laser by means of the Photon Analysis Delivery and Reduction System (PADReS). *Advances in X-Ray Free-Electron Lasers: Radiation Schemes, X-Ray Optics, and Instrumentation* **2011**, *8078*.
(120) Allaria, E.; Appio, R.; Badano, L.; Barletta, W. A.; Bassanese, S.; Biedron, S. G.; Borga, A.; Busetto, E.; Castronovo, D.; Cinquegrana, P.; Cleva, S.; Cocco, D.; Cornacchia, M.; Craievich, P.; Cudin, I.; D'Auria, G.; Dal Forno, M.; Danailov, M. B.; De Monte, R.; De Ninno, G.; Delgiusto, P.; Demidovich, A.; Di Mitri, S.; Diviacco, B.; Fabris, A.; Fabris, R.; Fawley, W.; Ferianis, M.; Ferrari, E.; Ferry, S.; Froehlich, L.; Furlan, P.; Gaio, G.; Gelmetti, F.; Giannessi, L.; Giannini, M.; Gobessi, R.; Ivanov, R.; Karantzoulis, E.; Lonza, M.; Lutman, A.; Mahieu, B.; Milloch, M.; Milton, S. V.; Musardo, M.; Nikolov, I.; Noe, S.; Parmigiani, F.; Penco, G.; Petronio, M.; Pivetta, L.; Predonzani, M.; Rossi, F.; Rumiz, L.; Salom, A.; Scafuri, C.; Serpico, C.; Sigalotti, P.; Spampinati, S.; Spezzani, C.; Svandrlik, M.; Svetina, C.; Tazzari, S.; Trovo, M.; Umer, R.; Vascotto, A.; Veronese, M.; Visintini, R.; Zaccaria, M.; Zangrando, D.; Zangrando, M.: Highly coherent and stable pulses from the FERMI seeded free-electron laser in the extreme ultraviolet. *Nat Photonics* **2012**, *6*, 699-704.
(121) Hara, T.: Fully coherent soft X-rays at FERMI. *Nat Photonics* **2013**, *7*, 851-854.
(122) Rehr, J. J.; Albers, R. C.: Theoretical approaches to x-ray absorption fine structure. *Rev Mod Phys* **2000**, *72*, 621-654.
(123) Filipponi, A.; Dicicco, A.; Tyson, T. A.; Natoli, C. R.: Abinitio Modeling of X-Ray Absorption-Spectra. *Solid State Commun* **1991**, *78*, 265-268.
(124) Natoli, C. R.; Benfatto, M.; Della Longa, S.; Hatada, K.: X-ray absorption spectroscopy: state-of-the-art analysis. *Journal of Synchrotron Radiation* **2003**, *10*, 26-42.
(125) Roscioni, O. M.; D'Angelo, P.; Chillemi, G.; Della Lonaga, S.; Benfatto, M.: Quantitative analysis of XANES spectra of disordered systems based on molecular dynamics. *Journal of Synchrotron Radiation* **2005**, *12*, 75-79.
(126) Oyanagi, H.: X-ray absorption fine structure. In *Applications of synchrotron radiation to material science*; Saisho, H. G., Y., Ed.; Elsevier Science B. V., 1996.
(127) Benfatto, M.; Della Longa, S.: Geometrical fitting of experimental XANES spectra by a full multiple-scattering procedure. *Journal of Synchrotron Radiation* **2001**, *8*, 1087-1094.
(128) Joly, Y.: X-ray absorption near-edge structure calculations beyond the muffin-tin approximation. *Physical Review B* **2001**, *63*, art. no.-125120.
(129) Bergmann, U.; Glatzel, P.: X-ray emission spectroscopy. *Photosynth Res* **2009**, *102*, 255-266.
(130) Hämäläinen, K.; Manninen, S.: Resonant and non-resonant inelastic x-ray scattering. *Journal of Physics: Condensed Matter* **2001**, *13*, 7539.
(131) Goulon, J.; Goulon-Ginet, C.; Cortes, R.; Dubois, J. M.: On experimental attenuation factors of the amplitude of the EXAFS oscillations in absorption, reflectivity and luminescence measurements. *J. Phys. France* **1982**, *43*, 539-548.
(132) Glatzel, P.; Jacquamet, L.; Bergmann, U.; de Groot, F. M. F.; Cramer, S. P.: Site-Selective EXAFS in Mixed-Valence Compounds Using High-Resolution Fluorescence Detection: A Study of Iron in Prussian Blue. *Inorg Chem* **2002**, *41*, 3121-3127.
(133) Yano, J.; Pushkar, Y.; Glatzel, P.; Lewis, A.; Sauer, K.; Messinger, J.; Bergmann, U.; Yachandra, V.: High-Resolution Mn EXAFS of the Oxygen-Evolving Complex in Photosystem II: Structural Implications for the Mn4Ca Cluster. *Journal of the American Chemical Society* **2005**, *127*, 14974-14975.
(134) Kramers, H. A.; Heisenberg, W.: Über die Streuung von Strahlung durch Atome. *Zeitschrift für Physik* **1925**, *31*, 681-708.
(135) Ament, L. J. P.; van Veenendaal, M.; Devereaux, T. P.; Hill, J. P.; van den Brink, J.: Resonant inelastic x-ray scattering studies of elementary excitations. *Rev Mod Phys* **2011**, *83*, 705-767.
(136) Kotani, A.; Shin, S.: Resonant inelastic x-ray scattering spectra for electrons in solids. *Rev Mod Phys* **2001**, *73*, 203-246.
(137) Glatzel, P.; Bergmann, U.: High resolution 1s core hole X-ray spectroscopy in 3d transition metal complexes - electronic and structural information. *Coordin Chem Rev* **2005**, *249*, 65-95.
(138) Hamalainen, K.; Manninen, S.; Suortti, P.; Collins, S. P.; Cooper, M. J.; Laundy, D.: Resonant Raman scattering and inner-shell hole widths in Cu, Zn and Ho. *Journal of Physics: Condensed Matter* **1989**, *1*, 5955.
(139) Delgado-Jaime, M. U.; Dible, B. R.; Chiang, K. P.; Brennessel, W. W.; Bergmann, U.; Holland, P. L.; DeBeer, S.: Identification of a Single Light Atom within a Multinuclear Metal Cluster Using Valence-to-Core X-ray Emission Spectroscopy. *Inorg Chem* **2011**, *50*, 10709-10717.
(140) Lancaster, K. M.; Roemelt, M.; Ettenhuber, P.; Hu, Y.; Ribbe, M. W.; Neese, F.; Bergmann, U.; DeBeer, S.: X-ray Emission Spectroscopy Evidences a Central Carbon in the Nitrogenase Iron-Molybdenum Cofactor. *Science* **2011**, *334*, 974-977.
(141) Szlachetko, J.; Cotte, M.; Morse, J.; Salome, M.; Jagodzinski, P.; Dousse, J.-C.; Hoszowska, J.; Kayser, Y.; Susini, J.: Wavelength-dispersive spectrometer for X-ray microfluorescence analysis at the X-ray microscopy beamline ID21 (ESRF). *Journal of Synchrotron Radiation* **2010**, *17*, 400-408.
(142) Gel'mukhanov, F.; Ågren, H.: Resonant X-ray Raman scattering. *Physics Reports* **1999**, *312*, 87-330.

(143) De Groot, F.; Kotani, A.: *Core Level Spectroscopy of Solids*; Taylor & Francis: New York, 2008.
(144) Szlachetko, J.; Nachtegaal, M.; de Boni, E.; Willimann, M.; Safonova, O.; Sa, J.; Smolentsev, G.; Szlachetko, M.; van Bokhoven, J. A.; Dousse, J. C.; Hoszowska, J.; Kayser, Y.; Jagodzinski, P.; Bergamaschi, A.; Schmitt, B.; David, C.; Lucke, A.: A von Hamos x-ray spectrometer based on a segmented-type diffraction crystal for single-shot x-ray emission spectroscopy and time-resolved resonant inelastic x-ray scattering studies. *Review of Scientific Instruments* **2012**, *83*.
(145) Josefsson, I.; Kunnus, K.; Schreck, S.; Fohlisch, A.; de Groot, F.; Wernet, P.; Odelius, M.: Ab Initio Calculations of X-ray Spectra: Atomic Multiplet and Molecular Orbital Effects in a Multiconfigurational SCF Approach to the L-Edge Spectra of Transition Metal Complexes. *J Phys Chem Lett* **2012**, *3*, 3565-3570.
(146) Kas, J. J.; Rehr, J. J.; Soininen, J. A.; Glatzel, P.: Real-space Green's function approach to resonant inelastic x-ray scattering. *Physical Review B* **2011**, *83*, 235114.
(147) McMorrow, D.; Als-Nielsen, J.: *Elements of modern X-ray physics*; 2nd ed.; Wiley: Hoboken, 2011.
(148) Warren, B. E.: *X-ray diffraction*; Dover ed.; Dover Publications: New York, 1990.
(149) Bratos, S.; Leicknam, J. C.; Mirloup, F.; Vuilleumier, R.; Gallot, G.; Wulff, M.; Plech, A.; Pommeret, S.: Real time visualizing of atomic motions in dense phases. *Novel Approaches to the Structure and Dynamics of Liquids: Experiments, Theories and Simulations* **2004**, 111-128.
(150) Kjær, K. S.; van Driel, T. B.; Kehres, J.; Haldrup, K.; Khakhulin, D.; Bechgaard, K.; Cammarata, M.; Wulff, M.; Sørensen, T. J.; Nielsen, M. M.: Introducing a standard method for experimental determination of the solvent response in laser pump, X-ray probe time-resolved wide-angle X-ray scattering experiments on systems in solution. *Phys Chem Chem Phys* **2013**, *15*, 15003-15016.
(151) Cammarata, M.; Lorenc, M.; Kim, T. K.; Lee, J. H.; Kong, Q. Y.; Pontecorvo, E.; Lo Russo, M.; Schiro, G.; Cupane, A.; Wulff, M.; Ihee, H.: Impulsive solvent heating probed by picosecond x-ray diffraction. *J Chem Phys* **2006**, *124*, -.
(152) Sheldrick, G. M.: A short history of SHELX. *Acta Crystallogr A* **2008**, *64*, 112-122.
(153) Petricek, V.; Dusek, M.; Palatinus, L.: Crystallographic Computing System JANA2006: General features. *Z Kristallogr* **2014**, *229*, 345-352.
(154) Landau, L. D.: On the theory of phase transitions. I. *Zh. Eksp. Teor. Fiz.* **1937**, *11*, 19.
(155) Gao, M.; Lu, C.; Jean-Ruel, H.; Liu, L. C.; Marx, A.; Onda, K.; Koshihara, S.; Nakano, Y.; Shao, X. F.; Hiramatsu, T.; Saito, G.; Yamochi, H.; Cooney, R. R.; Moriena, G.; Sciaini, G.; Miller, R. J. D.: Mapping molecular motions leading to charge delocalization with ultrabright electrons. *Nature* **2013**, *496*, 343-346.
(156) Collet, E.; Buron-Le Cointe, M.; Lemee-Cailleau, M. H.; Cailleau, H.; Toupet, L.; Meven, M.; Mattauch, S.; Heger, C.; Karl, N.: Structural evidence of ferrielectric neutral-ionic layered ordering in 2,6-dimethyltetrathiafulvalene-p-chloranil. *Physical Review B* **2001**, *63*.
(157) Buron-Le Cointe, M.; Lemee-Cailleau, M. H.; Cailleau, H.; Ravy, S.; Berar, J. F.; Rouziere, S.; Elkaim, E.; Collet, E.: One-dimensional fluctuating nanodomains in the charge-transfer molecular system TTF-CA and their first-order crystallization. *Physical Review Letters* **2006**, *96*.
(158) Guerin, L.; Hebert, J.; Cointe, M. B. L.; Adachi, S.; Koshihara, S.; Cailleau, H.; Collet, E.: Capturing One-Dimensional Precursors of a Photoinduced Transformation in a Material. *Physical Review Letters* **2010**, *105*, -.
(159) Gawelda, W.; Johnson, M.; de Groot, F. M. F.; Abela, R.; Bressler, C.; Chergui, M.: Electronic and molecular structure of photoexcited [Ru-II(bpy)(3)](2+) probed by picosecond X-ray absorption spectroscopy. *Journal of the American Chemical Society* **2006**, *128*, 5001-5009.
(160) Tarnovsky, A. N.; Gawelda, W.; Johnson, M.; Bressler, C.; Chergui, M.: Photexcitation of aqueous ruthenium(II)-tris-(2,2 '-bipyridine) with high-intensity femtosecond laser pulses. *J Phys Chem B* **2006**, *110*, 26497-26505.
(161) König, E.; Watson, K. J.: *Chem Phys Lett* **1970**, *6*, 457-459.
(162) Benfatto, M.; Della Longa, S.; Hatada, K.; Hayakawa, K.; Gawelda, W.; Bressler, C.; Chergui, M.: A full multiple scattering model for the analysis of time-resolved X-ray difference absorption spectra. *J Phys Chem B* **2006**, *110*, 14035-14039.
(163) Yersin, H.; Braun, D.: Localization in Excited-States of Molecules - Application to [Ru(Bpy)3]2+. *Coordin Chem Rev* **1991**, *111*, 39-46.
(164) Nozaki, K.; Takamori, K.; Nakatsugawa, Y.; Ohno, T.: Theoretical studies of phosphorescence spectra of tris(2,2 '-bipyridine) transition metal compounds. *Inorg Chem* **2006**, *45*, 6161-6178.
(165) Alary, F.; Heully, J. L.; Bijeire, L.; Vicendo, P.: Is the (MLCT)-M-3 the only photoreactive state of polypyridyl complexes? *Inorg Chem* **2007**, *46*, 3154-3165.
(166) Zhang, X. Y.; Smolentsev, G.; Guo, J. C.; Attenkofer, K.; Kurtz, C.; Jennings, G.; Lockard, J. V.; Stickrath, A. B.; Chen, L. X.: Visualizing Interfacial Charge Transfer in Ru-Dye-Sensitized TiO2 Nanoparticles Using X-ray Transient Absorption Spectroscopy. *J Phys Chem Lett* **2011**, *2*, 628-632.
(167) Sato, T.; Nozawa, S.; Tomita, A.; Hoshino, M.; Koshihara, S.-y.; Fujii, H.; Adachi, S.-i.: Coordination and electronic structure of ruthenium (II)-tris-2, 2′-bipyridine in the triplet metal-to-ligand charge-transfer excited state observed by picosecond time-resolved Ru K-edge XAFS. *The Journal of Physical Chemistry C* **2012**, *116*, 14232-14236.
(168) Van Kuiken, B. E.; Huse, N.; Cho, H.; Strader, M. L.; Lynch, M. S.; Schoenlein, R. W.; Khalil, M.: Probing the Electronic Structure of a Photoexcited Solar Cell Dye with Transient X-ray Absorption Spectroscopy. *J Phys Chem Lett* **2012**, *3*, 1695-1700.
(169) Borfecchia, E.; Garino, C.; Salassa, L.; Ruiu, T.; Gianolio, D.; Zhang, X.; Attenkofer, K.; Chen, L. X.; Gobetto, R.; Sadler, P. J.: X-ray transient absorption structural characterization of the 3 MLCT triplet excited state of cis-[Ru (bpy) 2 (py) 2] 2+. *Dalton T* **2013**, *42*, 6564-6571.
(170) Van Kuiken, B. E.; Valiev, M.; Daifuku, S. L.; Bannan, C.; Strader, M. L.; Cho, H.; Huse, N.; Schoenlein, R. W.; Govind, N.; Khalil, M.: Simulating Ru L3-edge x-ray absorption spectroscopy with time-dependent density functional theory: Model complexes and electron localization in mixed-valence metal dimers. *The Journal of Physical Chemistry A* **2013**, *117*, 4444-4454.
(171) de Graaf, C.; Sousa, C.: Study of the Light-Induced Spin Crossover Process of the [Fe(II)(bpy)(3)](2+) Complex. *Chem-Eur J* **2010**, *16*, 4550-4556.
(172) Shaw, G. B.; Grant, C. D.; Shirota, H.; Castner, E. W.; Meyer, G. J.; Chen, L. X.: Ultrafast structural rearrangements in the MLCT excited state for copper(I) bis-phenanthrolines in solution. *Journal of the American Chemical Society* **2007**, *129*, 2147-2160.
(173) Lockard, J. V.; Kabehie, S.; Zink, J. I.; Smolentsev, G.; Soldatov, A.; Chen, L. X.: Influence of Ligand Substitution on Excited State Structural Dynamics in Cu(I) Bisphenanthroline Complexes. *J Phys Chem B* **2010**, *114*, 14521-14527.
(174) Huang, J.; Buyukcakir, O.; Mara, M. W.; Coskun, A.; Dimitrijevic, N. M.; Barin, G.; Kokhan, O.; Stickrath, A. B.; Ruppert, R.; Tiede, D. M.; Stoddart, J. F.; Sauvage, J. P.; Chen, L. X.: Highly Efficient Ultrafast Electron Injection from the Singlet MLCT Excited State of Copper(I) Diimine Complexes to TiO2 Nanoparticles. *Angew Chem Int Edit* **2012**, *51*, 12711-12715.
(175) Iwamura, M.; Takeuchi, S.; Tahara, T.: Real-time observation of the photoinduced structural change of bis(2,9-dimethyl-1,10-phenanthroline)copper(I) by femtosecond fluorescence spectroscopy: A realistic potential curve of the Jahn-Teller distortion. *Journal of the American Chemical Society* **2007**, *129*, 5248-5256.

(176) Iwamura, M.; Watanabe, H.; Ishii, K.; Takeuchi, S.; Tahara, T.: Excited-State Nuclear Wavepacket Motion of an Ultrafast Inorganic Molecular Switch. *Springer Series Chem* **2009**, *92*, 382-384
1031.
(177) Chen, L. X.; Shaw, G. B.; Novozhilova, I.; Liu, T.; Jennings, G.; Attenkofer, K.; Meyer, G. J.; Coppens, P.: MLCT state structure and dynamics of a copper(I) diimine complex characterized by pump-probe X-ray and laser spectroscopies and DFT calculations. *Journal of the American Chemical Society* **2003**, *125*, 7022-7034.
(178) Smolentsev, G.; Soldatov, A. V.; Chen, L. X.: Three-dimensional local structure of photoexcited cu diimine complex refined by quantitative XANES analysis. *Journal of Physical Chemistry A* **2008**, *112*, 5363-5367.
(179) Rossenaar, B. D.; Stufkens, D. J.; Vlcek, A.: Halide-dependent change of the lowest-excited-state character from MLCT to XLCT for the complexes Re(X)(CO)(3)(alpha-diimine) (X=Cl, Br, I; alpha-diimine equals bpy, iPr-PyCa, iPr-DAB) studied by resonance Raman, time-resolved absorption, and emission spectroscopy. *Inorg Chem* **1996**, *35*, 2902-2909.
(180) Rodriguez, A. M. B.; Gabrielsson, A.; Motevalli, M.; Matousek, P.; Towrie, M.; Sebera, J.; Zalis, S.; Vlcek, A.: Ligand-to-diimine/metal-to-diimine charge-transfer excited states of [Re(NCS)(CO)(3)(alpha-diimine)] (alpha-diimine=2,2 '-bipyridine, di-Pr-i-N,N-1,4-diazabutadiene). A spectroscopic and computational study. *Journal of Physical Chemistry A* **2005**, *109*, 5016-5025.
(181) El Nahhas, A.; van der Veen, R. M.; Penfold, T. J.; Pham, V. T.; Lima, F. A.; Abela, R.; Blanco-Rodriguez, A. M.; Zalis, S.; Vlcek, A.; Tavernelli, I.; Rothlisberger, U.; Milne, C. J.; Chergui, M.: X-ray Absorption Spectroscopy of Ground and Excited Rhenium-Carbonyl Diimine-Complexes: Evidence for a Two-Center Electron Transfer. *Journal of Physical Chemistry A* **2013**, *117*, 361-369.
(182) Penfold, T. J.; Karlsson, S.; Capano, G.; Lima, F. A.; Rittmann, J.; Reinhard, M.; Rittmann-Frank, M. H.; Braem, O.; Baranoff, E.; Abela, R.; Tavernelli, I.; Rothlisberger, U.; Milne, C. J.; Chergui, M.: Solvent-Induced Luminescence Quenching: Static and Time-Resolved X-Ray Absorption Spectroscopy of a Copper(I) Phenanthroline Complex. *Journal of Physical Chemistry A* **2013**, *117*, 4591-4601.
(183) McMillin, D. R.; Kirchhoff, J. R.; Goodwin, K. V.: Exciplex quenching of photo-excitd copper complexes. *Coordin Chem Rev* **1985**, *64*, 83-92.
(184) Capano, G.; Chergui, M.; Rothlisberger, U.; Tavernelli, I.; Penfold, T. J.: A Quantum Dynamics Study of the Ultrafast Relaxation in a Prototypical Cu(I)-Phenanthroline. *Journal of Physical Chemistry A* **2014**, *118*, 9861-9869.
(185) Capano, G.; Milne, C. J.; Chergui, M.; Rothlisberger, U.; Tavernelli, I.; Penfold, T. J.: Probing wavepacket dynamics using ultrafast x-ray spectroscopy. *Journal of Physics B: Atomic, Molecular and Optical Physics* **2015**, *48*, 214001.
(186) Chen, L. X.; Jennings, G.; Liu, T.; Gosztola, D. J.; Hessler, J. P.; Scaltrito, D. V.; Meyer, G. J.: Rapid excited-state structural reorganization captured by pulsed X-rays. *Journal of the American Chemical Society* **2002**, *124*, 10861-10867.
(187) Takeuchi, S.; Tahara, T.: Coherent nuclear wavepacket motions in ultrafast excited-state intramolecular proton transfer: Sub-30-fs resolved pump-probe absorption spectroscopy of 10-hydroxybenzo[h]quinoline in solution. *Journal of Physical Chemistry A* **2005**, *109*, 10199-10207.
(188) Iwamura, M.; Watanabe, H.; Ishii, K.; Takeuchi, S.; Tahara, T.: Coherent Nuclear Dynamics in Ultrafast Photoinduced Structural Change of Bis(diimine)copper(I) Complex. *Journal of the American Chemical Society* **2011**, *133*, 7728-7736.
(189) Hauser, A.: Light-induced spin crossover and the high-spin -> low-spin relaxation. *Spin Crossover in Transition Metal Compounds Ii* **2004**, *234*, 155-198.
(190) Goodwin, H. A.: Spin crossover in cobalt(II) systems. *Spin Crossover in Transition Metal Compounds Ii* **2004**, *234*, 23-47.
(191) Decurtins, S.; Gutlich, P.; Hasselbach, K. M.; Hauser, A.; Spiering, H.: Light-Induced Excited-Spin-State Trapping in Iron(Ii) Spin-Crossover Systems - Optical Spectroscopic and Magnetic-Susceptibility Study. *Inorg Chem* **1985**, *24*, 2174-2178.
(192) Marino, A.; Chakraborty, P.; Servol, M.; Lorenc, M.; Collet, E.; Hauser, A.: The Role of Ligand- Field States in the Ultrafast Photophysical Cycle of the Prototypical Iron(II) Spin- Crossover Compound [Fe(ptz)(6)](BF4). *Angew Chem Int Edit* **2014**, *53*, 3863-3867.
(193) Lawthers, I.; Mcgarvey, J. J.: Spin-State Relaxation Dynamics in Iron(Iii) Complexes - Photochemical Perturbation of the 2t Reversible 6a Spin Equilibrium by Pulsed-Laser Irradiation in the Ligand-to-Metal Charge-Transfer Absorption-Band. *Journal of the American Chemical Society* **1984**, *106*, 4280-4282.
(194) Gawelda, W.; Pham, V. T.; El Nahhas, A.; Kaiser, M.; Zaushytsin, Y.; Johnson, S.; Grolimund, D.; Abela, R.; Hauser, A.; Bressler, C.; Chergui, M.: Capturing Transient Electronic and Molecular Structures in Liquids by Picosecond X-Ray Absorption Spectroscopy. *AIP Conference Proceedings* **2007**, *882*, 31.
(195) Consani, C.; Premont-Schwarz, M.; ElNahhas, A.; Bressler, C.; van Mourik, F.; Cannizzo, A.; Chergui, M.: Vibrational Coherences and Relaxation in the High-Spin State of Aqueous [Fe-II(bpy)(3)](2+). *Angew Chem Int Edit* **2009**, *48*, 7184-7187.
(196) Bräm, O.; Messina, F.; El-Zohry, A.; Cannizzo, A.; Chergui, M.: Polychromatic femtosecond fluorescence studies of metal-polypyridine complexes in solution *Chem Phys* **2012**, *393*, 51-57.
(197) Zhang, W. K.; Alonso-Mori, R.; Bergmann, U.; Bressler, C.; Chollet, M.; Galler, A.; Gawelda, W.; Hadt, R. G.; Hartsock, R. W.; Kroll, T.; Kjaer, K. S.; Kubicek, K.; Lemke, H. T.; Liang, H. Y. W.; Meyer, D. A.; Nielsen, M. M.; Purser, C.; Robinson, J. S.; Solomon, E. I.; Sun, Z.; Sokaras, D.; van Driel, T. B.; Vanko, G.; Weng, T. C.; Zhu, D. L.;

Gaffney, K. J.: Tracking excited-state charge and spin dynamics in iron coordination complexes. *Nature* **2014**, *509*, 345-+.

(198) Aubock, G.; Chergui, M.: Sub-50-fs photoinduced spin crossover in [Fe(bpy)(3)](2+). *Nat Chem* **2015**, *7*, 629-633.

(199) Guionneau, P.; Costa, J. S.; Letard, J. F.: Revisited crystal symmetry of the high-spin form of the iron(II) spin-crossover complex dicyano[2,13-dimethyl-6,9-dioxa-3,12,18-triazabicyclo[12.3.1]octadeca-1(18),2,12,14,16-pentaene]iron(II) monohydrate. *Acta Crystallogr C* **2004**, *60*, M587-M589.

(200) Oyanagi, H.; Tayagaki, T.; Tanaka, K.: Photo-induced phase transitions probed by X-ray absorption spectroscopy: Fe(II) spin crossover complex. *Journal of Physics and Chemistry of Solids* **2004**, *65*, 1485-1489.

(201) Oyanagi, H.; Tayagaki, T.; Tanaka, K.: Synchrotron radiation study of photo-induced spin-crossover transitions: Microscopic origin of nonlinear phase transition. *J Lumin* **2006**, *119*, 361-369.

(202) Daku, L. M. L.; Vargas, A.; Hauser, A.; Fouqueau, A.; Casida, M. E.: Assessment of density functionals for the high-spin/low-spin energy difference in the low-spin iron(II) tris(2,2 '-bipyridine) complex. *Chemphyschem* **2005**, *6*, 1393-1410.

(203) Khalil, M.; Marcus, M. A.; Smeigh, A. L.; McCusker, J. K.; Chong, H. H. W.; Schoenlein, R. W.: Picosecond X-ray absorption spectroscopy of a photoinduced iron(II) spin crossover reaction in solution. *Journal of Physical Chemistry A* **2006**, *110*, 38-44.

(204) Gawelda, W.; Pham, V. T.; van der Veen, R. M.; Grolimund, D.; Abela, R.; Chergui, M.; Bressler, C.: Structural analysis of ultrafast extended x-ray absorption fine structure with subpicometer spatial resolution: Application to spin crossover complexes. *J Chem Phys* **2009**, *130*, -.

(205) Vanko, G.; Glatzel, P.; Pham, V. T.; Abela, R.; Grolimund, D.; Borca, C. N.; Johnson, S. L.; Milne, C. J.; Bressler, C.: Picosecond Time-Resolved X-Ray Emission Spectroscopy: Ultrafast Spin-State Determination in an Iron Complex. *Angew Chem Int Edit* **2010**, *49*, 5910-5912.

(206) Haldrup, K.; Vanko, G.; Gawelda, W.; Galler, A.; Doumy, G.; March, A. M.; Kanter, E. P.; Bordage, A.; Dohn, A.; van Driel, T. B.; Kjaer, K. S.; Lemke, H. T.; Canton, S. E.; Uhlig, J.; Sundstrom, V.; Young, L.; Southworth, S. H.; Nielsen, M. M.; Bressler, C.: Guest-Host Interactions Investigated by Time-Resolved X-ray Spectroscopies and Scattering at MHz Rates: Solvation Dynamics and Photoinduced Spin Transition in Aqueous Fe(bipy)(3)(2+). *Journal of Physical Chemistry A* **2012**, *116*, 9878-9887.

(207) Monat, J. E.; McCusker, J. K.: Femtosecond excited-state dynamics of an iron(II) polypyridyl solar cell sensitizer model. *Journal of the American Chemical Society* **2000**, *122*, 4092-4097.

(208) Juban, E. A.; Smeigh, A. L.; Monat, J. E.; McCusker, J. K.: Ultrafast dynamics of ligand-field excited states. *Coordin Chem Rev* **2006**, *250*, 1783-1791.

(209) Briois, V.; Sainctavit, P.; Long, G. J.; Grandjean, F.: Importance of photoelectron multiple scattering in the iron K-edge X-ray absorption spectra of spin-crossover complexes: Full multiple scattering calculations for several iron(II) trispyrazolylborate and trispyrazolylmethane complexes. *Inorg Chem* **2001**, *40*, 912-918.

(210) Huse, N.; Cho, H.; Hong, K.; Jamula, L.; de Groot, F. M. F.; Kim, T. K.; McCusker, J. K.; Schoenlein, R. W.: Femtosecond Soft X-ray Spectroscopy of Solvated Transition-Metal Complexes: Deciphering the Interplay of Electronic and Structural Dynamics. *J Phys Chem Lett* **2011**, *2*, 880-884.

(211) Lemke, H. T.; Bressler, C.; Chen, L. X.; Fritz, D. M.; Gaffney, K. J.; Galler, A.; Gawelda, W.; Haldrup, K.; Hartsock, R. W.; Ihee, H.; Kim, J.; Kim, K. H.; Lee, J. H.;

Nielsen, M. M.; Stickrath, A. B.; Zhang, W. K.; Zhu, D. L.; Cammarata, M.: Femtosecond X-ray Absorption Spectroscopy at a Hard X-ray Free Electron Laser: Application to Spin Crossover Dynamics. *Journal of Physical Chemistry A* **2013**, *117*, 735-740.

(212) Vanko, G.; Bordage, A.; Glatzel, P.; Gallo, E.; Rovezzi, M.; Gawelda, W.; Galler, A.; Bressler, C.; Doumy, G.; March, A. M.; Kanter, E. P.; Young, L.; Southworth, S. H.; Canton, S. E.; Uhlig, J.; Smolentsev, G.; Sundstrom, V.; Haldrup, K.; van Driel, T. B.; Nielsen, M. M.; Kjaer, K. S.; Lemke, H. T.: Spin-state studies with XES and RIXS: From static to ultrafast. *Journal of Electron Spectroscopy and Related Phenomena* **2013**, *188*, 166-171.

(213) Lemke, H. T.; Kjær, K. S.; Hartsock, R.; Brandt van Driel, T.; Chollet, M.; Glownia, J. M.; Song, S.; Zhu, D.; Pace, E.; Matar, S. F.; Nielsen, M. N.; Benfatto, M.; Gaffney, K. J.; Collet, E.; Cammarata, M.: Coherent structural trapping through wave packet dispersion during photoinduced spin state switching. *Nat Commun* **2017**.

(214) Biasin, E.; van Driel, T. B.; Kjær, K. S.; Dohn, A. O.; Christensen, M.; Harlang, T.; Chabera, P.; Liu, Y.; Uhlig, J.; Pápai, M.: Femtosecond X-Ray Scattering Study of Ultrafast Photoinduced Structural Dynamics in Solvated [Co (terpy) 2] 2+. *Physical Review Letters* **2016**, *117*, 013002.

(215) Penfold, T. J.; Tavernelli, I.; Abela, R.; Chergui, M.; Rothlisberger, U.: Ultrafast anisotropic x-ray scattering in the condensed phase. *New J Phys* **2012**, *14*.

(216) Miaja-Avila, L.; O'Neil, G. C.; Joe, Y. I.; Alpert, B. K.; Damrauer, N. H.; Doriese, W. B.; Fatur, S. M.; Fowler, J. W.; Hilton, G. C.; Jimenez, R.; Reintsema, C. D.; Schmidt, D. R.; Silverman, K. L.; Swetz, D. S.; Tatsuno, H.; Ullom, J. N.: Ultrafast Time-Resolved Hard X-Ray Emission Spectroscopy on a Tabletop. *Physical Review X* **2016**, *6*, 031047.

(217) Vlcek, A.: The life and times of excited states of organometallic and coordination compounds. *Coordin Chem Rev* **2000**, *200*, 933-977.

(218) van der Veen, R. M.; Bressler, C.; Milne, C. J.; Pham, V. T.; El Nahhas, A.; Lima, F. A.; Gawelda, W.; Borca, C. N.; Abela, R.; Chergui, M.: Retrieving photochemically active structures by time-resolved EXAFS spectroscopy. *J Phys Conf Ser* **2009**, *190*, -4855.

(219) van der Veen, R. M.; Kas, J. J.; Milne, C. J.; Pham, V. T.; El Nahhas, A.; Lima, F. A.; Vithanage, D. A.; Rehr, J. J.; Abela, R.; Chergui, M.: L-edge XANES analysis of photoexcited metal complexes in solution. *Phys Chem Chem Phys* **2010**, *12*, 5551-5561.

(220) van der Veen, R. M.; Milne, C. J.; El Nahhas, A.; Lima, F. A.; Pham, V. T.; Best, J.; Weinstein, J. A.; Borca, C. N.; Abela, R.; Bressler, C.; Chergui, M.: Structural Determination of a Photochemically Active Diplatinum Molecule by Time-Resolved EXAFS Spectroscopy. *Angew Chem Int Edit* **2009**, *48*, 2711-2714.

(221) Novozhilova, I. V.; Volkov, A. V.; Coppens, P.: Theoretical analysis of the triplet excited state of the [Pt-2(H2P2O5)(4)](4-) ion and comparison with time-resolved x-ray and spectroscopic results. *Journal of the American Chemical Society* **2003**, *125*, 1079-1087.

(222) Christensen, M.; Haldrup, K.; Bechgaard, K.; Feidenhans'l, R.; Kong, Q. Y.; Cammarata, M.; Lo Russo, M.; Wulff, M.; Harrit, N.; Nielsen, M. M.: Time-Resolved X-ray Scattering of an Electronically Excited State in Solution. Structure of the (3)A(2u) State of Tetrakis-mu-pyrophosphitodiplatinate(II). *Journal of the American Chemical Society* **2009**, *131*, 502-508.

(223) Lockard, J. V.; Rachford, A. A.; Smolentsev, G.; Stickrath, A. B.; Wang, X. H.; Zhang, X. Y.; Atenkoffer, K.; Jennings, G.; Soldatov, A.; Rheingold, A. L.; Castellano, F. N.; Chen, L. X.: Triplet Excited State Distortions in a Pyrazolate Bridged Platinum Dimer

Measured by X-ray Transient Absorption Spectroscopy. *Journal of Physical Chemistry A* **2010**, *114*, 12780-12787.

(224) Stiegman, A. E.; Rice, S. F.; Gray, H. B.; Miskowski, V. M.: Electronic Spectroscopy of D8-D8 Diplatinum Complexes - 1a2u(Dsigma Star-]P-Sigma), 3eu(Dxz,Dyz-]P-Sigma), and 3,1b2u(Dsigma Star-] Dx2-Y2) Excited-States of Pt2(P2o5h2)44-. *Inorg Chem* **1987**, *26*, 1112-1116.

(225) van der Veen, R. M.; Cannizzo, A.; van Mourik, F.; Vlcek, A.; Chergui, M.: Vibrational Relaxation and Intersystem Crossing of Binuclear Metal Complexes in Solution. *Journal of the American Chemical Society* **2011**, *133*, 305-315.

(226) Penfold, T. J.; Curchod, B. F. E.; Tavernelli, I.; Abela, R.; Rothlisberger, U.; Chergui, M.: Simulations of X-ray absorption spectra: the effect of the solvent. *Phys Chem Chem Phys* **2012**, *14*, 9444-9450.

(227) Maroncelli, M.: The Dynamics of Solvation in Polar Liquids. *J Mol Liq* **1993**, *57*, 1-37.

(228) Jeannin, C.; Porrella-Oberli, M. T.; Jimenez, S.; Vigliotti, F.; Lang, B.; Chergui, M.: Femtosecond dynamics of electronic 'bubbles' in solid argon: viewing the inertial response and the bath coherences. *Chem Phys Lett* **2000**, *316*, 51-59.

(229) Vigliotti, F.; Bonacina, L.; Chergui, M.: Ultrafast structural dynamics in electronically excited solid neon. I. Real-time probing of the electronic bubble formation. *Physical Review B* **2003**, *67*, art. no.-115118.

(230) Vigliotti, F.; Bonacina, L.; Chergui, M.: Structural dynamics in quantum solids. II. Real-time probing of the electronic bubble formation in solid hydrogens. *J Chem Phys* **2002**, *116*, 4553-4562.

(231) Bonacina, L.; Larregaray, P.; van Mourik, F.; Chergui, M.: Lattice response of quantum solids to an impulsive local perturbation. *Physical Review Letters* **2005**, *95*, 015301.

(232) Larregaray, P.; Cavina, A.; Chergui, M.: Ultrafast solvent response upon a change of the solute size in non-polar supercritical fluids. *Chem Phys* **2005**, *308*, 13-25.

(233) Pham, V. T.; Gawelda, W.; Zaushitsyn, Y.; Kaiser, M.; Grolimund, D.; Johnson, S. L.; Abela, R.; Bressler, C.; Chergui, M.: Observation of the solvent shell reorganization around photoexcited atomic solutes by picosecond X-ray absorption spectroscopy. *Journal of the American Chemical Society* **2007**, *129*, 1530-+.

(234) Pham, V. T.; Penfold, T. J.; van der Veen, R. M.; Lima, F.; El Nahhas, A.; Johnson, S. L.; Beaud, P.; Abela, R.; Bressler, C.; Tavernelli, I.; Milne, C. J.; Chergui, M.: Probing the Transition from Hydrophilic to Hydrophobic Solvation with Atomic Scale Resolution. *Journal of the American Chemical Society* **2011**, *133*, 12740-12748.

(235) Penfold, T. J.; Tavernelli, I.; Doemer, M.; Abela, R.; Rothlisberger, U.; Chergui, M.: Solvent rearrangements during the transition from hydrophilic to hydrophobic solvation. *Chem Phys* **2013**, *410*, 25-30.

(236) Penfold, T. J.; Milne, C. J.; Tavernelli, I.; Chergui, M.: Hydrophobicity with atomic resolution: Steady-state and ultrafast X-ray absorption and molecular dynamics studies. *Pure Appl Chem* **2013**, *85*, 53-60.

(237) Moret, M. E.; Tavernelli, I.; Chergui, M.; Rothlisberger, U.: Electron Localization Dynamics in the Triplet Excited State of [Ru(bpy)(3)](2+) in Aqueous Solution. *Chem-Eur J* **2010**, *16*, 5889-5894.

(238) Daku, L. M. L.; Hauser, A.: Ab Initio Molecular Dynamics Study of an Aqueous Solution of [Fe(bpy)(3)](Cl)(2) in the Low-Spin and in the High-Spin States. *J Phys Chem Lett* **2010**, *1*, 1830-1835.

(239) Haldrup, K.; Gawelda, W.; Abela, R.; Alonso-Mori, R.; Bergmann, U.; Bordage, A.; Cammarata, M.; Canton, S. E.; Dohn, A. O.; Van Driel, T. B.: Observing

Solvation Dynamics with Simultaneous Femtosecond X-ray Emission Spectroscopy and X-ray Scattering. *The Journal of Physical Chemistry B* **2016**, *120*, 1158-1168.

(240) Franck, J.; Rabinowitsch, E.: Some remarks about free radicals and the photochemistry of solutions. *T Faraday Soc* **1934**, *30*, 120-130.

(241) Chergui, M.: Ultrafast Photophysics of Transition Metal Complexes. *Accounts Chem Res* **2015**, *48*, 801-808.

(242) Shirom, M.; Stein, G.: Excited State Chemistry of Ferrocyanide Ion in Aqueous Solution .1. Formation of Hydrated Electron. *J Chem Phys* **1971**, *55*, 3372-&.

(243) Shirom, M.; Stein, G.: Excited State Chemistry of Ferrocyanide Ion in Aqueous Solution .2. Photoaquation. *J Chem Phys* **1971**, *55*, 3379-&.

(244) Reinhard, M.; Penfold, T. J.; Lima, F. A.; Rittmann, J.; Rittmann-Frank, M. H.; Abela, R.; Tavernelli, I.; Rothlisberger, U.; Milne, C. J.; Chergui, M.: Photooxidation and photoaquation of iron hexacyanide in aqueous solution: A picosecond X-ray absorption study. *Structural Dynamics* **2014**, *1*, 024901.

(245) Aziz, E. F.; Rittmann-Frank, M. H.; Lange, K. M.; Bonhommeau, S.; Chergui, M.: Charge transfer to solvent identified using dark channel fluorescence-yield L-edge spectroscopy. *Nat Chem* **2010**, *2*, 853-857.

(246) Penfold, T. J.; Reinhard, M.; Rittmann-Frank, M. H.; Tavernelli, I.; Rothlisberger, U.; Milne, C. J.; Glatzel, P.; Chergui, M.: X-ray Spectroscopic Study of Solvent Effects on the Ferrous and Ferric Hexacyanide Anions. *Journal of Physical Chemistry A* **2014**, *118*, 9411-9418.

(247) Trushin, S. A.; Fuss, W.; Kompa, K. L.; Schmid, W. E.: Femtosecond dynamics of Fe(CO)(5) photodissociation at 267 nm studied by transient ionization. *Journal of Physical Chemistry A* **2000**, *104*, 1997-2006.

(248) Banares, L.; Baumert, T.; Bergt, M.; Kiefer, B.; Gerber, G.: The ultrafast photodissociation of Fe (CO) 5 in the gas phase. *J Chem Phys* **1998**, *108*.

(249) Wrighton, M. S.; Ginley, D.; Schroeder, M.; Morse, D.: Generation of catalysts by photolysis of transition metal complexes. *Pure Appl Chem* **1975**, *41*, 671-697.

(250) Poliakoff, M.; Weitz, E.: Shedding light on organometallic reactions: the characterization of tetracarbonyliron (Fe (CO) 4), a prototypical reaction intermediate. *Accounts Chem Res* **1987**, *20*, 408-414.

(251) Portius, P.; Yang, J. X.; Sun, X. Z.; Grills, D. C.; Matousek, P.; Parker, A. W.; Towrie, M.; George, M. W.: Unraveling the photochemistry of Fe(CO)(5) in solution: Observation of Fe(CO)(3) and the conversion between Fe-3(CO)(4) and Fe-1(CO)(4)(solvent). *Journal of the American Chemical Society* **2004**, *126*, 10713-10720.

(252) Besora, M.; Carreon-Macedo, J. L.; Cowan, A. J.; George, M. W.; Harvey, J. N.; Portius, P.; Ronayne, K. L.; Sun, X. Z.; Towrie, M.: A Combined Theoretical and Experimental Study on the Role of Spin States in the Chemistry of Fe(CO)(5) Photoproducts. *Journal of the American Chemical Society* **2009**, *131*, 3583-3592.

(253) Snee, P. T.; Payne, C. K.; Kotz, K. T.; Yang, H.; Harris, C. B.: Triplet organometallic reactivity under ambient conditions: An ultrafast UV pump/IR probe study. *Journal of the American Chemical Society* **2001**, *123*, 2255-2264.

(254) Snee, P. T.; Payne, C. K.; Mebane, S. D.; Kotz, K. T.; Harris, C. B.: Dynamics of photosubstitution reactions of Fe(CO)(5): An ultrafast infrared study of high spin reactivity. *Journal of the American Chemical Society* **2001**, *123*, 6909-6915.

(255) Yang, H.; Snee, P. T.; Kotz, K. T.; Payne, C. K.; Harris, C. B.: Femtosecond infrared study of the dynamics of solvation and solvent caging. *Journal of the American Chemical Society* **2001**, *123*, 4204-4210.

(256) Ahr, B.; Chollet, M.; Adams, B.; Lunny, E. M.; Laperle, C. M.; Rose-Petruck, C.: Picosecond X-ray absorption measurements of the ligand substitution dynamics of Fe(CO)(5) in ethanol. *Phys Chem Chem Phys* **2011**, *13*, 5590-5599.

(257) Jiang, Y.; Lee, T.; Rose-Petruck, C. G.: Structure of solvated Fe(CO)(5): FTIR measurements and density functional theory calculations. *Journal of Physical Chemistry A* **2003**, *107*, 7524-7538.

(258) Wernet, P.; Kunnus, K.; Josefsson, I.; Rajkovic, I.; Quevedo, W.; Beye, M.; Schreck, S.; Grubel, S.; Scholz, M.; Nordlund, D.; Zhang, W.; Hartsock, R. W.; Schlotter, W. F.; Turner, J. J.; Kennedy, B.; Hennies, F.; de Groot, F. M. F.; Gaffney, K. J.; Techert, S.; Odelius, M.; Fohlisch, A.: Orbital-specific mapping of the ligand exchange dynamics of Fe(CO)5 in solution. *Nature* **2015**, *520*, 78-81.

(259) Kunnus, K.; Josefsson, I.; Rajkovic, I.; Schreck, S.; Quevedo, W.; Beye, M.; Weniger, C.; Grübel, S.; Scholz, M.; Nordlund, D.; Zhang, W.; Hartsock, R. W.; Gaffney, K. J.; Schlotter, W. F.; Turner, J. J.; Kennedy, B.; Hennies, F.; de Groot, F. M. F.; Techert, S.; Odelius, M.; Wernet, P.; Föhlisch, A.: Identification of the dominant photochemical pathways and mechanistic insights to the ultrafast ligand exchange of Fe(CO)5 to Fe(CO)4EtOH. *Structural Dynamics* **2016**, *3*, 043204.

(260) Linsebigler, A. L.; Lu, G. Q.; Yates, J. T.: Photocatalysis on Tio2 Surfaces - Principles, Mechanisms, and Selected Results. *Chem Rev* **1995**, *95*, 735-758.

(261) Kalyanasundaram, K.; Gratzel, M.: Applications of functionalized transition metal complexes in photonic and optoelectronic devices. *Coordin Chem Rev* **1998**, *177*, 347-414.

(262) Gray, H. B.; Winkler, J. R.: Electron tunneling through proteins. *Q Rev Biophys* **2003**, *36*, 341-372.

(263) Bellelli, A.; Brunori, M.; Brzezinski, P.; Wilson, M. T.: Photochemically induced electron transfer. *Methods* **2001**, *24*, 139-152.

(264) Valis, L.; Wang, Q.; Raytchev, M.; Buchvarov, I.; Wagenknecht, H. A.; Fiebig, T.: Base pair motions control the rates and distance dependencies of reductive and oxidative DNA charge transfer. *P Natl Acad Sci USA* **2006**, *103*, 10192-10195.

(265) Fujishima, A.; Zhang, X. T.; Tryk, D. A.: TiO2 photocatalysis and related surface phenomena. *Surf Sci Rep* **2008**, *63*, 515-582.

(266) Hagfeldt, A.; Boschloo, G.; Sun, L. C.; Kloo, L.; Pettersson, H.: Dye-Sensitized Solar Cells. *Chem Rev* **2010**, *110*, 6595-6663.

(267) Nazeeruddin, M. K.; Baranoff, E.; Gratzel, M.: Dye-sensitized solar cells: A brief overview. *Sol Energy* **2011**, *85*, 1172-1178.

(268) Wang, Z.; Wen, B.; Hao, Q.; Liu, L.-M.; Zhou, C.; Mao, X.; Lang, X.; Yin, W.-J.; Dai, D.; Selloni, A.: Localized Excitation of Ti3+ Ions in the Photoabsorption and Photocatalytic Activity of Reduced Rutile TiO2. *Journal of the American Chemical Society* **2015**, *137*, 9146-9152.

(269) Chen, X.; Selloni, A.: Introduction: Titanium Dioxide (TiO2) Nanomaterials. *Chem Rev* **2014**, *114*, 9281-9282.

(270) Katz, J. E.; Gilbert, B.; Zhang, X. Y.; Attenkofer, K.; Falcone, R. W.; Waychunas, G. A.: Observation of Transient Iron(II) Formation in Dye-Sensitized Iron Oxide Nanoparticles by Time-Resolved X-ray Spectroscopy. *J Phys Chem Lett* **2010**, *1*, 1372-1376.

(271) Rittmann-Frank, M. H.; Milne, C. J.; Rittmann, J.; Reinhard, M.; Penfold, T. J.; Chergui, M.: Mapping of the Photoinduced Electron Traps in TiO2 by Picosecond X-ray Absorption Spectroscopy. *Angew Chem Int Edit* **2014**, *53*, 5858-5862.

(272) Santomauro, F. G.; Lubcke, A.; Rittmann, J.; Baldini, E.; Ferrer, A.; Silatani, M.; Zimmermann, P.; Grubel, S.; Johnson, J. A.; Mariager, S. O.; Beaud, P.; Grolimund, D.;

Borca, C.; Ingold, G.; Johnson, S. L.; Chergui, M.: Femtosecond X-ray absorption study of electron localization in photoexcited anatase TiO2. *Sci Rep-Uk* **2015**, *5*, 14834.

(273) Amidani, L.; Naldoni, A.; Malvestuto, M.; Marelli, M.; Glatzel, P.; Dal Santo, V.; Boscherini, F.: Probing Long-Lived Plasmonic-Generated Charges in TiO2/Au by High-Resolution X-ray Absorption Spectroscopy. *Angew Chem Int Edit* **2015**, *54*, 5413-5416.

(274) Santomauro, F. G.; Grilj, J.; Mewes, L.; Nedelcu, G.; Yakunin, S.; Rossi, T.; Capano, G.; Haddad, A. A.; Budarz, J.; Kinschel, D.; Ferreira, D. S.; Rossi, G.; Tovar, M. G.; Grolimund, D.; Samson, V.; Nachtegaal, M.; Smolentsev, G.; Kovalenko, M. V.; Chergui, M.: Localized holes and delocalized electrons in photoexcited inorganic perovskites: Watching each atomic actor by picosecond X-ray absorption spectroscopy. *Structural Dynamics* **2017**, *4*, 044002.

(275) Neppl, S.; Gessner, O.: Time-resolved X-ray photoelectron spectroscopy techniques for the study of interfacial charge dynamics. *Journal of Electron Spectroscopy and Related Phenomena* **2015**, *200*, 64-77.

(276) Neppl, S.; Shavorskiy, A.; Zegkinoglou, I.; Fraund, M.; Slaughter, D. S.; Troy, T.; Ziemkiewicz, M. P.; Ahmed, M.; Gul, S.; Rude, B.; Zhang, J. Z.; Tremsin, A. S.; Glans, P. A.; Liu, Y. S.; Wu, C. H.; Guo, J. H.; Salmeron, M.; Bluhm, H.; Gessner, O.: Capturing interfacial photoelectrochemical dynamics with picosecond time-resolved X-ray photoelectron spectroscopy. *Faraday Discussions* **2014**, *171*, 219-241.

(277) Siefermann, K. R.; Pemmaraju, C. D.; Neppl, S.; Shavorskiy, A.; Cordones, A. A.; Vura-Weis, J.; Slaughter, D. S.; Sturm, F. P.; Weise, F.; Bluhm, H.; Strader, M. L.; Cho, H.; Lin, M.-F.; Bacellar, C.; Khurmi, C.; Guo, J.; Coslovich, G.; Robinson, J. S.; Kaindl, R. A.; Schoenlein, R. W.; Belkacem, A.; Neumark, D. M.; Leone, S. R.; Nordlund, D.; Ogasawara, H.; Krupin, O.; Turner, J. J.; Schlotter, W. F.; Holmes, M. R.; Messerschmidt, M.; Minitti, M. P.; Gul, S.; Zhang, J. Z.; Huse, N.; Prendergast, D.; Gessner, O.: Atomic-Scale Perspective of Ultrafast Charge Transfer at a Dye–Semiconductor Interface. *The Journal of Physical Chemistry Letters* **2014**, *5*, 2753-2759.

(278) Canton, S. E.; Kjaer, K. S.; Vanko, G.; van Driel, T. B.; Adachi, S. I.; Bordage, A.; Bressler, C.; Chabera, P.; Christensen, M.; Dohn, A. O.; Galler, A.; Gawelda, W.; Gosztola, D.; Haldrup, K.; Harlang, T.; Liu, Y. Z.; Moller, K. B.; Nemeth, Z.; Nozawa, S.; Papai, M.; Sato, T.; Sato, T.; Suarez-Alcantara, K.; Togashi, T.; Tono, K.; Uhlig, J.; Vithanage, D. A.; Warnmark, K.; Yabashi, M.; Zhang, J. X.; Sundstrom, V.; Nielsen, M. M.: Visualizing the non-equilibrium dynamics of photoinduced intramolecular electron transfer with femtosecond X-ray pulses. *Nat Commun* **2015**, *6*, 6359.

(279) Thomas, J. M.: Crystal engineering: origins, early adventures and some current trends. *Crystengcomm* **2011**, *13*, 4304-4306.

(280) Naumov, P.; Bharadwaj, P. K.: Single-crystal-to-single-crystal transformations. *Crystengcomm* **2015**, *17*, 8775-8775.

(281) Nasu, K.: Itinerant type many-body theories for photo-induced structural phase transitions. *Reports on Progress in Physics* **2004**, *67*, 1607.

(282) Decurtins, S.; Gütlich, P.; Köhler, C.; Spiering, H.; Hauser, A.: Light-induced excited spin state trapping in a transition-metal complex: The hexa-1-propyltetrazole-iron (II) tetrafluoroborate spin-crossover system. *Chem Phys Lett* **1984**, *105*, 1-4.

(283) Goujon, A.; Varret, F.; Boukheddaden, K.; Chong, C.; Jeftić, J.; Garcia, Y.; Naik, A.; Ameline, J.-C.; Collet, E.: An optical microscope study of photo-switching and relaxation in single crystals of the spin transition solid [Fe (ptz) 6](BF 4) 2, with image processing. *Inorg Chim Acta* **2008**, *361*, 4055-4064.

(284) Bertoni, R.; Lorenc, M.; Tissot, A.; Servol, M.; Boillot, M. L.; Collet, E.: Femtosecond Spin-State Photoswitching of Molecular Nanocrystals Evidenced by Optical Spectroscopy. *Angew Chem Int Edit* **2012**, *51*, 7485-7489.
(285) Tissot, A.; Bertoni, R.; Collet, E.; Toupet, L.; Boillot, M. L.: The cooperative spin-state transition of an iron(III) compound [Fe-III(3-MeO-SalEen)(2)]PF6: thermal- vs. ultra-fast photo-switching. *J Mater Chem* **2011**, *21*, 18347-18353.
(286) Bonhommeau, S.; Molnár, G.; Galet, A.; Zwick, A.; Real, J. A.; McGarvey, J. J.; Bousseksou, A.: One Shot Laser Pulse Induced Reversible Spin Transition in the Spin-Crossover Complex [Fe (C4H4N2){Pt (CN) 4}] at Room Temperature. *Angewandte Chemie* **2005**, *117*, 4137-4141.
(287) Collet, E.; Henry, L.; Piñeiro-López, L.; Toupet, L.; Antonio Real, J.: Single laser shot spin state switching of {FeII (pz)[Pt (CN) 4]} inside thermal hysteresis studied by x-ray diffraction. *Current Inorganic Chemistry* **2016**, *6*, 61-66.
(288) Bertoni, R.; Cammarata, M.; Lorenc, M.; Matar, S. F.; Letard, J. F.; Lemke, H. T.; Collet, E.: Ultrafast Light-Induced Spin-State Trapping Photophysics Investigated in Fe(phen)(2)(NCS)(2) Spin-Crossover Crystal. *Accounts Chem Res* **2015**, *48*, 774-781.
(289) Bertoni, R.; Lorenc, M.; Graber, T.; Henning, R.; Moffat, K.; Letard, J. F.; Collet, E.: Cooperative elastic switching vs. laser heating in [Fe(phen)(2)(NCS)(2)] spin-crossover crystals excited by a laser pulse. *Crystengcomm* **2016**, *18*, 7269-7275.
(290) Cammarata, M.; Bertoni, R.; Lorenc, M.; Cailleau, H.; Di Matteo, S.; Mauriac, C.; Matar, S. F.; Lemke, H.; Chollet, M.; Ravy, S.; Laulhe, C.; Letard, J. F.; Collet, E.: Sequential Activation of Molecular Breathing and Bending during Spin-Crossover Photoswitching Revealed by Femtosecond Optical and X-Ray Absorption Spectroscopy. *Physical Review Letters* **2014**, *113*.
(291) Marino, A.; Cammarata, M.; Matar, S. F.; Létard, J.-F.; Chastanet, G.; Chollet, M.; Glownia, J. M.; Lemke, H. T.; Collet, E.: Activation of coherent lattice phonon following ultrafast molecular spin-state photo-switching: A molecule-to-lattice energy transfer. *Structural Dynamics* **2016**, *3*, 023605.
(292) Freyer, B.; Zamponi, F.; Juve, V.; Stingl, J.; Woerner, M.; Elsaesser, T.; Chergui, M.: Ultrafast inter-ionic charge transfer of transition-metal complexes mapped by femtosecond X-ray powder diffraction. *J Chem Phys* **2013**, *138*, 144504.
(293) Bertoni, R.; Lorenc, M.; Cailleau, H.; Tissot, A.; Laisney, J.; Boillot, M. L.; Stoleriu, L.; Stancu, A.; Enachescu, C.; Collet, E.: Elastically driven cooperative response of a molecular material impacted by a laser pulse. *Nat Mater* **2016**, *15*, 606-610.
(294) van der Veen, R. M.; Kwon, O. H.; Tissot, A.; Hauser, A.; Zewail, A. H.: Single-nanoparticle phase transitions visualized by four-dimensional electron microscopy. *Nat Chem* **2013**, *5*, 395-402.
(295) Chernyshov, D.; Hostettler, M.; Tornroos, K. W.; Burgi, H. B.: Ordering phenomena and phase transitions in a spin-crossover compound-uncovering the nature of the intermediate phase of [Fe(2-PiC)(3)]Cl-2 center dot EtOH. *Angew Chem Int Edit* **2003**, *42*, 3825-3830.
(296) Fitzpatrick, A. J.; Trzop, E.; Muller-Bunz, H.; Dirtu, M. M.; Garcia, Y.; Collet, E.; Morgan, G. G.: Electronic vs. structural ordering in a manganese(III) spin crossover complex. *Chem Commun* **2015**, *51*, 17540-17543.
(297) Brefuel, N.; Collet, E.; Watanabe, H.; Kojima, M.; Matsumoto, N.; Toupet, L.; Tanaka, K.; Tuchagues, J. P.: Nanoscale Self-Hosting of Molecular Spin-States in the Intermediate Phase of a Spin-Crossover Material. *Chem-Eur J* **2010**, *16*, 14060-14068.
(298) Collet, E.; Lorenc, M.; Cammarata, M.; Guerin, L.; Servol, M.; Tissot, A.; Boillot, M. L.; Cailleau, H.; Buron-Le Cointe, M.: 100 Picosecond Diffraction Catches

Structural Transients of Laser-Pulse Triggered Switching in a Spin-Crossover Crystal. *Chem-Eur J* **2012**, *18*, 2051-2055.

(299) Murnaghan, K. D.; Carbonera, C.; Toupet, L.; Griffin, M.; Dirtu, M. M.; Desplanches, C.; Garcia, Y.; Collet, E.; Letard, J. F.; Morgan, G. G.: Spin-State Ordering on One Sub-lattice of a Mononuclear Iron(III) Spin Crossover Complex Exhibiting LIESST and TIESST. *Chem-Eur J* **2014**, *20*, 5613-5618.

(300) Trzop, E.; Zhang, D. P.; Pineiro-Lopez, L.; Valverde-Munoz, F. J.; Munoz, M. C.; Palatinus, L.; Guerin, L.; Cailleau, H.; Real, J. A.; Collet, E.: First Step Towards a Devil's Staircase in Spin-Crossover Materials. *Angew Chem Int Edit* **2016**, *55*, 8675-8679.

(301) Watanabe, H.; Tanaka, K.; Brefuel, N.; Cailleau, H.; Letard, J. F.; Ravy, S.; Fertey, P.; Nishino, M.; Miyashita, S.; Collet, E.: Ordering phenomena of high-spin/low-spin states in stepwise spin-crossover materials described by the ANNNI model. *Physical Review B* **2016**, *93*.

(302) Marino, A.; Buron-Le Cointe, M.; Lorenc, M.; Toupet, L.; Henning, R.; DiChiara, A. D.; Moffat, K.; Brefueld, N.; Collet, E.: Out-of-equilibrium dynamics of photoexcited spin-state concentration waves. *Faraday Discussions* **2015**, *177*, 363-379.

(303) Sokolowski-Tinten, K.; Blome, C.; Blums, J.; Cavalleri, A.; Dietrich, C.; Tarasevitch, A.; Uschmann, I.; Forster, E.; Kammler, M.; Horn-von-Hoegen, M.; von der Linde, D.: Femtosecond X-ray measurement of coherent lattice vibrations near the Lindemann stability limit. *Nature* **2003**, *422*, 287-289.

(304) Fritz, D. M.: Ultrafast bond softening in bismuth: Mapping a solid's interatomic potential with x-rays (vol 315, pg 633, 2007). *Science* **2007**, *315*, 940-940.

(305) Beaud, P.; Caviezel, A.; Mariager, S. O.; Rettig, L.; Ingold, G.; Dornes, C.; Huang, S. W.; Johnson, J. A.; Radovic, M.; Huber, T.; Kubacka, T.; Ferrer, A.; Lemke, H. T.; Chollet, M.; Zhu, D.; Glownia, J. M.; Sikorski, M.; Robert, A.; Wadati, H.; Nakamura, M.; Kawasaki, M.; Tokura, Y.; Johnson, S. L.; Staub, U.: A time-dependent order parameter for ultrafast photoinduced phase transitions. *Nat Mater* **2014**, *13*, 923-927.

(306) Woerner, M.; Zamponi, F.; Ansari, Z.; Dreyer, J.; Freyer, B.; Premont-Schwarz, M.; Elsaesser, T.: Concerted electron and proton transfer in ionic crystals mapped by femtosecond x-ray powder diffraction. *J Chem Phys* **2010**, *133*, -.

(307) Techert, S.; Schotte, F.; Wulff, M.: Picosecond x-ray diffraction probed transient structural changes in organic solids. *Physical Review Letters* **2001**, *86*, 2030-2033.

(308) Braun, M.; Schmising, C. v. K.; Kiel, M.; Zhavoronkov, N.; Dreyer, J.; Bargheer, M.; Elsässer, T.; Root, C.; Schrader, T.; Gilch, P.: Ultrafast changes of molecular crystal structure induced by dipole solvation. *Physical review letters* **2007**, *98*, 248301.

(309) Kim, C. D.; Pillet, S.; Wu, G.; Fullagar, W. K.; Coppens, P.: Excited-state structure by time-resolved X-ray diffraction. *Acta Crystallogr A* **2002**, *58*, 133-137.

(310) Coppens, P.; Vorontsov, I. I.; Graber, T.; Gembicky, M.; Kovalevsky, A. Y.: The structure of short-lived excited states of molecular complexes by time-resolved X-ray diffraction. *Acta Crystallogr A* **2005**, *61*, 162-172.

(311) Makal, A.; Trzop, E.; Sokolow, J.; Kalinowski, J.; Benedict, J.; Coppens, P.: The development of Laue techniques for single-pulse diffraction of chemical complexes: time-resolved Laue diffraction on a binuclear rhodium metal-organic complex. *Acta Crystallogr A* **2011**, *67*, 319-326.

(312) Coppens, P.: Perspective: On the relevance of slower-than-femtosecond time scales in chemical structural-dynamics studies. *Structural Dynamics* **2015**, *2*.

(313) Makal, A.; Benedict, J.; Trzop, E.; Sokolow, J.; Fournier, B.; Chen, Y.; Kalinowski, J. A.; Graber, T.; Henning, R.; Coppens, P.: Restricted Photochemistry in the Molecular Solid State: Structural Changes on Photoexcitation of Cu(I) Phenanthroline Metal-

to-Ligand Charge Transfer (MLCT) Complexes by Time-Resolved Diffraction. *Journal of Physical Chemistry A* **2012**, *116*, 3359-3365.

(314) Koshihara, S.; Takahashi, Y.; Sakai, H.; Tokura, Y.; Luty, T.: Photoinduced cooperative charge transfer in low-dimensional organic crystals. *J Phys Chem B* **1999**, *103*, 2592-2600.

(315) Lecointe, M.; Lemeecailleau, M. H.; Cailleau, H.; Toudic, B.; Toupet, L.; Heger, G.; Moussa, F.; Schweiss, P.; Kraft, K. H.; Karl, N.: Symmetry-Breaking and Structural-Changes at the Neutral-to-Ionic Transition in Tetrathiafulvalene-P-Chloranil. *Physical Review B* **1995**, *51*, 3374-3386.

(316) Iwai, S.; Ishige, Y.; Tanaka, S.; Okimoto, Y.; Tokura, Y.; Okamoto, H.: Coherent control of charge and lattice dynamics in a photoinduced neutral-to-ionic transition of a charge-transfer compound. *Physical Review Letters* **2006**, *96*.

(317) Collet, E.; Lemee-Cailleau, M. H.; Buron-Le Cointe, M.; Cailleau, H.; Wulff, M.; Luty, T.; Koshihara, S. Y.; Meyer, M.; Toupet, L.; Rabiller, P.; Techert, S.: Laser-induced ferroelectric structural order in an organic charge-transfer crystal. *Science* **2003**, *300*, 612-615.

(318) Helliwell, J. R.; Rentzepis, P. M.: *Time-resolved diffraction*; Oxford University Press: Oxford, 1997.

(319) Mills, D. M.; Lewis, A.; Harootunian, A.; Huang, J.; Smith, B.: Time-Resolved X-Ray Absorption-Spectroscopy of Carbon-Monoxide Myoglobin Recombination after Laser Photolysis. *Science* **1984**, *223*, 811-813.

(320) Clozza, A.; Castellano, A. C.; Dellalonga, S.; Giovannelli, A.; Bianconi, A.: Apparatus for Time-Resolved X-Ray Absorption-Spectroscopy Using Flash-Photolysis. *Review of Scientific Instruments* **1989**, *60*, 2519-2521.

(321) Chance, M. R.; Wirt, M. D.; Miller, L. M.; Scheuring, E. M.; Xie, A.; Sidelinger, D. E.: Time-Resolved X-Ray Absorption-Spectroscopy on a 5 Mu-S Timescale. *Biophysical Journal* **1993**, *64*, A42-a42.

(322) Chen, L. X.; Zhang, X. Y.; Wasinger, E. C.; Attenkofer, K.; Jennings, G.; Muresan, A. Z.; Lindsey, J. S.: Tracking electrons and atoms in a photoexcited metalloporphyrin by X-ray transient absorption spectroscopy. *Journal of the American Chemical Society* **2007**, *129*, 9616-+.

(323) Chen, L. X.; Zhang, X. Y.; Wasinger, E. C.; Lockard, J. V.; Stickrath, A. B.; Mara, M. W.; Attenkofer, K.; Jennings, G.; Smolentsev, G.; Soldatov, A.: X-ray snapshots for metalloporphyrin axial ligation. *Chem Sci* **2010**, *1*, 642-650.

(324) Mara, M. W.; Shelby, M.; Stickrath, A.; Harpham, M.; Huang, J. E.; Zhang, X. Y.; Hoffman, B. M.; Chen, L. X.: Electronic and Nuclear Structural Snapshots in Ligand Dissociation and Recombination Processes of Iron Porphyrin in Solution: A Combined Optical/X-ray Approach. *J Phys Chem B* **2013**, *117*, 14089-14098.

(325) Stickrath, A. B.; Mara, M. W.; Lockard, J. V.; Harpham, M. R.; Huang, J.; Zhang, X. Y.; Attenkofer, K.; Chen, L. X.: Detailed Transient Heme Structures of Mb-CO in Solution after CO Dissociation: An X-ray Transient Absorption Spectroscopic Study. *J Phys Chem B* **2013**, *117*, 4705-4712.

(326) Silatani, M.; Lima, F. A.; Penfold, T. J.; Rittmann, J.; Reinhard, M. E.; Rittmann-Frank, H. M.; Borca, C.; Grolimund, D.; Milne, C. J.; Chergui, M.: NO binding kinetics in myoglobin investigated by picosecond Fe K-edge absorption spectroscopy. *P Natl Acad Sci USA* **2015**, *112*, 12922-12927.

(327) Ye, X.; Demidov, A.; Champion, P. M.: Measurements of the photodissociation quantum yields of MbNO and MbO(2) and the vibrational relaxation of the

six-coordinate heme species. *Journal of the American Chemical Society* **2002**, *124*, 5914-5924.

(328) Schotte, F.; Anfinrud, P. A.; Hummer, G.; Wulff, M.: Picosecond crystallography: Snapshots of a protein at work. *Biophysical Journal* **2004**, *86*, 525A-525A.

(329) Bourgeois, D.; Vallone, B.; Arcovito, A.; Sciara, G.; Schotte, F.; Anfinrud, P. A.; Brunori, M.: Extended subnanosecond structural dynamics of myoglobin revealed by Laue crystallography. *P Natl Acad Sci USA* **2006**, *103*, 4924-4929.

(330) Schotte, F.; Lim, M. H.; Jackson, T. A.; Smirnov, A. V.; Soman, J.; Olson, J. S.; Phillips, G. N.; Wulff, M.; Anfinrud, P. A.: Watching a protein as it functions with 150-ps time-resolved X-ray crystallography. *Science* **2003**, *300*, 1944-1947.

(331) Schotte, F.; Soman, J.; Olson, J. S.; Wulff, M.; Anfinrud, P. A.: Picosecond time-resolved X-ray crystallography: probing protein function in real time. *Journal of Structural Biology* **2004**, *147*, 235-246.

(332) Ahn, S.; Kim, K. H.; Kim, Y.; Kim, J.; Ihee, H.: Protein Tertiary Structural Changes Visualized by Time-Resolved X-ray Solution Scattering. *J Phys Chem B* **2009**, *113*, 13131-13133.

(333) Ihee, H.; Kim, K. H.; Oang, K. Y.; Kim, J.; Lee, J. H.; Kim, Y.: Direct observation of myoglobin structural dynamics from 100 picoseconds to 1 microsecond with picosecond X-ray solution scattering. *Chem Commun* **2011**, *47*, 289-291.

(334) Oang, K. Y.; Kim, J. G.; Yang, C.; Kim, T. W.; Kim, Y.; Kim, K. H.; Kim, J.; Ihee, H.: Conformational Substates of Myoglobin Intermediate Resolved by Picosecond X-ray Solution Scattering. *The Journal of Physical Chemistry Letters* **2014**, *5*, 804-808.

(335) Oang, K. Y.; Kim, J. G.; Yang, C.; Kim, T. W.; Kim, Y.; Kim, K. H.; Kim, J. H.; Ihee, H.: Conformational Substates of Myoglobin Intermediate Resolved by Picosecond X‑ray Solution Scattering. *J Phys Chem Lett* **2014**, *5*, 804−808.

(336) Kim, K. H.; Kim, J.; Lee, J. H.; Ihee, H.: Topical Review: Molecular reaction and solvation visualized by time-resolved X-ray solution scattering: Structure, dynamics, and their solvent dependence. *Structural Dynamics* **2014**, *1*.

(337) Kim, K. H.; Muniyappan, S.; Oang, K. Y.; Kim, J. G.; Nozawa, S.; Sato, T.; Koshihara, S. Y.; Henning, R.; Kosheleva, I.; Ki, H.; Kim, Y.; Kim, T. W.; Kim, J.; Adachi, S.; Ihee, H.: Direct Observation of Cooperative Protein Structural Dynamics of Homodimeric Hemoglobin from 100 ps to 10 ms with Pump-Probe X-ray Solution Scattering. *Journal of the American Chemical Society* **2012**, *134*, 7001-7008.

(338) Kim, J. G.; Muniyappan, S.; Oang, K. Y.; Kim, T. W.; Yang, C.; Kim, K. H.; Kim, J.; Ihee, H.: Cooperative protein structural dynamics of homodimeric hemoglobin linked to water cluster at subunit interface revealed by time-resolved X-ray solution scattering. *Structural Dynamics* **2016**, *3*.

(339) Kern, J.; Yachandra, V. K.; Yano, J.: Metalloprotein structures at ambient conditions and in real-time: biological crystallography and spectroscopy using X-ray free electron lasers. *Current Opinion in Structural Biology* **2015**, *34*, 87-98.

(340) Levantino, M.; Lemke, H. T.; Schirò, G.; Glownia, M.; Cupane, A.; Cammarata, M.: Observing heme doming in myoglobin with femtosecond X-ray Absorption Spectroscopy. *Structural Dynamics* **2015**, *2*, 041713.

(341) Miller, N. A.; Deb, A.; Alonso-Mori, R.; Garabato, B. D.; Glownia, J. M.; Kiefer, L. M.; Koralek, J.; Sikorski, M.; Spears, K. G.; Wiley, T. E.; Zhu, D.; Kozlowski, P. M.; Kubarych, K. J.; Penner-Hahn, J. E.; Sension, R. J.: Polarized XANES Monitors Femtosecond Structural Evolution of Photoexcited Vitamin B12. *Journal of the American Chemical Society* **2017**, *139*, 1894-1899.

(342) Levantino, M.; Schirò, G.; Lemke, H. T.; Cottone, G.; Glownia, J. M.; Zhu, D.; Chollet, M.; Ihee, H.; Cupane, A.; Cammarata, M.: Ultrafast myoglobin structural dynamics observed with an X-ray free-electron laser. *Nat Commun* **2015**, *6*, 6772.

(343) Barends, T. R. M.; Foucar, L.; Ardevol, A.; Nass, K.; Aquila, A.; Botha, S.; Doak, R. B.; Falahati, K.; Hartmann, E.; Hilpert, M.; Heinz, M.; Hoffmann, M. C.; Köfinger, J.; Koglin, J. E.; Kovacsova, G.; Liang, M.; Milathianaki, D.; Lemke, H. T.; Reinstein, J.; Roome, C. M.; Shoeman, R. L.; Williams, G. J.; Burghardt, I.; Hummer, G.; Boutet, S.; Schlichting, I.: Direct observation of ultrafast collective motions in CO Myoglobin upon Ligand Dissociation. *Science* **2015**, *350*, 445-450.

(344) Hutchison, C. D. M.; van Thor, J. J.: Populations and Coherence in femtosecond time resolved X-ray crystallography of the photoactive yellow protein. *Int Rev Phys Chem* **2017**, *36*, 117-143.

(345) Schmidt, M.: A short history of structure based research on the photocycle of photoactive yellow protein. *Structural Dynamics* **2017**, *4*, 032201.

(346) Nango, E.; Royant, A.; Kubo, M.; Nakane, T.; Wickstrand, C.; Kimura, T.; Tanaka, T.; Tono, K.; Song, C.; Tanaka, R.; Arima, T.; Yamashita, A.; Kobayashi, J.; Hosaka, T.; Mizohata, E.; Nogly, P.; Sugahara, M.; Nam, D.; Nomura, T.; Shimamura, T.; Im, D.; Fujiwara, T.; Yamanaka, Y.; Jeon, B.; Nishizawa, T.; Oda, K.; Fukuda, M.; Andersson, R.; Båth, P.; Dods, R.; Davidsson, J.; Matsuoka, S.; Kawatake, S.; Murata, M.; Nureki, O.; Owada, S.; Kameshima, T.; Hatsui, T.; Joti, Y.; Schertler, G.; Yabashi, M.; Bondar, A.-N.; Standfuss, J.; Neutze, R.; Iwata, S.: A three-dimensional movie of structural changes in Bacteriorhodopsin. *Science* **2016**, *354*, 1552-1557.

(347) Sauter, N. K.; Echols, N.; Adams, P. D.; Zwart, P. H.; Kern, J.; Brewster, A. S.; Koroidov, S.; Alonso-Mori, R.; Zouni, A.; Messinger, J.: No observable conformational changes in PSII. *Nature* **2016**, *533*, E1-E2.

(348) Pande, K.; Hutchison, C. D. M.; Groenhof, G.; Aquila, A.; Robinson, J. S.; Tenboer, J.; Basu, S.; Boutet, S.; DePonte, D. P.; Liang, M.; White, T. A.; Zatsepin, N. A.; Yefanov, O.; Morozov, D.; Oberthuer, D.; Gati, C.; Subramanian, G.; James, D.; Zhao, Y.; Koralek, J.; Brayshaw, J.; Kupitz, C.; Conrad, C.; Roy-Chowdhury, S.; Coe, J. D.; Metz, M.; Xavier, P. L.; Grant, T. D.; Koglin, J. E.; Ketawala, G.; Fromme, R.; Šrajer, V.; Henning, R.; Spence, J. C. H.; Ourmazd, A.; Schwander, P.; Weierstall, U.; Frank, M.; Fromme, P.; Barty, A.; Chapman, H. N.; Moffat, K.; van Thor, J. J.; Schmidt, M.: Femtosecond structural dynamics drives the trans/cis isomerization in photoactive yellow protein. *Science* **2016**, *352*, 725-729.

(349) Kuramochi, H.; Takeuchi, S.; Yonezawa, K.; Kamikubo, H.; Kataoka, M.; Tahara, T.: Probing the early stages of photoreception in photoactive yellow protein with ultrafast time-domain Raman spectroscopy. *Nat Chem* **2017**, *advance online publication*.

(350) Winter, B.; Faubel, M.: Photoemission from liquid aqueous solutions. *Chem Rev* **2006**, *106*, 1176-1211.

(351) Ekimova, M.; Quevedo, W.; Faubel, M.; Wernet, P.; Nibbering, E. T. J.: A liquid flatjet system for solution phase soft-x-ray spectroscopy. *Structural Dynamics* **2015**, *2*.

(352) Link, O.; Lugovoy, E.; Siefermann, K.; Liu, Y.; Faubel, M.; Abel, B.: Ultrafast electronic spectroscopy for chemical analysis near liquid water interfaces: concepts and applications. *Appl Phys a-Mater* **2009**, *96*, 117-135.

(353) Faubel, M.; Siefermann, K. R.; Liu, Y.; Abel, B.: Ultrafast Soft X-ray Photoelectron Spectroscopy at Liquid Water Microjets. *Accounts Chem Res* **2012**, *45*, 120-130.

(354) Al-Obaidi, R.; Wilke, M.; Borgwardt, M.; Metje, J.; Moguilevski, A.; Engel, N.; Tolksdorf, D.; Raheem, A.; Kampen, T.; Mähl, S.: Ultrafast photoelectron spectroscopy of solutions: space-charge effect. *New J Phys* **2015**, *17*, 093016.

(355) Ojeda, J.; Arrell, C. A.; Grilj, J.; Frassetto, F.; Mewes, L.; Zhang, H.; van Mourik, F.; Poletto, L.; Chergui, M.: Harmonium: A pulse preserving source of monochromatic extreme ultraviolet (30–110 eV) radiation for ultrafast photoelectron spectroscopy of liquids. *Structural Dynamics* **2016**, *3*, 023602.

(356) Johnson, A.; Miseikis, L.; Wood, D.; Austin, D.; Brahms, C.; Jarosch, S.; Strüber, C.; Ye, P.; Marangos, J.: Measurement of sulfur L2, 3 and carbon K edge XANES in a polythiophene film using a high harmonic supercontinuum. *Structural Dynamics* **2016**, *3*, 062603.

(357) Vura-Weis, J.; Jiang, C.-M.; Liu, C.; Gao, H.; Lucas, J. M.; de Groot, F. M. F.; Yang, P.; Alivisatos, A. P.; Leone, S. R.: Femtosecond M2,3-Edge Spectroscopy of Transition-Metal Oxides: Photoinduced Oxidation State Change in α-Fe2O3. *The Journal of Physical Chemistry Letters* **2013**, *4*, 3667-3671.

(358) Jiang, C. M.; Baker, L. R.; Lucas, J. M.; Vura-Weis, J.; Alivisatos, A. P.; Leone, S. R.: Characterization of Photo-Induced Charge Transfer and Hot Carrier Relaxation Pathways in Spinel Cobalt Oxide (Co3O4). *J Phys Chem C* **2014**, *118*, 22774-22784.

(359) Borja, L. J.; Zürch, M.; Pemmaraju, C.; Schultze, M.; Ramasesha, K.; Gandman, A.; Prell, J. S.; Prendergast, D.; Neumark, D. M.; Leone, S. R.: Extreme ultraviolet transient absorption of solids from femtosecond to attosecond timescales. *JOSA B* **2016**, *33*, C57-C64.

(360) Szlachetko, J.; Milne, C. J.; Hoszowska, J.; Dousse, J.-C.; Błachucki, W.; Sà, J.; Kayser, Y.; Messerschmidt, M.; Abela, R.; Boutet, S.; David, C.; Williams, G.; Pajek, M.; Patterson, B. D.; Smolentsev, G.; van Bokhoven, J. A.; Nachtegaal, M.: Communication: The electronic structure of matter probed with a single femtosecond hard x-ray pulse. *Structural Dynamics* **2014**, *1*, 021101.

(361) Mukamel, S.: *Principles of nonlinear optical spectroscopy*; Oxford University Press: New York, 1995.

(362) Bencivenga, F.; Cucini, R.; Capotondi, F.; Battistoni, A.; Mincigrucci, R.; Giangrisostomi, E.; Gessini, A.; Manfredda, M.; Nikolov, I. P.; Pedersoli, E.; Principi, E.; Svetina, C.; Parisse, P.; Casolari, F.; Danailov, M. B.; Kiskinova, M.; Masciovecchio, C.: Four-wave mixing experiments with extreme ultraviolet transient gratings. *Nature* **2015**, *520*, 205-U149.

(363) Szlachetko, J.; Hoszowska, J.; Dousse, J.-C.; Nachtegaal, M.; Błachucki, W.; Kayser, Y.; Sà, J.; Messerschmidt, M.; Boutet, S.; Williams, G. J.: Establishing nonlinearity thresholds with ultraintense X-ray pulses. *Sci Rep-Uk* **2016**, *6*.

(364) Dean, M.; Cao, Y.; Liu, X.; Wall, S.; Zhu, D.; Mankowsky, R.; Thampy, V.; Chen, X.; Vale, J.; Casa, D.: Ultrafast energy-and momentum-resolved dynamics of magnetic correlations in the photo-doped Mott insulator Sr2IrO4. *Nat Mater* **2016**, *15*, 601-605.

(365) Badali, D. S.; Gengler, R. Y.; Miller, R.: Ultrafast electron diffraction optimized for studying structural dynamics in thin films and monolayers. *Structural Dynamics* **2016**, *3*, 034302.

(366) Franssen, J.; Frankort, T.; Vredenbregt, E.; Luiten, O.: Pulse length of ultracold electron bunches extracted from a laser cooled gas. *Structural Dynamics* **2017**, *4*, 044010.

(367) Hamm, P.; Zanni, M. T.: *Concepts and methods of 2d infrared spectroscopy*; Cambridge University Pres: Cambridge ; New York, 2011.

(368) Fayer, M. D.: *Ultrafast infrared vibrational spectroscopy*; Taylor & Francis: Boca Raton, 2013.
(369) Hamm, P.; Lim, M.; Hochstrasser, R. M.: Ultrafast dynamics of amide-I vibrations. *Biophysical Journal* **1998**, *74*, A332-A332.